1976

The optimal dimensions of pennsylvania highway drainage inlets in paved channels, M.S. thesis, 1976.

Andrew Day Spear

THE OPTIMAL DIMENSIONS OF PENNSYLVANIA HIGHWAY DRAINAGE INLETS IN PAVED CHANNELS

by

Andrew Day Spear

A Thesis

Presented to the Graduate Committee

of Lehigh University

in Candidacy for the Degree of

Master of Science

in

Civil Engineering

Lehigh University

1976

This thesis is accepted and approved in partial fulfillment of the requirements for the Degree of Master of Science.

12 December 1975
(Date)

Professor in Charge

Chairman of Department

ACKNOWLEDGEMENTS

This research was sponsored by the Pennsylvania Department of Transportation in conjunction with the United States Federal Highway Administration. It was conducted in Fritz Engineering Laboratory (Department of Civil Engineering) of Lehigh University in Bethlehem, Pennsylvania, by the following personnel of the Hydraulics Department: Dr. Arthur W. Brune, Project Director, Dr. Willard A. Murray, Assistant Project Director, and Andrew D. Spear, Research Assistant.

The Director of Fritz Engineering Laboratory is Dr. Lynn S. Beedle; the Chairman of the Department of Civil Engineering is Dr. David A. VanHorn; the Director of the Office of Research is Professor George R. Jenkins.

The author is indebted to Mr. Elias Dittbrenner who assisted in the work, to the secretaries of Fritz Laboratory who typed the manuscript, and to John M. Gera who prepared the drawings.

Recognition is here given to personnel of PennDOT and FHWA who aided materially in the study and Mr. Kenneth L. Heilman, PE, PennDOT, the Research Coordinator, whose guidance was very

ACKNOWLEDGEMENTS

helpful. Additionally, the author offers his thanks to Mr. Ming Tsai, PennDOT, Mr. Kennth Foster, FHWA, and especially to Dr. D. C. Woo whose careful observations were very valuable in accomplishing this work.

TABLE OF CONTENTS

TABLE OF CONTENTS - continued

TABLE OF CONTENTS - continued

APPENDIX

LIST OF TABLES

LIST OF FIGURES

LIST OF FIGURES (Cont.)

LIST OF FIGURES (Cont.)

NOMENCLATURE

A	:	area of flow, m^2 (ft^2)
A'	:	effective area, m^2 (ft^2)
BB	:	backslope width of flow, m (ft)
BS	:	swale slope width of flow, m (ft)
c	:	constant
C', Co	:	Chezy's constant
D	:	depth of flow m (ft)
D'	:	depth of flow at invert when bypassing flow exists m (ft)
E_u	:	Euler number
f	:	Darcy's friction factor
F_r	:	Froude number
g	:	gravitational acceleration, m/sec^2 (ft/sec^2)
ΔH	:	change in head, m (in.)
L	:	length of inlet, cm (in.)
L_b	:	bar width in grate, cm (in.)
L_o	:	length of falling flow, m (ft)
Lp, L'	:	length of flow around inlet, m (ft)
L_r	:	scale ratio
L_s	:	space width in grate, cm (in.)
m	:	Li's grating variable
n	:	Manning's roughness coefficient
ΔP	:	pressure difference gm/cm^2 (psi)

NOMENCLATURE (cont)

Q	:	flow rate, cms (cfs)
Q_1	:	total flow rate, cms (cfs)
Q_2	:	intercepted flow rate, cms (cfs)
Q_3	:	bypassing flow rate, cms (cfs)
R_e	:	Reynolds number
R_h	:	hydraulic radius, m (ft)
s	:	slope of energy line
S_B	:	backslope
S_o	:	longitudinal slope, grade
S_s	:	swaleslope
v	:	velocity, mps (fps)
V	:	volume, m^3 (ft^3)
w	:	width of inlet, m (ft)
W	:	wetted perimeter, m (ft)
x	:	variable
y	:	width of flow, m (ft)
z	:	Murray tragectory theory term
Z	:	constant for flow over situation calculations
η	:	efficiency
θ	:	swale slope angle
ρ	:	density, gm/cm^3 (pcf)
μ	:	dynamic viscosity, kg/m-hr (lb/ft-hr)

NOMENCLATURE (cont)

cfs	:	cubic feet per second
cms	:	cubic meters per second
FHWA	:	Federal Highway Administration
PennDOT	:	Pennsylvania Department of Transportation
p subscripted	:	prototype
m subscripted	:	model

ABSTRACT

An experimental model investigation is presented of the optimal dimensions of highway drainage gratings installed in paved channels along highways in Pennsylvania. Further work is introduced in an effort to describe the flow situation into the grating through analytical theory and equations. The ultimate goal of this study was to determine an optimal length to width ratio of an inlet grating based upon maximal inflow rate efficiency.

The channel considered was triangular in shape with swale slopes ranging from 48:1 to 12:1 and back slopes ranging from 3:1 to 1/8:1. Longitudinal slopes used during the tests were 1/2%, 2%, and 4%. The grating width was held constant while the length was modified.

The model inlet grating was built to half the scale of the prototype, and through model laws, other prototype:model relationships were established. The capacity of the grating was determined by actual measurements, and equations based upon these measurements were formulated.

A series of curves are presented which relate 100%-efficient inflow rates to the grating length. These curves show that the longer drains intercept more water and that the channels with the 12:1 swale slopes yield higher maximal efficiency flow rates

than do those with 48:1 swale slopes. Also curves are presented which indicate, for 48:1 swale slopes, shorter gratings are used more efficiently, with respect to the surface area of the drain, than longer ones, whereas the opposite is true with 12:1 swale slopes.

The information contained herein should be useful in the design of highway drainage systems - grate sizes, spacing, and preferred channel configurations for paved channels.

1.1 INTRODUCTION

1.1.1 Problem Statement

Runoff along highways from precipitation must be removed from the paved surfaces and adjacent areas. The surface runoff is channeled into drainage inlets and is removed by way of a subsurface system of conduits. the drainage inlets are spaced along the roadway at intervals which are determined by the design engineer.

Two difficulties exist with inlets currently being installed in drainage channels by the Pennsylvania Department of Transportation: (1) water bypasses the inlet owing to the fact that the inlet is to narrow; and (2) part of the inlet grating is not covered entirely with water at times of maximal efficiency flow.

In consideration of these problems, a program of research was undertaken using a model of a paved channel in an effort to determine the optimal ratio of length:width of grating based upon the efficiency of the inlet grating in catching channeled surface drainage flow. Different channel configurations were included in the testing program: back slopes 3:1 and 1/8:1, swale slopes of 48:1 and 12:1; longitudinal slopes of 4%, 2% and 1/2%; and prototype grating lengths of 45.8 (1.50 ft), 53.4 cm (1.75 ft), 61.0 cm

(2.00 ft), 68.6 cm (2.25 ft), and 76.2 (2.50 ft). The width was constant at 91.5 cm (3.0 ft).

Next, an analytical evaluation of the various flow regimes measured in these tests was made, which will be presented in Chapter Two of this report.

1.1.2 Background

The problem of draining highway pavements has been solved commonly by employing empirical or intuitional approaches, notwithstanding that drainage systems are of paramount importance in highway design. Drainage channels and inlets are placed along the roadways to catch surface runoff and to guide it into a subsurface drainage system. Without such drainage, flooding would occur causing damage to the pavement and base materials, deposition of sediment in low-lying areas, and hinderances to traffic safety.

Until recently, estimation of the capacity of drainage inlets had been based on past experience; furthermore, little consideration was given to different channel configurations or irregularities in the channel surface. Obviously, the hydraulic performance of any drainage inlet must be known before it can properly be utilized along the highway.

PennDOT Research Project 68-31 at Lehigh University entitled "Development of Improved Drainage Inlets", which also used a model study, was completed in January, 1973 in accordance with PennDOT Agreement Numbers 42237 through 42237-H between Lehigh University and the Commonwealth of Pennsylvania. As a result of this project, reports were presented to PennDOT summarizing and evaluating (1) the results of past papers and studies pertaining to highway drainage inlets (Yucel, 1969); (2) new capacities for inlets installed in paved channels (Yee, 1972), and (3) new capacities for inlets installed in grass channels (Appel, 1973).

The investigators noted throughout the investigation that, for high flow rates, some water in the channel bypassed the drainage inlet because the width of the inlet, perpendicular to the direction of flow, was too narrow. This bypassing of water could be prevented by increasing the width of the drain.

Another observation of some importance was that the entire grating surface was not utilized in catching water flowing toward it during maximum efficiency flow situations. Part of some bars on the grating and all of other bars were exposed to the atmosphere in many instances. Specifically, those in the downstream portion of the grating near the channel invert were not covered by water.

Based upon these observations, an investigation was warranted to determine the optimal arrangement of the length:width ratio for an inlet grating which most efficiently utilized the surficial area of the grating and intercepted the maximal amount of inflow.

1.1.3 Objectives

The objectives of this research program are:

1. To develop a single grating for installation in paved highway drainage channels based upon maximum surficial efficiency and inflow interception rates.
2. To analyze analytically the flow situation surrounding the inlet grating for all channel configurations tested through the use of theory, equations, and computer.
3. To document, by means of photographs, those conditions which determine the optimal length of each respective inlet grating for every channel configuration.

1.2 MODEL LAWS

1.2.1 General Remarks

Two common procedures in solving hydraulic problems are analytical methods and model studies. An analytical approach will be presented in Chapter Two. Model studies can simulate the prototype situation while providing visual as well as statistical means of evaluation. A model is usually smaller than its prototype, and consequently is easier to fabricate. Also working with a smaller apparatus in a controlled environment provides greater ease in handling, preparation, and repair. For these reasons, a model study was chosen to study the highway drainage inlets.

Prior to testing, the similitude between relevant properties of the model and the prototype must be computed, so that events noted in the model study can be properly related to the prototype. This similitude is determined through model laws. Once the basic model:prototype scale ratio is known, data from the model study can be changed into different physical quantities, such as velocity, discharge, and depth, in the corresponding prototype.

The length ratio of 2:1 was determined for the prototype: model after considering (a) the space available in the laboratory, (b) the available pumping facilities, (c) the cost of fabricating and operating a model of that size, and (d) the effect of surface tension.

It should be noted that the literature available on model laws is extensive and complete. (Stevens et al., 1942; Morris, 1963; Hansen, 1967; and Graf, 1971.)

1.2.2 Hydraulic Similitude

The correlation between physical quantities in the model and the prototype is called the similitude. For complete similarity between model and prototype, three similarities must be satisfied; they are geometric, kinematic, and dynamic similitudes.

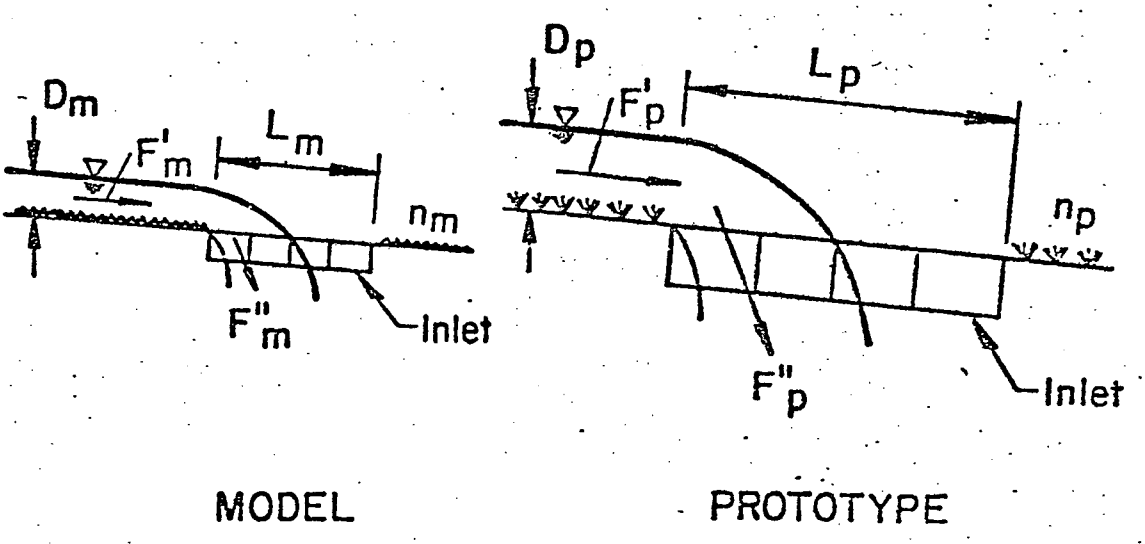

Figure 1.1: Similitude of Highway Drainage Inlets

1.2.2.1 Geometric Similitude

Two objects are said to be geometrically similar provided the ratios of corresponding dimensions are equal. From the model

and prototype illustrated in Figure 1.1, geometric similitude will exist provided

$$L_R = \frac{D_p}{D_m} = \frac{L_p}{L_m} \qquad \text{Eq. 1.1}$$

where L denotes the length of the grating, D the depth of flow, and L_R the scale ratio. The subscripts, p and m, indicate prototype and model, respectively. The similarity between areas and volumes can be obtained as well from the scale ratio:

$$L_R^2 = \frac{A_p}{A_m} \qquad \text{and} \qquad \text{Eq. 1.2a}$$

$$L_R^3 = \frac{V_p}{V_m} \qquad \text{Eq. 1.2b}$$

where A and V are representative area and volume, respectively.

1.2.2.2 Kinematic Similitude

Two flow regimes are said to be kinematically similar provided (1) the flow fields have the same shape, and (2) the prototype:model ratios of velocities and accelerations are the same.

1.2.2.3 Dynamic Similitude

Dynamic similitude exists between prototype and model if corresponding forces are parallel and have the same prototype: model ratio of forces for all related points in the flow fields.

From Fig. 1.1, the force ratios can be expressed as:

$$F_R = \frac{F_p'}{F_m''} = \frac{F_p'}{F_m''} \qquad \text{Eq. 1.3}$$

where F_R is the force ratio; F_p' and F_p'' are forces in the prototype, and F_m' and F_m'' are corresponding forces in the model. The forces which can affect a flow field are those due to inertia F_I, gravity F_g, pressure F_p, viscosity F_v, elasticity F_e, and surface tension F_t. Inasmuch as water is nearly incompressible and the model is fairly large, the forces of elasticity and surface tension are negligible and can be ignored in this study. Thus, for complete dynamic similitude, the following equation must be satisfied:

$$F_R = \frac{(F_I)_p}{(F_I)_m} = \frac{(F_g)_p}{(F_g)_m} = \frac{(F_p)_p}{(F_p)_m} = \frac{(F_v)_p}{(F_v)_m} \qquad \text{Eq. 1.4}$$

1.2.3 Dimensionless Numbers

In a hydraulic model study, certain combinations of variables forming dimensionless numbers are more valuable than individual variables. In this case, the Euler Number E_u, the Froude Number F_r, and the Reynolds Number R_e are important. These dimensionless numbers are expressed in the following manner:

$$E_u = \frac{F_p}{F_I} = \frac{\Delta p}{\rho v^2} \qquad \text{Eq. 1.5}$$

$$F_r = \left(\frac{F_I}{F_g}\right)^{1/2} \frac{v}{(gL)^{1/2}} \qquad \text{Eq. 1.6}$$

$$R_e = \frac{F_I}{F_v} = \frac{\rho v L}{\mu} \qquad \text{Eq. 1.7}$$

where ρ is density, v is characteristic velocity, Δp is a pressure difference, g is the gravitational acceleration, and μ is the dynamic viscosity. Only two of these three dimensionless numbers are independent, which means that the third number can be obtained provided the other two are known; thus dynamic similitude is achieved if two of these numbers are simultaneously satisfied. Unfortunately, acquiring complete similarity using only two of these numbers is usually impossible owing to limitations, such as: certain characteristics of water and the limited facilities available. In most hydraulic engineering problems, however, some forces are orders of magnitude greater than others, which allows some relationships to be ignored. In this way, dynamic similitude is obtainable using but one dimensionless number. For this study, the force of gravity is much greater than the force of friction due to the smoothness of the surface, which indicates that Froude similarity alone is sufficient to ensure dynamic similarity between the model and the prototype.

1.2.4 Froude Model Law

The Froude Number for both the model and prototype can be expressed as follows:

$$F_R = \left.\frac{v}{\sqrt{gL}}\right|_p = \left.\frac{v}{\sqrt{gL}}\right|_m \qquad \text{Eq. 1.8}$$

For equal accelerations of gravity, the resulting velocity ratio is:

$$\frac{V_p}{V_m} = \left(\frac{L_p}{L_m}\right)^{1/2} \qquad \text{Eq. 1.9a}$$

For a scale ratio of 2, as used in the present study, the velocity ratio becomes:

$$\frac{V_p}{V_m} = 1.41 \qquad \text{Eq. 1.9b}$$

The flow-ratio can be computed in a similar manner to yield:

$$\frac{Q_p}{Q_m} = (L_R)^{2.5} = 5.66 \qquad \text{Eq. 1.10}$$

Using this equation with the model flow rate, the corresponding prototype flow rate can be calculated. A complete list of Froude model similarities is presented in Table 1.1.

1.2.5 Manning Model Law

The effect of frictional forces on the flow regime has been ignored thus far, yet the friction from the channel roughness

(pavement) must influence the flow pattern - the type of channel flow as well as the efficiency of the drainage grating - to some extent. Hence, it is necessary to consider both the frictional and gravity forces simultaneously. As mentioned in Section 1.2.3, satisfying both the Froude and Reynolds Numbers simultaneously is virtually impossible provided the same fluid is used in both the model and the prototype. Another means of correlating friction and gravity must be adopted.

For open-channel flow, this correlation is achieved most effectively by introducing the Manning Analogy which is derived from the Manning equation:

$$v = \frac{1.49\, R_h^{2/3}\, S_o^{1/2}}{n} \qquad \text{Eq. 1.11}$$

where R_h is the hydraulic radius, S_o is the grade or longitudinal slope for uniform flow, v is the mean velocity, and n is the Manning roughness coefficient. Because geometric and kinematic similitudes exist between the model and prototype, the Manning Analogy is expressed as:

$$\left(\frac{L^{2/3}}{vn}\right)_p = \left(\frac{L^{2/3}}{vn}\right)_m \qquad \text{Eq. 1.12}$$

Using Eq. 1.9a, Eq. 1.12 can be expressed as:

		Froude Similitude	Lehigh Scale	Manning Similitude	Lehigh Scale Paved Channel
Physical Properties	Length, L_r	L_r	2.0	L_r	2.0
	Area, A_r	L_r^2	4.0	L_r^2	4.0
	Volume, V_r	L_r^3	8.0	L_r^3	8.0
Kinematic Properties	Time, T_r	$L_r^{1/2}$	1.41	$\frac{L_r^{1/3}}{n_r}$	1.47
	Velocity, v_r	$L_r^{1/2}$	1.41	$\frac{L_r^{2/3}}{n_r}$	1.36
	Discharge, Q_r	$L_r^{5/2}$	5.66	$\frac{L_r^{8/3}}{n_r}$	5.44

$n_r = \frac{0.014}{0.012}$

Table 1.1 Model Scales for Froude and Manning Similitudes

$$\frac{n_p}{n_m} = \frac{L_p^{1/6}}{L_m} \qquad \text{Eq. 1.13}$$

Since the discharge relationship between prototype and model is of prime interest, Eq. 1.13 can be rearranged to yield:

$$\frac{Q_p}{Q_m} = \frac{L_p^{8/3}}{L_m} \frac{n_m}{n_p} \qquad \text{Eq. 1.14a}$$

This relationship and other flow characteristics for Manning similitude are shown in Table 1.1.

To evaluate Eq. 1.14a, the roughness coefficients for the model and prototype must be known. The Manning coefficient for pavement as used by the Pennsylvania Department of Transportation is n = 0.014, which is in good agreement with the literature (Chow, 1959). Plywood of 1.91 cm (0.75 in.) thickness has been used in the model to simulate the paved surface of the prototype. The Manning coefficient of plywood was determined from flume tests performed at Lehigh University to be n = 0.012 which again is in accordance with the literature (Chow, 1959). These roughness coefficient values were used throughout the study.

Introducing the n_p:n_m ratio and the length ratio $L_R = 2.0$, Eq. 1.14a then becomes:

$$\frac{Q_p}{Q_m} = 5.45 \qquad \text{Eq. 1.14b}$$

The application of the Manning formula requires turbulent flow both in the model and the prototype. Almost all open-channel flow in nature is turbulent, whereas flow occurring in a simulating model might very well not be turbulent. To ensure turbidity, the model should be operated in such a way as to yeild a high Reynolds Number, R_e.

The Reynolds Number ratio is

$$\frac{(R_e)_p}{(R_e)_m} = \frac{(vL)_p}{(vL)_m} = 2.72 \qquad \text{Eq. 1.15}$$

A preliminary test was performed in the model, from which it was determined that turbulent flow does exist in the model ($R_e > 7000$).

1.2.6 Concluding Remarks

Table 1.1 shows that the Froude similitude, involving gravitational effects, and the Manning Analogy, involving frictional effects, give similar results. Either set of numbers could be used in this study. Because gravitational forces are to be of the most importance in this case, Froude similitude has been selected to transform model results into prototype data.

1.3 EXPERIMENTAL INVESTIGATION

1.3.1 Laboratory Equipment

1.3.1.1 General Requirements of the Model

A full-sized model is ideal in performance tests of different inlet openings; however, as mentioned in Section 1.2.1, owing to the limitations placed upon the project, a prototype:model length ratio of 2:1 was chosen.

Uniform flow was required in the channel upstream from the inlet; consequently the model had to be long enough with little distortion to ensure this. Baffles and vanes were installed at the headwater of the channel to aid in forming uniform flow.

The frame supporting the model had to be rigid yet versatile. Uncontrolled fluctuations in slopes during testing would lead to faulty data, whereas controlled slopes were required to enable a full testing program of the inlet grating. Simple and rugged mechanisms for changing slopes and inlet grating lengths were necessary in order to reduce the time interval between tests.

The surface roughness of the channel must be designed to resemble closely the surface of the prototype (pavement).

For accurate results, care must be taken that no leakage occurs in the entire system and that flow rates be measured as accurately as possible.

1.3.1.2 Apparatus

A schematic diagram of the testing arrangement is shown in Fig. 1.2. Either or both pumps (B) raise water from the main sump (A) into the pressure tank (D). The two pumps could be operated separately or in parallel by adjusting the three valves (C).

Each pump was driven by a Westinghouse 9B Type HF, 220 volt AC, induction motor equipped with rheostatic control. One motor was rated at 40-hp, and the other at 35-hp. During a test, the pumps were adjusted to a rate of discharge that was constant over a period of time.

The pumps were DeLaval single-stage, double-suction, centrifugal types (Type I). One pump had a 25.4 cm (10.0 in.) suction line and a 20.3 cm (8.0 in.) discharge line, whereas the other had a 20.3 cm (8.0 in.) suction line and a 15.2 cm (6.0 in.) discharge line.

The cylindrical pressure tank (D) was 1.54 m (5.5 ft) in diameter, and 18.7 m (34.0 ft) high. The rate of discharge delivered to the manifold discharge pipe (M) in the head tank (N) was controlled by means of the supply value (E). The rate of inflow was measured using a 10.2 cm (4.0 in.) orifice (H) placed upstream

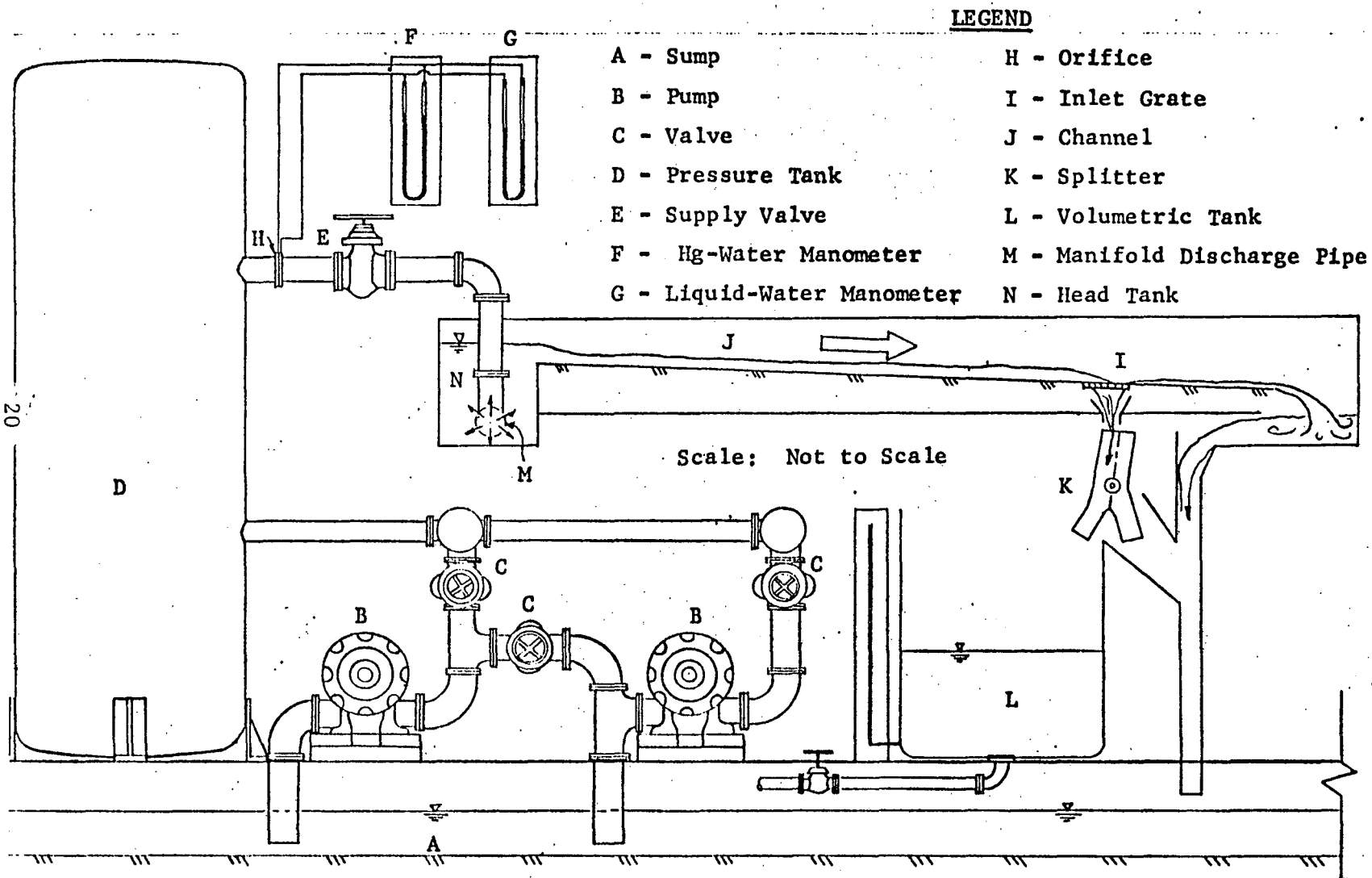

Fig. 1.2: Schematic Diagram of Model

from the supply valve in a 30.5 cm (12.0 in.) pipe, and a mercury-water manometer (F). The orifice had been calibrated numerous times over the previous five years and was rechecked twice during the testing period, each time with the same result, given as:

$$Q = 0.428\ H^{0.500} \qquad \text{Eq. 1.16}$$

where H is the pressure drop across the orifice in feet of water and Q is the discharge in cubic feet per second.

From the head tank (N), the water flowed down the channel (J) toward the inlet (I). The water intercepted by the inlet grating was directed by a manual splitter (K) into a 11.9 m^3 (420 ft^3) volumetric tank (L). Any flow that bypassed the inlet was channeled into the main sump (A).

The testing tank which held the model was rectanular in shape (See Fig. 1.3): 10.1 m (33.0 ft) long, 4.9 m (16.0 ft) wide, and 0.9 m (3.0 ft) deep. The tank was constructed on 0.64 cm (0.25 in.) steel plates framed by 7.6 cm (3.0 in.) by 7.6 cm (3.0 in.) angle irons, and it rested on 5.1 cm (2 in.) by 17.8 cm (7 in.) channel beams which were placed transversely on 1.2 m (4.0 ft) centers along the entire length of the testing tank.

The head tank containing the manifold discharge pipe was 0.76 m (2.5 ft) long, 4.9 m (16.0 ft) wide, and 1.2 m (4.0 ft) deep.

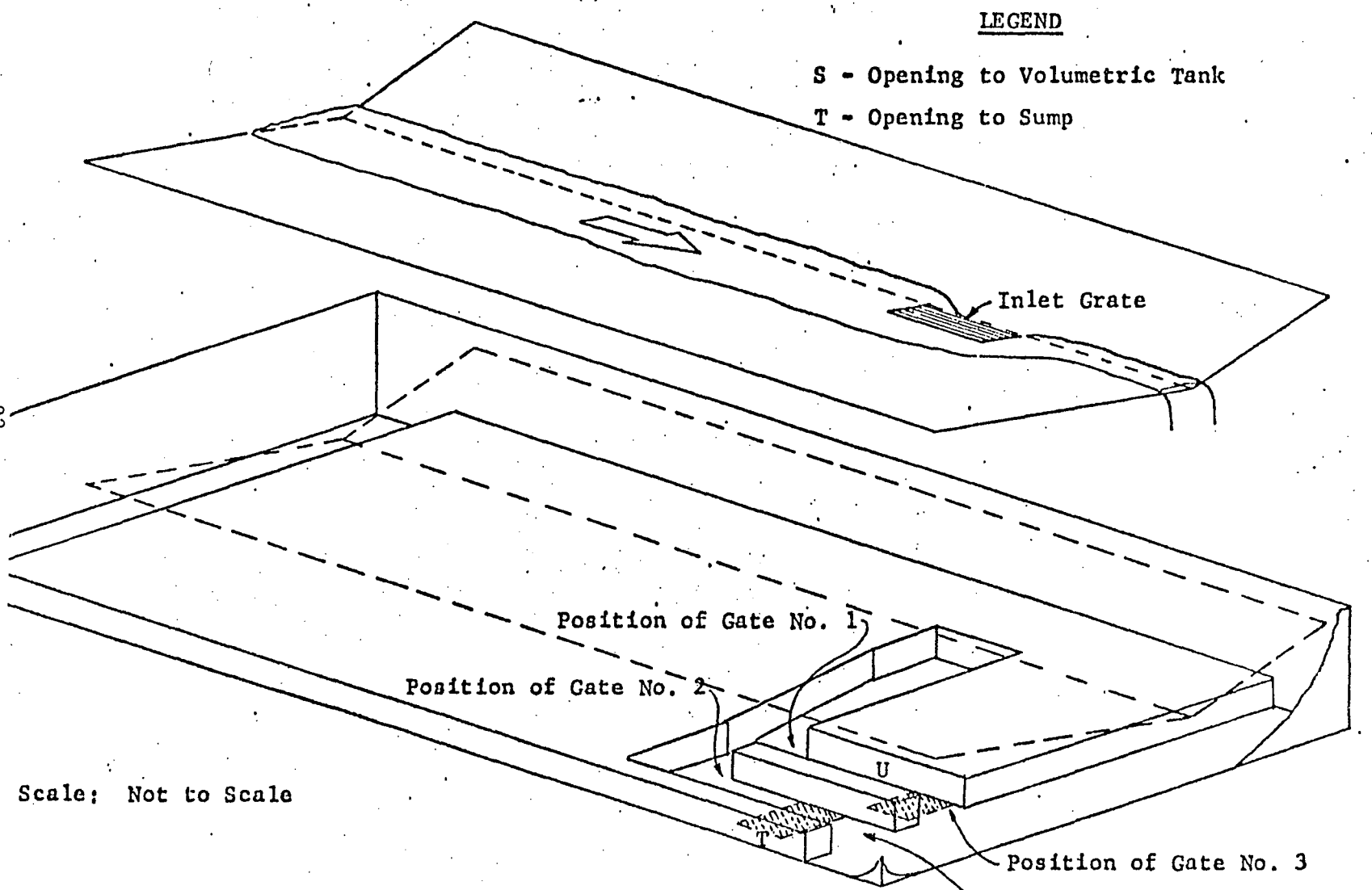

Fig. 1.3: Cutaway View of Testing Tank

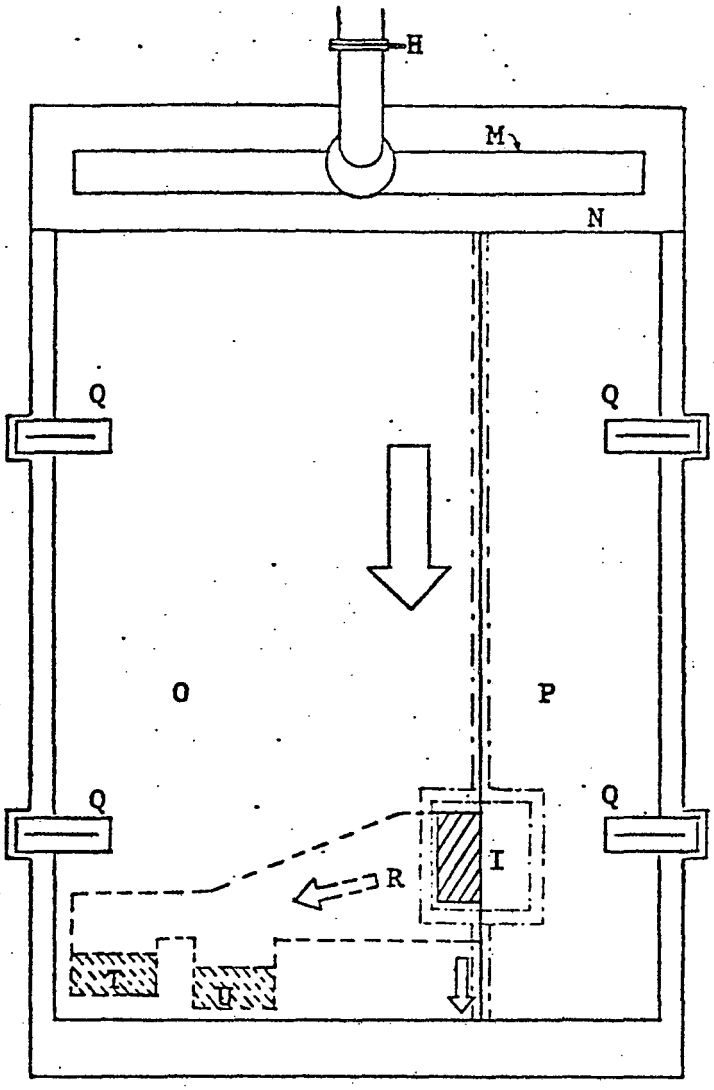

(a) Plan View

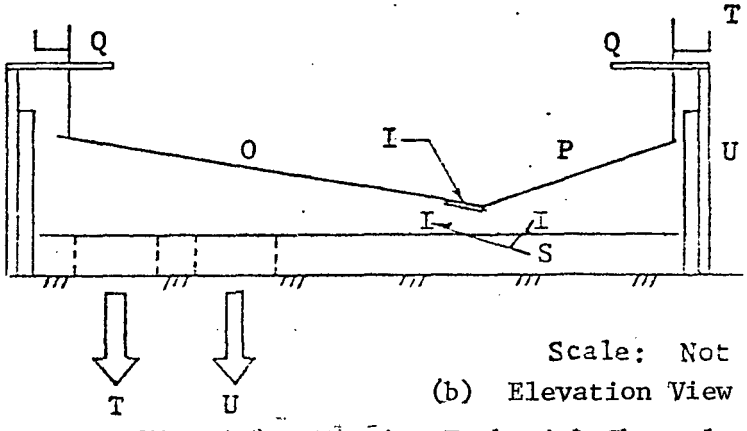

(b) Elevation View

LEGEND

H - Orifice

M - Manifold Discharge Pipe

N - Head Tank

O - Swale Slope

P - Back Slope

Q - Side-Slope Adjustment Rods

R - Conveyance Channel

S - Main Supporting I-Beam

I - Inlet Grates

T - Opening to Volumetric Tank

U - Opening to Sump

Scale: Not to Scale

Fig. 1.4: Testing Tank with Channel and Inlet Grate

Fig. 1.3 is a cutaway view of the testing tank, and Fig. 1.4 shows the model placed in the testing tank. A conveyance channel (R) carried the water intercepted by the drainage inlet to an opening (T) which was connected to the splitter and thence either to the volumetric tank or to the main sump. Another opening (U) nearer the downstream end of the testing tank directed the by-passing flow directly to the main sump. During the actual testing period, gates 1 and 4 were closed so that all intercepted flow went to the splitter for measurement if desired and all bypassing flow went directly to the main sump.

1.3.1.3 Model Construction

Two steel frames were constructed to support the swale slope (O) and back slope (P) which formed a triangular channel, as shown in Fig. 1.4. The swale and back slopes, which were 8.53 m (28.0 ft) long and 3.66 m (12.0 ft) and 1.07 m (3.5 ft) wide, respectively, were representations of similar situations in the field. Both frames were made of 54 X 9.5 I-beams welded together. The welded joints were reinforced by clip angles to prevent failure and to minimize deflection. The outer edges of the frames were made of 57 X 15.3 I-beams.

Both frames were covered with 1.9 cm (0.75 in.) outdoor plywood. Each piece, measuring 1.2 m (4.0 ft) by 2.4 m (8.0 ft),

was treated with preservative and with enamel paint. The joints of the plywood were covered with 5.1 cm (2 in.) self-adhesive tape which was then also painted. Hinges were welded to the invert of the channel to prevent lateral separation of the two side slopes, and also to allow rotation of the frames about the invert whenever changes in the side slopes were desired.

The invert rested on a W8 X 40 I-beam (S), which was 8.8 m (29 ft) long and was hinged at the downstream end. The proper longitudinal slope (grade) was obtained by providing the proper height of support. This was performed by manually placing blocks under the upstream end of the I-beam with the downstream end being fixed. Supports at various points along the I-beam were also installed to prevent any midpoint deflection. A survey using a rod and level was made of the channel to measure the grade. An overhead crane in the laboratory was used to raise the upstream end of the model into position.

The main supporting beam was cut just upstream and downstream from the inlet (See Fig. 1.4) and a box section, made of the same type of I-beam was installed to replace the piece that was removed. This modification was made to enable the water intercepted by the grating to fall directly into the conveyance channel without splashing over any obstacle and to facilitate emplacement of the grating itself.

The outer edge of each frame was supported by two 1,9 cm (0.75 in.) threaded tension rods (Q), which allowed the changing of each side slope independently of the other. Layers of 1.3 cm (0.5 in.) hardware cloth were soldered together to form a 0.30 m (1,0 ft) thick mat which was placed at the upstream end of the channel near the head tank, which acted as a baffle to aid in developing uniform flow in the channel upstream from the inlet.

1.3.2 The Drainage Inlet

The drainage inlet grating used in this study was made of wood with diagonal bars (See Fig. 1.5). The overall grating size of the model was 0.92 m (36 in.) in length and 0.61 m (24 in.) in width, corresponding to 1.84 m (72 in.) by 1.22 m (48 in.) in the prototype. The grating was installed parallel and coincidentally with the swale slope with the one side directly along the invert. The width was held constant at 0.46 m (1.50 ft) for the model, 0.92 m (3.00 ft) for the prototype, while the length of the grating was altered by covering downstream portions of it with thin metal plates. A rubber skirt was installed around the inlet and under the plates to prevent leakage. The plates were painted with enamel paint to give continuity of surface roughness.

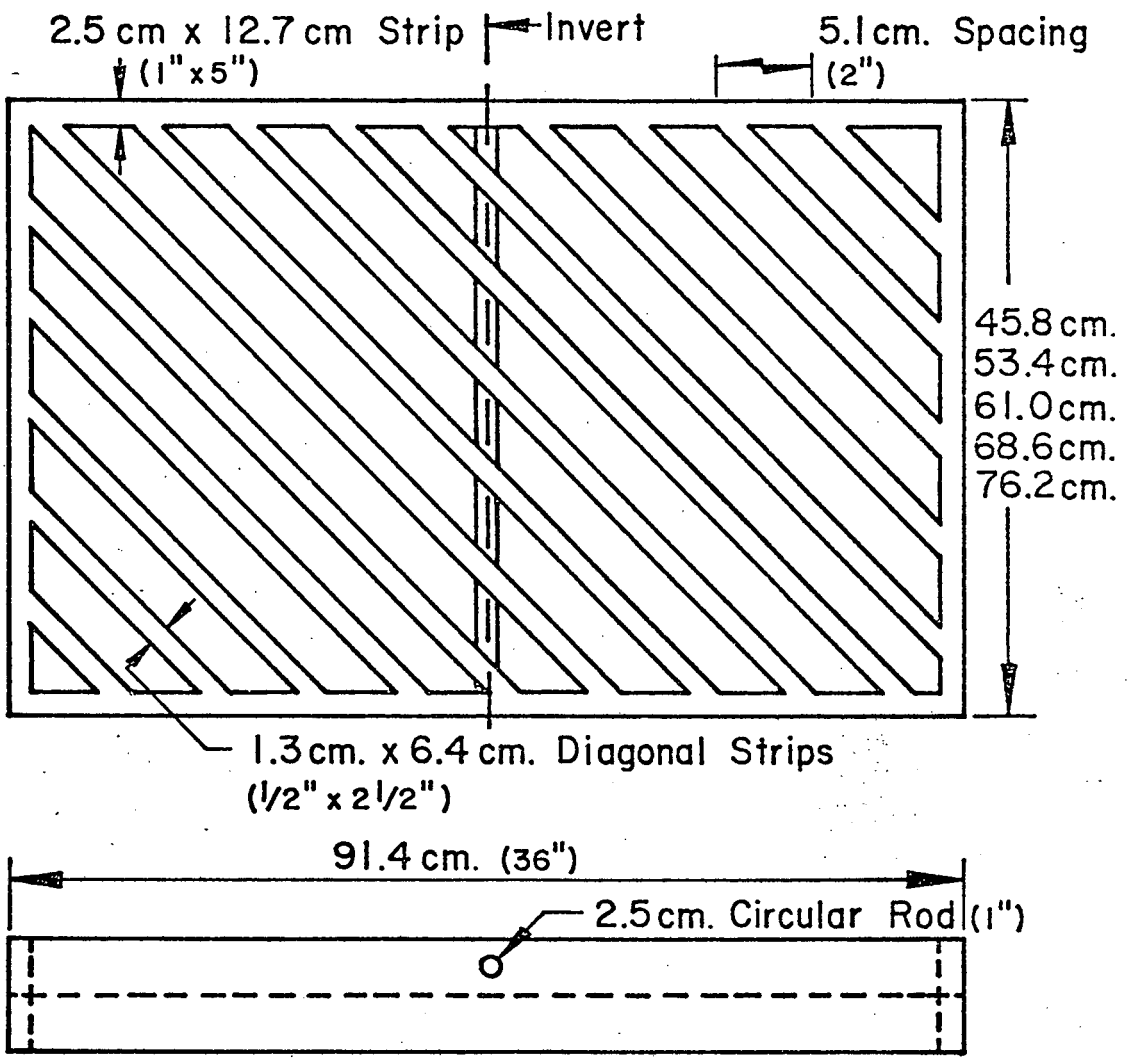

Fig. 1.5: Prototype Inlet Grating Used for Testing

1.3.3 Procedure

1.3.3.1 Flow Measurements

As mentioned in Section 1.3.1.2, the flow rate into the head tank and subsequently into the channel was determined by reading manometers attached to a calibrated 10.2 cm (4.0 in.) orifice installed in the supply line. The mercury in the manometer had a specific gravity of 13.6.

Water flowed down the channel and was totally or partly intercepted by the inlet depending upon the flow rate. The intercepted water was channeled to the splitter which directed it to a volumetric tank for measurement or to the main sump for recirculation. The flow which bypassed the inlet was directed into the main sump. The total flow, Q_1, was calculated from the manometer reading and from Eq. 1.16. The intercepted flow, Q_2, was determined by measuring water levels in the volumetric tank over a suitable time interval (60 sec). The bypassing flow, Q_3, was obtained by taking the difference between Q_1 and Q_2.

1.3.3.2 Depth and Width Measurements

Depth measurements were taken in the invert at stations 0.30 m (1.0 ft), 0.61 m (2.0 ft), and 0.92 m (3.0 ft) upstream from the inlet during each test. A point gage, graduated to 0.03 cm

(0.001 ft), was used for all depth measurements. The depth was determined by subtracting the gage reading for the channel bottom at the invert from the gage reading at the water surface. The point gage was mounted on wheels on an aluminum beam 7.6 cm (3.0 in.) by 12.7 cm (5.0 in.) which spanned the model perpendicular to the channel invert. The beam was supported by a monorail system at each end which enabled it to travel freely above the channel. This set-up facilitated depth measurements at any point in the channel.

For this experiment, steady uniform flow was required upstream from the grating for accurate measurements. Near the drain, reduction in the vertical and lateral dimensions of the flow occurred due to the convergence of the water into the inlet, disturbing the uniform flow. In this situation, it was desirable to maintain a cross-sectional area of constant shape. Thus width of flow measurements were taken at the same 0.30 m (1.0 ft), 0.61 m (2.0 ft), and 0.92 m (3.0 ft) stations as mentioned above to serve as a constant shape check. A tape measure mounted on the aluminum cross beam was used as a range finder together with a plumb bob that was lowered to the water's edge.

1.3.3.3 Technique

Before each test, the appropriate longitudinal slope was set using a surveyor's level. Next the slide slopes were adjusted as required using a triangular template and a carpenter's

level, and then the length of the grating was set. Inasmuch as altering the longitudinal slope was the most difficult and time consuming of the adjustments, all tests with the same longitudinal slope were performed in succession, thus reducing the number of these tedious changes to a minimum.

Subsequently, the pumps were started, and the supply valve was opened to provide a flow rate which was visually determined to be the maximum flow rate possible without allowing any water to bypass the drainage inlet.

After a period of several minutes had elapsed to allow steady flow to develop, the splitter was used to direct the intercepted flow into the volumetric tank for 60 seconds. The increase in volume divided by the time increment gave Q_2. Next, the manometer for the orifice in the supply line was read giving the total influent Q_1, and consequenntly Q_3, the difference between Q_1 and Q_2 was determined; Q_3 was zero for no bypassing flow. Finally, the different depth and width measurements were made and recorded, and photographs were taken.

The run was completed by following the same procedure for flow rates of 300%, 250%, 200%, and 50% of the maximal flow rate as determined in the first step. Approximately 300 tests were made overall. The experimental data are in part summarized in Section 1.4. All of the data are summarized in Tables A-1, A-2 of the Appendix.

1.4 RESULTS

A summary of the results from the tests is shown in Table 1.2 which lists the different channel configurations and grating lengths with the corresponding maximal 100% efficient flow rate, Q_{max}, for each case. Q_{max} occurs if no more water can flow through the grating without some water bypassing the drain. Sixty runs were conducted for this study involving three-hundred different tests and flow rates including sub-and super-maximal flow rates. A complete summary of all data taken is given in tabular form in the Appendix.

Figures 1.6 through 1.11 are graphs which illustrate the maximum 100% efficient flow rate, Q_{max}, for each channel configuration plotted against the grating length, L.

Figures 1.12-1.13 represent the relative efficiencies of the different drain openings with respect to the amount of surface area of the grating used to capture water, Q_{max}/L, plotted against the length of the grating, L. The width was constant for all tests, thus the length is directly proportional to the surface area of the grate. Table 1.3 lists the values used to compile these figures.

	GRATING LENGTH				
	45.8 cm 18.0 in.	53.4 cm 21.0 in.	61.0 cm 24.0 in.	68.6 cm 27.0 in.	76.2 cm 30.0 in.
Grade = 4% Back Slope = 1/8:1 Swale Slope = 12:1	0.0110 0.40	0.0150 0.54	0.0200 0.70	0.0240 0.85	0.0350 1.22
Grade = 4% Back Slope = 3:1 Swale Slope = 12:1	0.0110 0.39	0.0150 0.54	0.0190 0.68	0.0240 0.85	0.0250 0.91
Grade = 2% Back Slope = 1/8:1 Swale Slope = 12:1	0.0250 0.91	0.0350 1.25	0.0400 1.42	0.0490 1.75	0.0560 1.98
Grade = 2% Back Slope = 3:1 Swale Slope = 12:1	0.0210 0.74	0.0250 0.88	0.0340 1.20	0.0360 1.27	0.0450 1.58
Grade = 1/2% Back Slope = 1/8:1 Swale Slope = 12:1	0.0420 1.47	0.0490 1.74	0.0500 1.77	0.0520 1.83	0.0590 2.09
Grade = 1/2% Back Slope = 3:1 Swale Slope = 12:1	0.0310 1.09	0.0450 1.61	0.0510 1.80	0.0570 2.03	0.0710 2.52
Grade = 4% Back Slope = 1/8:1 Swale Slope = 48:1	0.0074 0.26	0.0079 0.28	0.0079 0.28	0.0085 0.29	0.0108 0.37
Grade = 4% Back Slope = 3:1 Swale Slope = 48:1	0.0136 0.49	0.0142 0.54	0.0158 0.56	0.0169 0.59	0.0181 0.65
Grade = 2% Back Slope = 1/8:1 Swale Slope = 48:1	0.0085 0.29	0.0108 0.38	0.0110 0.40	0.0119 0.42	0.0125 0.45
Grade = 2% Back Slope = 3:1 Swale Slope = 48:1	0.0057 0.20	0.0062 0.22	0.0096* 0.34	0.0091 0.31	0.0125 0.45
Grade = 1/2% Back Slope = 1/8:1 Swale Slope = 48:1	0.0045 0.16	0.0045 0.17	0.0051 0.18	0.0057 0.20	0.0062 0.22
Grade 1/2% Back Slope = 3:1 Swale Slope = 48:1	0.0068 0.24	0.0074 0.26	0.0096* 0.34	0.0079 0.28	0.0079 0.29

*Faulty Data

Table 1.2 100% Maximum Efficient Flow Rates
(Prototype Values)

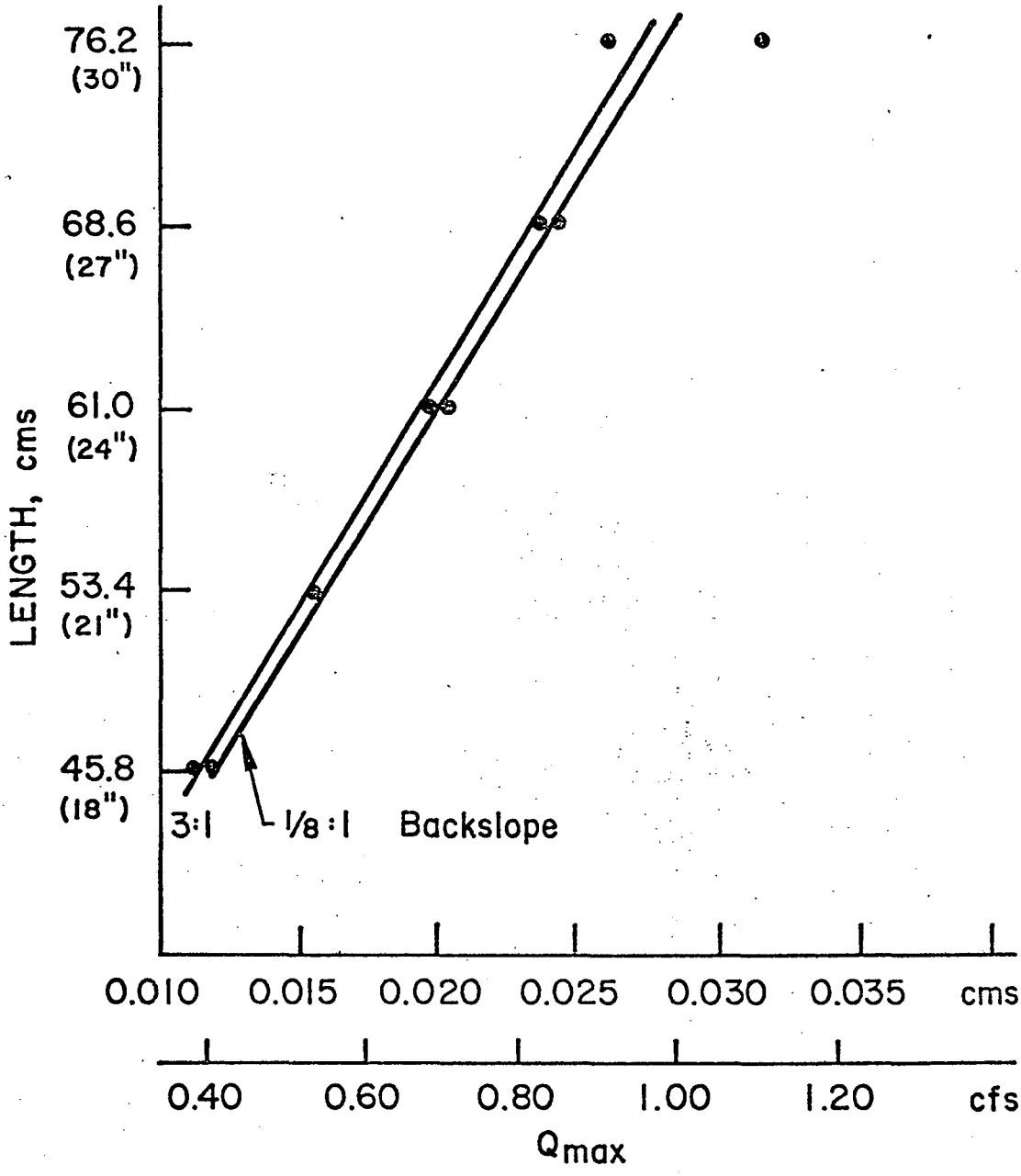

Grade = 4%
Swale = 12:1
Prototype Values

Fig. 1.6: Maximum 100% Efficient Flow vs. Length
(Long. Slope = 4%; Swale = 12:1)

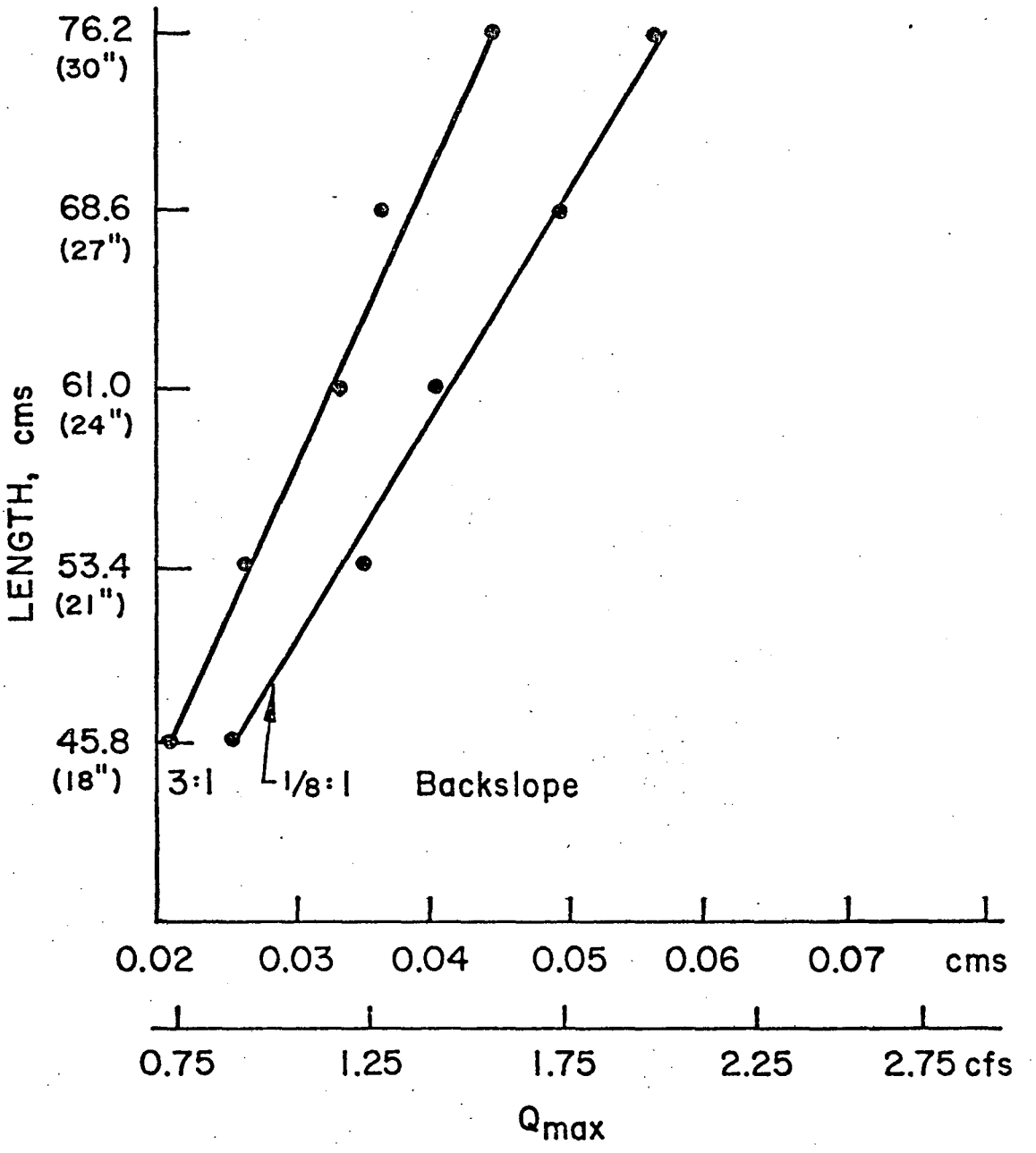

Fig. 1.7: Maximum 100% Efficient Flow Versus Length (Long. Slope = 2%; Swale = 12:1)

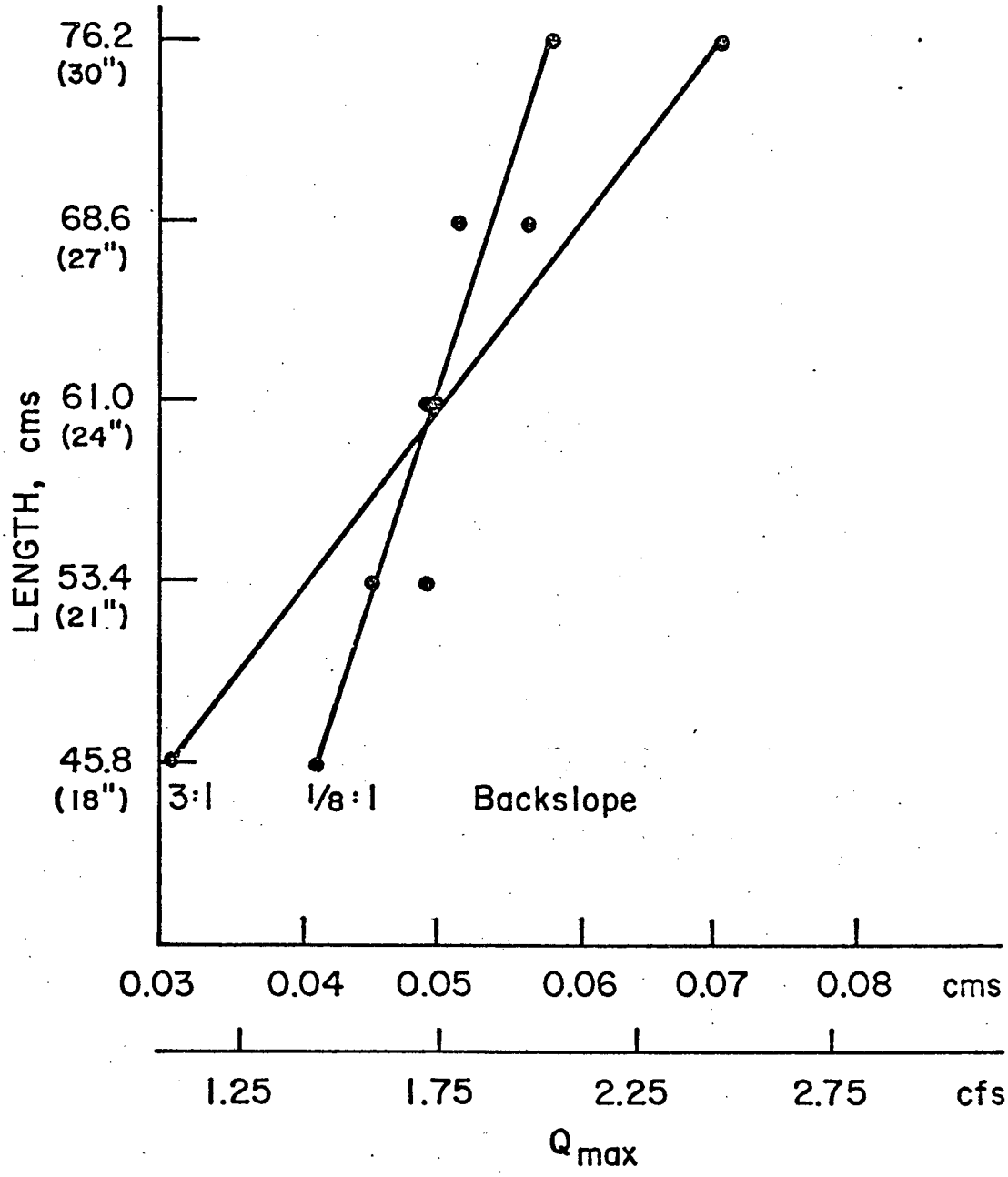

Fig. 1.8: Maximum 100% Efficient Flow Versus Length
(Long. Slope = 1/2%; Swale = 12:1)

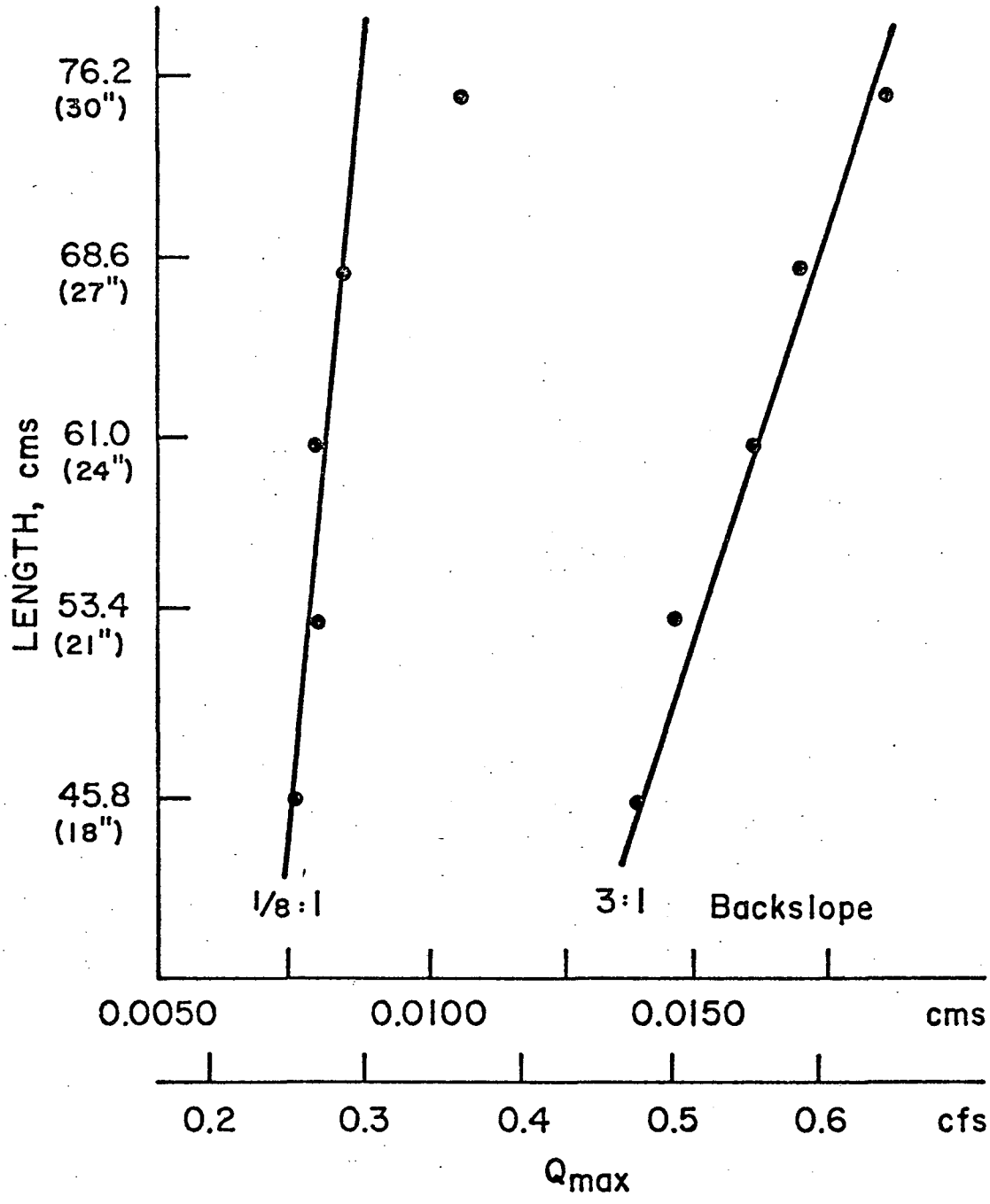

Fig. 1.9: Maximum 100% Efficient Flow Versus Length (Long. Slope = 4%; Swale = 48:1)

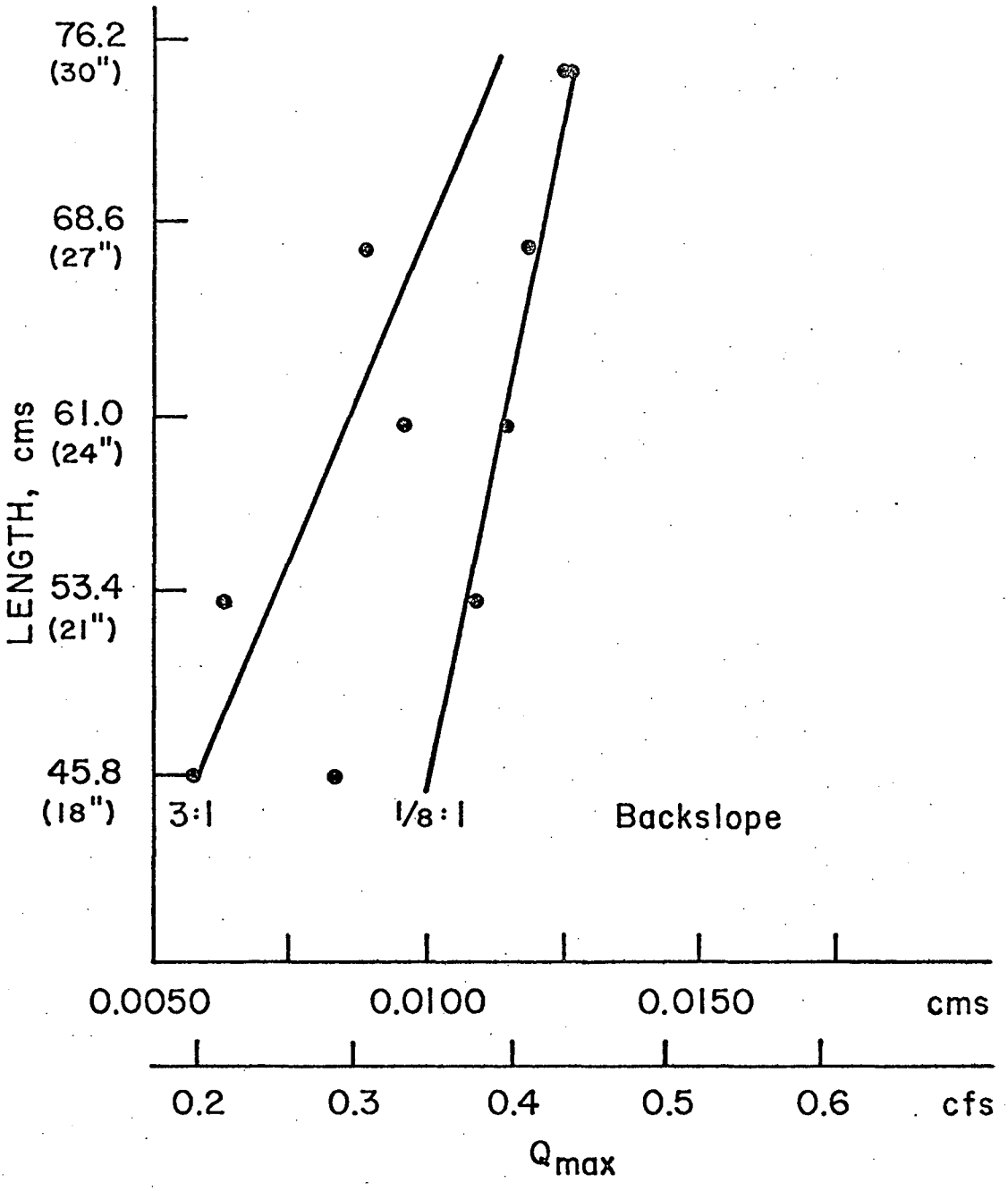

Fig. 1.10: Maximum 100% Efficient Flow Versus Length (Long. Slope = 2%; Swale = 48:1)

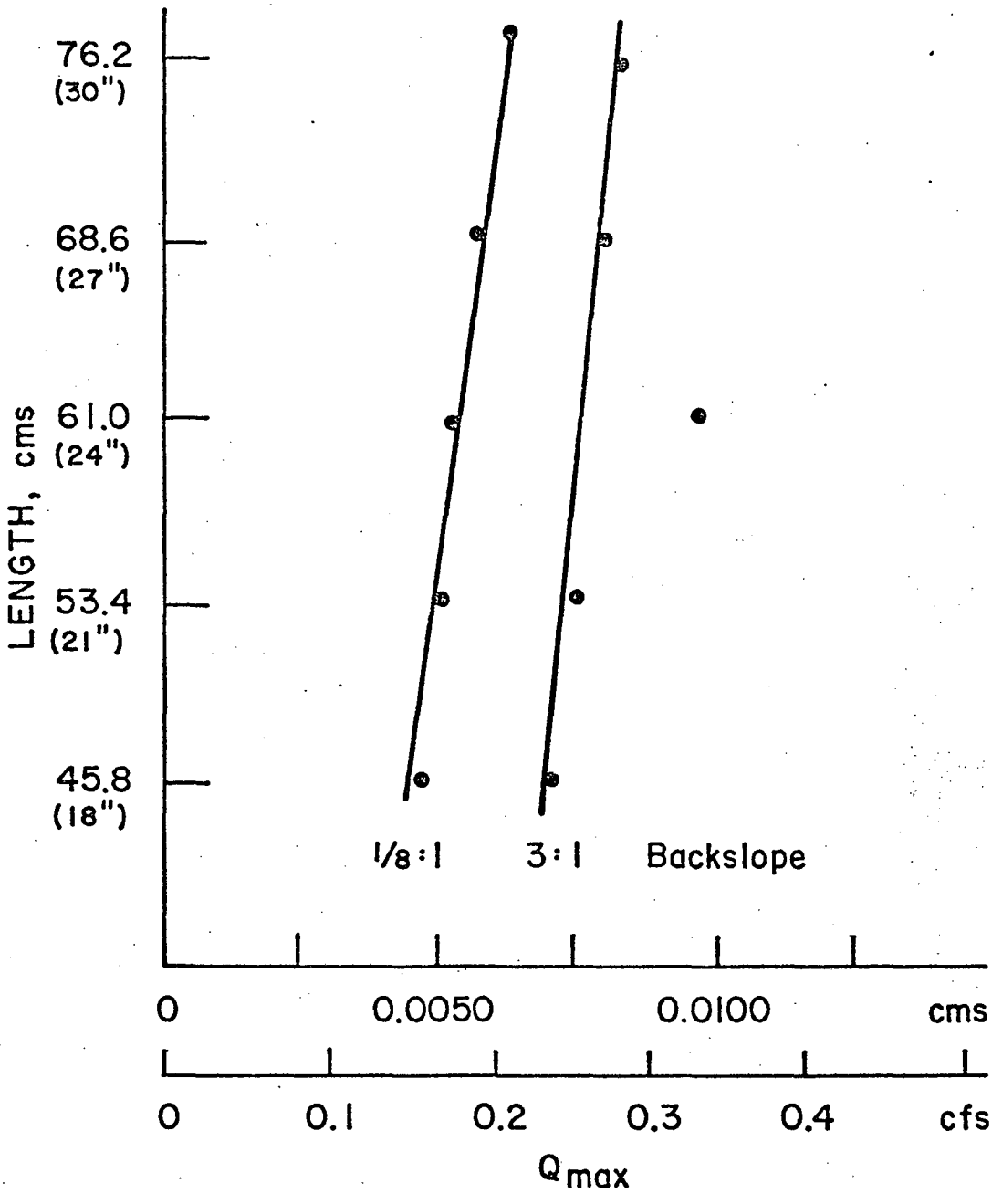

Grade = 1/2 %
Swale = 48 : 1
Prototype Values

Fig. 1.11: Maximum 100% Efficient Flow Versus Length (Long. Slope = 1/2%; Swale = 48:1)

	GRATING LENGTH				
	45.8 cm 18.0 in.	53.4 cm 21.0 in.	61.0 cm 24.0 in.	68.6 cm 27.0 in.	76.2 cm 30.0 in.
Grade = 4% Swale = 12:1 Back = 1/8:1	0.026 0.280	0.029 0.312	0.032 0.344	0.036 0.387	0.042 0.452
Grade = 4% Swale = 12:1 Back = 3:1	0.024 0.258	0.029 0.312	0.030 0.323	0.034 0.366	0.034 0.366
Grade = 2% Swale = 12:1 Back = 1/8:1	0.055 0.592	0.066 0.710	0.067 0.721	0.071 0.764	0.074 0.796
Grade = 2% Swale = 12:1 Back = 3:1	0.046 0.495	0.049 0.527	0.057 0.613	0.052 0.560	0.060 0.646
Grade = 1/2% Swale = 12:1 Back = 1/8:1	0.091 0.979	0.092 0.990	0.083 0.893	0.076 0.818	0.078 0.839
Grade = 1/2% Swale = 12:1 Back = 3:1	0.068 0.732	0.085 0.915	0.084 0.904	0.083 0.893	0.094 1.011
Grade = 4% Swale = 48:1 Back = 1/8:1	0.016 0.172	0.015 0.161	0.013 0.140	0.012 0.129	0.014 0.151
Grade = 4% Swale = 48:1 Back = 3:1	0.030 0.323	0.026 0.280	0.026 0.280	0.025 0.269	0.024 0.258
Grade = 2% Swale = 48:1 Back = 1/8:1	0.019 0.204	0.020 0.215	0.019 0.204	0.017 0.183	0.016 0.172
Grade = 2% Swale = 48:1 Back = 3:1	0.012 0.129	0.011 0.118	0.016 0.172	0.013 0.140	0.016 0.172
Grade = 1/2% Swale = 48:1 Back = 1/8:1	0.010 0.108	0.008 0.086	0.008 0.086	0.008 0.086	0.008 0.086
Grade = 1/2% Swale = 48:1 Back = 3:1	0.015 0.161	0.014 0.151	0.016 0.172	0.012 0.129	0.010 0.108

Table 1.3 Values for Maximum 100% Efficient Flow Rates Divided By Length of Grate, $\frac{Q_{max}}{L}$ cms/m (cfs/ft)

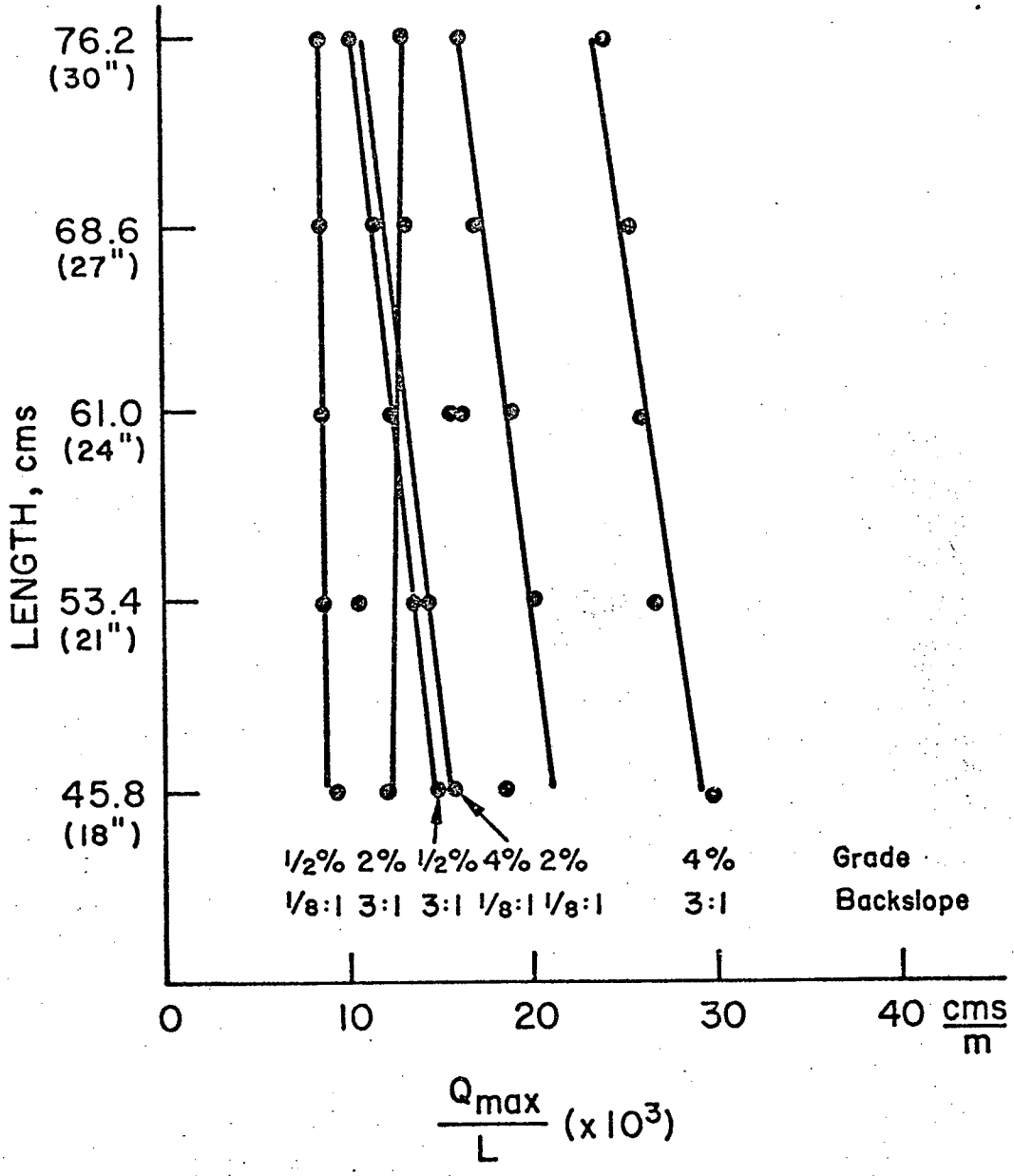

Fig. 1.12: Efficiency (Relative Surface Area Coverage of Grate) Versus Length (Swale = 48:1)

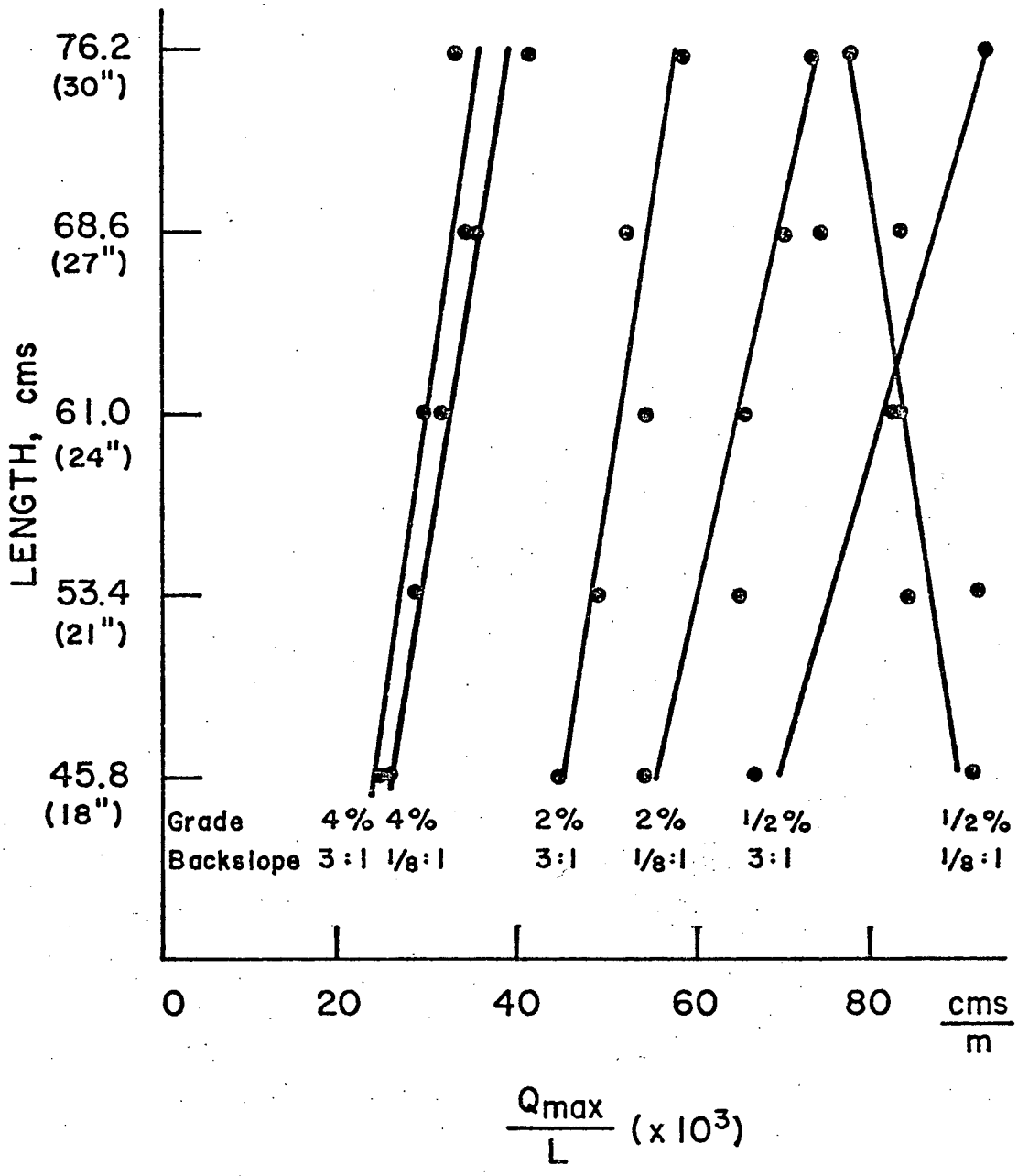

Fig. 1.13: Efficiency (Relative Surface Area Coverage of Grate) Versus Length (Swale = 12:1)

1.5 DISCUSSION

Prototype maximum 100% efficient flow rates ranged from just below 0.0050 cms (0.18 cfs) to just above 0.0700 cms (2.49 cfs), with the gratings in the channels with the 12:1 swale slopes intercepting the most water in most cases. Figures 1.6 to 1.11 show that for all channel configurations, the maximum 100% efficient flow rate, Q_{max}, increases with the length of the grating. This increase in flow capacity is much more pronounced in channels with the steeper (12:1) swale slopes, as displayed by the greater slope of these particular curves.

Figure 1.12 indicates that the grate surface is used more efficiently (more of the grate surface is covered by water) with the shorter gratings than with the longer ones for swale slopes of 48:1. On the other hand, Figure 1.13 displays just the opposite tendency for gratings placed in 12:1 swale slope channels. The longer the grate is, the more efficiently the grate surface is used.

1.6 CONCLUSION

Tests were run for the Pennsylvania Department of Transportation in a model study to determine an optimal length:width ratio of highway drainage inlets for paved channels. The effects of different longitudinal and slide slopes and of different discharges were investigated.

Results show that for all cases, the longest grating tested, 76.2 cm (30.0 in.), had the highest flow capacity for each particular channel configuration. However, the longer inlets did not always utilize their surface area most efficiently. For channels with 48:1 swale slopes, the smallest grating, 45.8 cm (18.0 in.), was consistently the most efficient. Although the plots do not indicate a percentage of surface area convered, for the 48:1 swale slopes, the percentage is very low as indicated by a photographic study. With the 12:1 swale slope channels, the surface coverage efficiency increases with the length of the grating. The percentage of coverage in this case is very high; as in most cases, flow around the inlet occurs at nearly the same time as flow over the inlet (See Fig. 1.14 and Fig. 1.15). Thus, flow enters the inlet through the grate from the swale slope, the back side, and the upstream side, simultaneously.

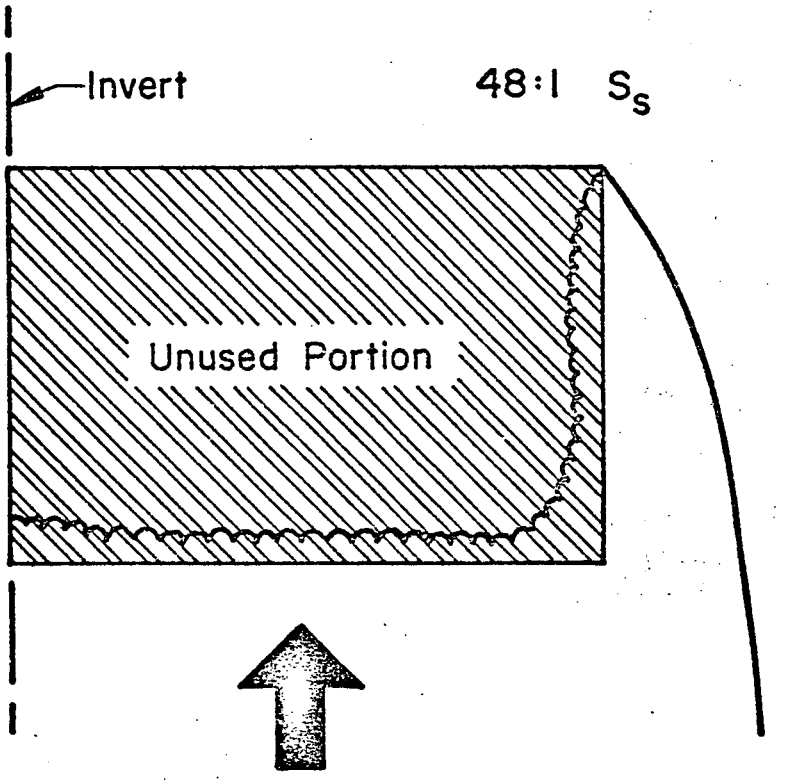

Fig. 1.14: Flow Into Grate with 48:1 Swale Slope

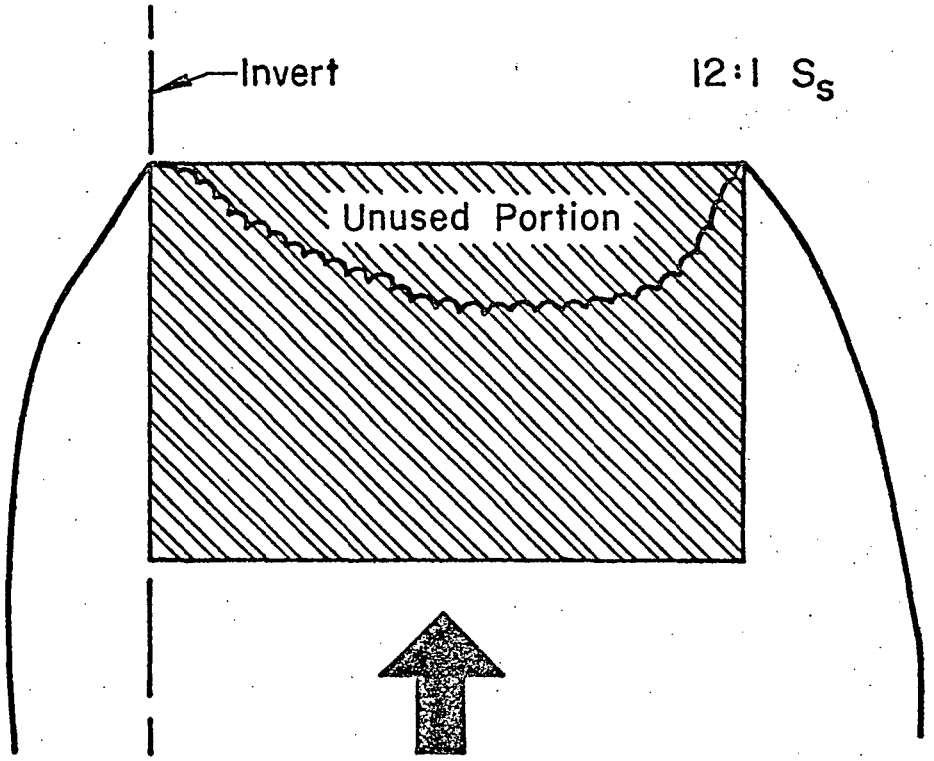

Fig. 1.15: Flow Into Grate with 12:1 Swale Slope

1.7 RECOMMENDATIONS

This study was charged with developing a grating for installation in paved channels along Pennsylvania highways which will be the most efficient in terms of flow capacity and surface area covered.

It is recommended that for channels with 48:1 swale slopes, a short grate, 45.8 cm (18.0 in.) should be used in the field for most efficient results. For the 12:1 swale slope channels, a long grate, 76.2 cm (30.0 in.) should be used.

It is also recommended that wherever possible, a 12:1 swale slope should be utilized in the field. Inlets placed in these channesl intercept upto eight times more water - especially in channels with 1/2% and 2% grades. With the higher capacities available in this case, fewer drains would be necessary and installation costs would be reduced considerably.

2. THEORETICAL ANALYSIS *

2.1 INTRODUCTION

After all the data had been collected and tabulated, it was desirable to establish analytical expressions based upon hydraulic theories which would corroborate with the measured results. First, it was necessary to research past studies related to this inlet study which might yield valuable information. Next, using these studies as a foundation, various theories were modified to fit the situation at hand, as closely as possible, and then comparisons between the measured and calculated results were begun. If the compared values did not resemble each other, reasons for their disparity were sought.

Ultimately, it was hoped that equations could be derived which would predict efficiencies and critical values of depth and flow for given channel and inlet configurations.

2.2 BACKGROUND

Most highway inlet studies concerned themselves, primarily, with finding inlet capacities for a particular situation using field or model data while giving little emphasis to the theoretical aspect of the flow regime. Three studies were very influential, however, in providing a foundation for this analytical work.

* All data and figures pertain to the model for this chapter.

The first two were published reports by Li (1954) and by Wasley (1961). The third study was performed by Dr. Willard A. Murray informally at Lehigh University in the Spring of 1975 using data from past tests conducted at the university. The pertinent information contained in the two reports and Dr. Murray's notes are summarized in the Appendix.

2.3 CALCULATING LI'S "m" FOR THIS GRATING

From trajectory theory, Li calculated that, with no grating in the inlet (a free fall situation), the length of falling flow "L_o" (see Fig. 2.1) was given by:

$$L_o = m(v)\ (\frac{D}{g})^{0.5} \qquad \text{Eq. 2.1 (A1.4)}$$

with "m" equal to $\sqrt{2}$, v equal to the average velocity of the flow, g equal to the gravitational acceleration, and D equal to the depth of flow upstream, which depth is assumed to be constant.

His analysis went on to suggest that this m-value would become larger as part of the inlet was filled in with bars contained in a grating. This also would increase L_o. The m-value would vary depending upon the shape and size of the installed grating.

In this study part of the interest was in obtaining an efficiency equation for flow passing over the drain. In many tests, specifically those with 12:1 swale slopes and with no flow

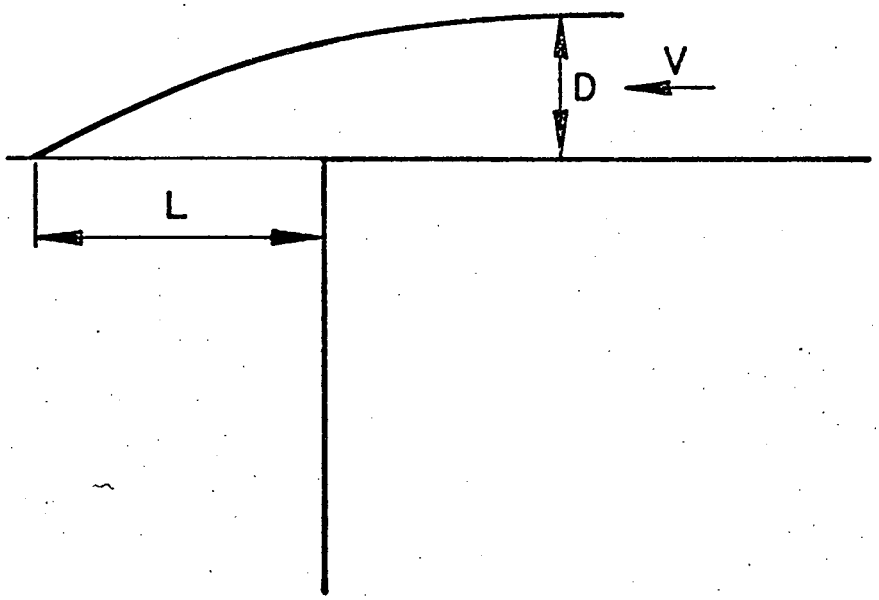

Fig. 2.1: Li's Diagram for "m" Calculation

around the drain, data were available from situations where the flow (Q_{max}) just traversed the grated inlet yet did not overflow the inlet. Thus, L_o equaled the length of the drain L. The depth of flow as well as the velocity calculated from the flow rate were part of the data, so that "m", for the grating used in this study, could be determined. This m-value, in turn, could be used in an efficiency equation, and the length of drain required for certain flow rates could be acquired. (It should be noted that throughout this study, the inlet width was a constant and was not considered in inlet size optimization).

At this point, the most critical problem encountered throughout this analytical work was first realized. That is: 'What is the most reliable, closest fitting expression for velocity of flow that should be used?' The flow is great enough to be turbulent in all situations allowing the assumption that velocity is essentially constant with depth. Velocity is not constant in the direction normal to the flow. The current on the outer extremes of the flow is much slower than that at the invert. Does this disallow average velocity expressions such as Q/A or the Manning Velocity? Wasley used a velocity expression which varied normal to the flow as a function of the square root of the depth.

Finally, it was decided to try all three velocities in arriving at the m-value for the grating. The m-value using $v = Q/A$ was simply equal to:

$$m = \frac{L(A)}{Q} \left(\frac{g}{D}\right)^{1/2} \qquad \text{Eq. 2.2}$$

The m-value for the Manning Velocity was equal to:

$$m = L \left(\frac{g}{D}\right)^{1/2} \frac{n}{1.49} \left(\frac{W}{A}\right)^{2/3} \left(\frac{1}{S_o}\right)1/2 \qquad \text{Eq. 2.3}$$

where n is the Manning roughness coefficient (n = 0.012), W is the wetted perimeter, A is the cross-sectional area of flow and S_o is the grade of the channel.

Wasley's velocity expression (see Appendix) for flow at the invert (y = D) of the channel is:

$$v = \frac{5}{2} \frac{Q}{S_s D^2} \qquad \text{Eq. 2.4 (A2.8)}$$

where Q is the flow, S_s is the inverse of the swale slope, and D the depth at the invert. With this velocity expression, "m" is equal to

$$m = \frac{2}{5} \left(\frac{L}{Q}\right) S_s D^{1.5} g^{0.5} \qquad \text{Eq. 2.5}$$

These expressions along with the appropriate data were fed into a CDC 6400 computer with the results summarized in Table 2.1.

The next step was to solve for "m" using data from situations where the efficiency of the drain was less than 100%. This called for a substitution of Eq. 2.1 into Li's efficiency equation for flow over the drain: (see Appendix)

$$Q_3 = Q \left(1 - L^2/L_o^2\right)^2 \qquad \text{Eq. 2.6 (A1.6)}$$

where Q_3 is the flow over the drain, L is the length of the inlet, and L_o is the computed necessary length of drain to catch all of the on-coming flow.

Substituting for L_o:

$$Q_3 = Q\ (1 - \frac{L^2 g}{m^2 v^2 D})^2 \qquad \text{Eq. 2.7}$$

solving for "m" and using the relationship $Q_3 = Q - Q_1$, where Q_1 is the flow intercepted by the inlet:

$$m = \frac{L^2 g}{v^2 D\ (1.- [1. - Q_1/Q]^{0.5})}^{0.5} \qquad \text{Eq. 2.8}$$

Q/A and Wasley's velocity expressions were then used for v. The results of this work are also contained in Table 2.1.

	Manning v	Average v	Wasley v
< 100% Eff.		4.57	3.21
100% Eff.	8.21	6.08	4.33

Table 2.1 Calculated Values for Li's m value.

The numbers contained in Table 2.1 are prototype values which, in turn, equal those of the model situation as well. The m-value is a function of the length of the drain, the velocity of flow,and the depth of flow. Through model:prototype relationships it is known that $L_p = 2L_m$, $D_p = 2D_m$, and $v_p = 1.41\ v_m$ using the

Froude Similitude (See Table 1.1). Replacing model values with prototype values gives an "m_p":

$$m_p = \frac{2(L_m)}{1.41(v_m)} \quad \frac{g}{2(D_m)} = 1.00\ m_m \qquad \text{Eq. 2.1}$$

Finally, an attempt was made to derive an m-value using the geometry of the drain. Figure 2.2 illustrates the grating set-up in the inlet. The total area of the drain is the drain width times its length. The effective area is the total area minus the area of the bars. For the grating used, $b/b' = 3.00$ and $A/A' = 1.33$ ($\Theta = 45°$). With the width held constant and with the width of flow equal to the width of the drain, an m-value could be found.

$$A' = 0.75A = w \times 0.75L \qquad \text{Eq. 2.9}$$

Since A is the area necessary to catch all of the flow, the length of the drain must be increased until $A = A'$.

$$w \times (0.75L + xL) = A$$

Obviously, x equals 0.25. The added length is the added open space L_s, but an additional bar width L_b must also be added.

$$L_b = \frac{L_s}{3}$$

Thus, the total added length to the inlet to catch all flow must be:

$$\Delta L = 0.25L_s + 0.25\ \frac{L_s}{3},$$

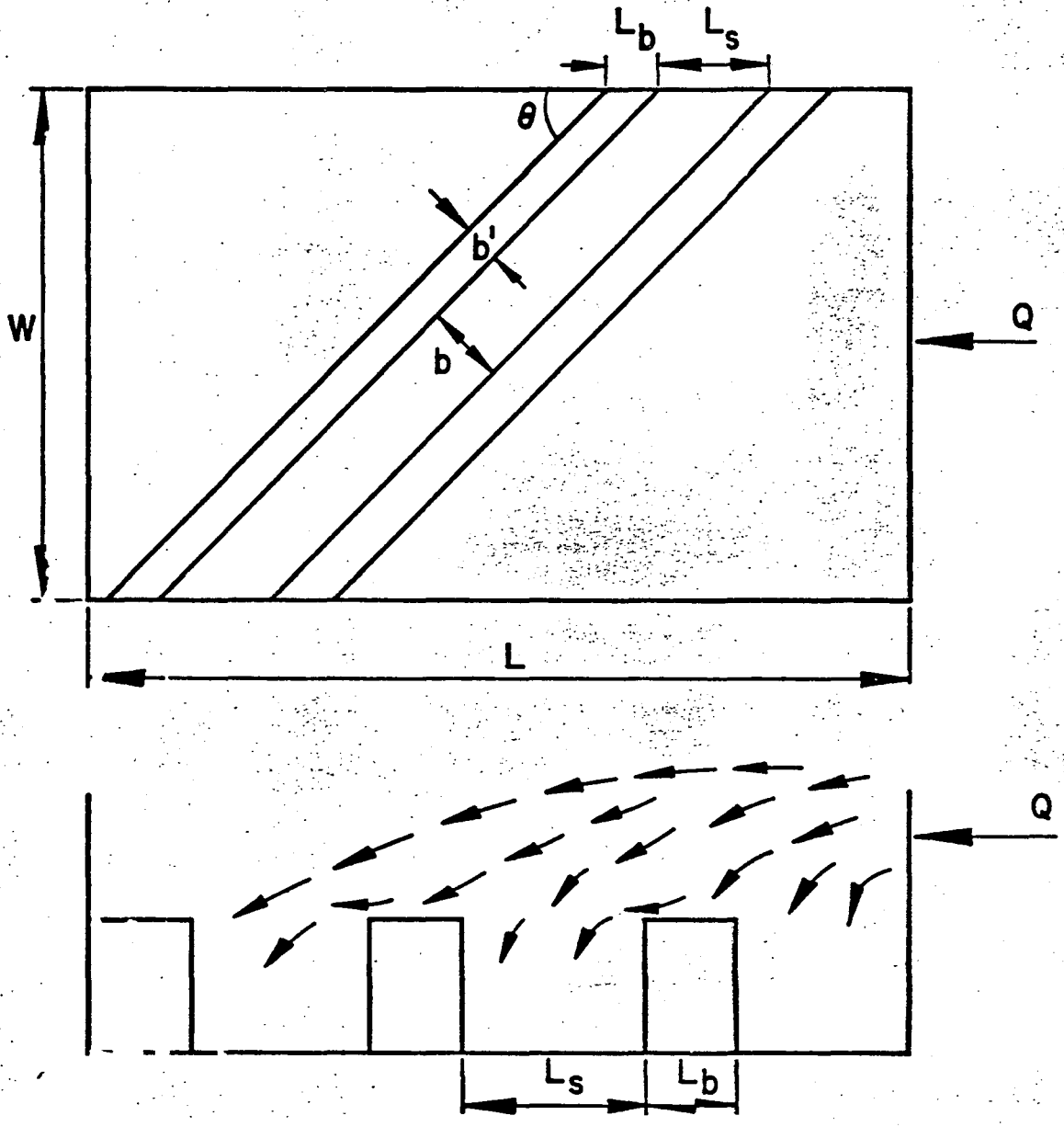

Fig. 2.2: Diagram for Geometric Calculation of "m".

$$\Delta L = 0.333\ L_s$$

Hence, to make A = A', L must be increased by ΔL. It can be assumed that the velocity and depth remain constant so Eq. 2.1 yields:

$$m_g = 1.333\ m_o = 1.89 \qquad \text{Eq. 2.10}$$

where m_g is with the grating in place and m_o is with no grating.

This value is below those calculated from actual tests which indicates that the situation was probably over-simplified. A further analysis was done using momentum theory but, after a series of cancellations, the length relationship surfaced again yielding the same m-value.

2.4 PASSING FLOW AROUND THE DRAIN

Most of the analytical literature cited in this report deals with passing flow around the drain. Murray, Wasley, and Li made attempts at determining efficiency equations which would hold for this inlet situation. The analysis presented begins with a check of Murray's work on efficiency equations and then investigates critical depth relationships with respect to an L' presented by Wasley and to the velocity of flow.

2.4.1 Murray Efficiencies

Dr. Murray derived two expressions for efficiency with respect to flow around the drain. The two expressions, shown below, differ only in the boundaries used to determine the Wasley velocity distribution. The derivations and explanations behind these equations are detailed in sections A3.2.1 and A3.2.2 of the Appendix. His equations are:

$$\frac{Q_2}{Q} = 1 - \frac{\frac{w}{DS_s}}{2} \left[1 - \sqrt{1 - R'}\right]^{2.5} \qquad \text{Eq. 2.11 (A3.7)}$$

where $R' = \dfrac{8gL^2D^3}{25Q^2(1 - \frac{w}{DS_s})^2}$

and

$$\frac{Q_2}{Q} = (1 - \frac{w}{DS_s})^{2.5} \left[1 - R''\right]^{2.5} \qquad \text{Eq. 2.12 (A3.9)}$$

where $R'' = \dfrac{gL^2D^2}{8Q^2(D - \frac{w}{S_s})^2}$

The data obtained in this study from test situations with flow around the drain was inserted into these equations. Eq. 2.11 did not give any worthwhile results, but Eq. 2.12 did provide efficiencies which generally matched those that were measured. Fig. 2.3 shows the plot of Murray's efficiency ($\eta = 1-Q_2/Q$) versus the measured efficiency. Unfortunately, the wide range of scatter pre-

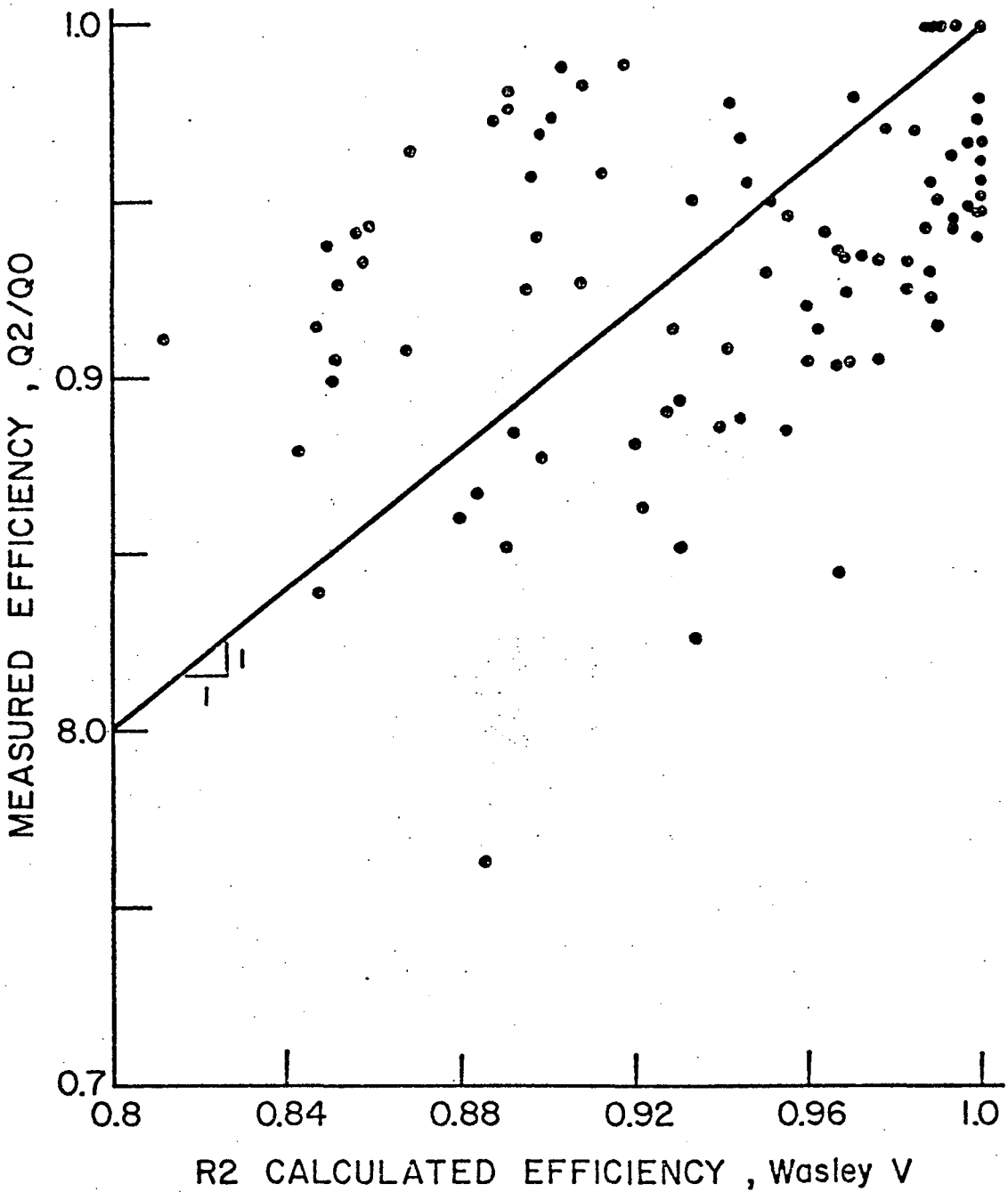

Fig. 2.3: Measured Efficiency Versus Murray's Calculated Efficiency

vents any recommendation of its use for efficiency estimates without further tests, perhaps involving lower efficiencies.

Another simpler expression for efficiency was also tested. Based upon the same equation:

$$\frac{Q_2}{Q} = \frac{D_A}{D}^{2.5} \qquad \text{Eq. 2.13 (A3.4)}$$

as illustrated in Figure 2.4, D_A is the depth of flow at point A and D is the depth at the invert of the channel. Knowing that:

$$D_A = D - \frac{w}{S_s} - \frac{L^2 g}{2v^2 S_s^2} \qquad \text{Eq. 2.14 (A3.5)}$$

and using a simple expression for v ($v = Q/A$), another calculated efficiency was found using the same data. Fig. 2.5 shows the plot of this efficiency versus the measured efficiency and Fig. 2.6 illustrates a comparison between Murray's efficiency and this simplified version. Again, a great deal of scatter is present with less variation appearing in the comparison of the two calculated efficiencies as would be expected due to their similarity of origin.

Since it was determined that more testing was necessary to pursue this line of analysis further, a new approach towards an analytical solution was begun through linear comparisons, that is, by computing theoretical maximum allowable depths and lengths and comparing them to their respective measured values.

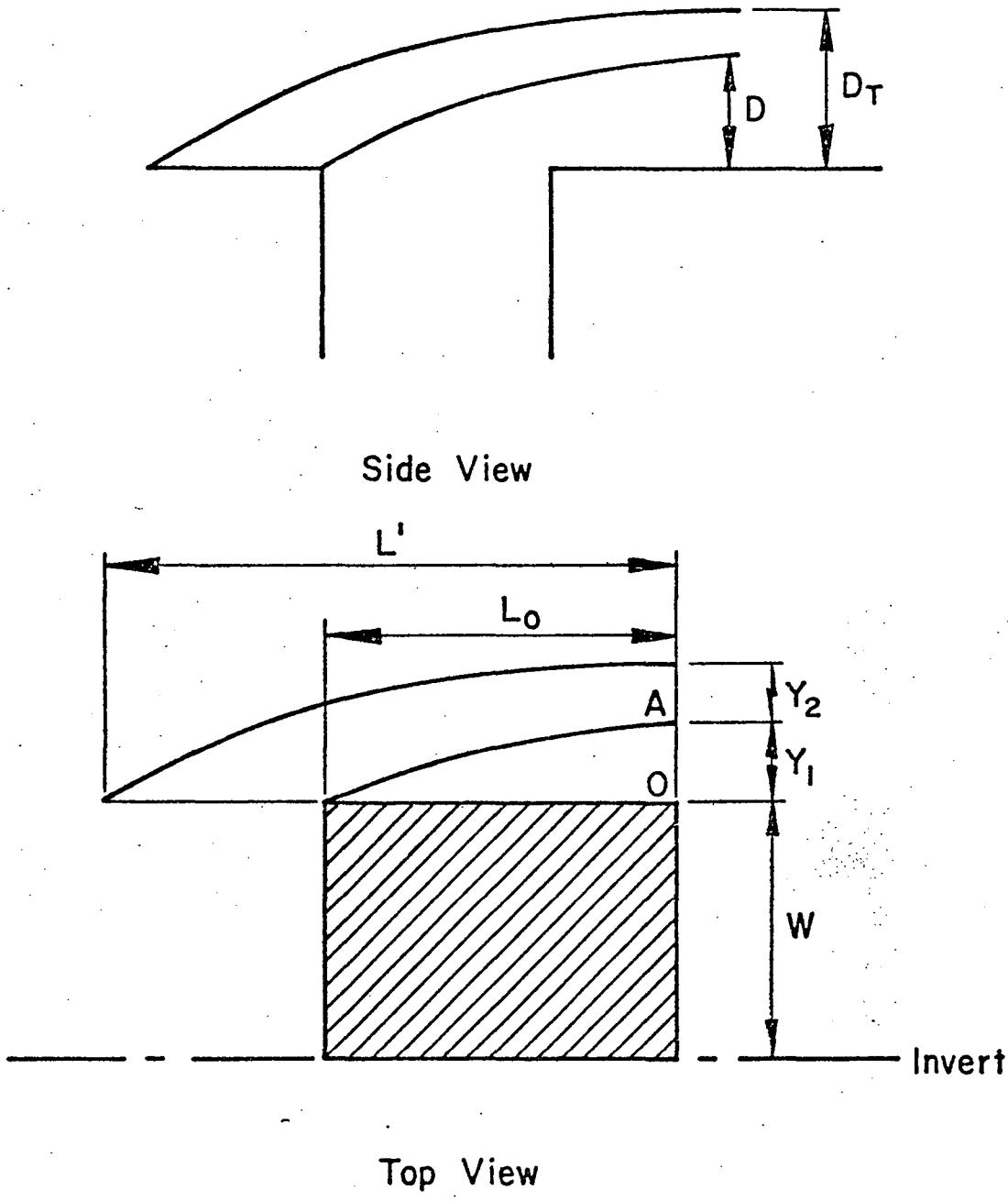

Fig. 2.4: Diagram for Efficiency Calculations

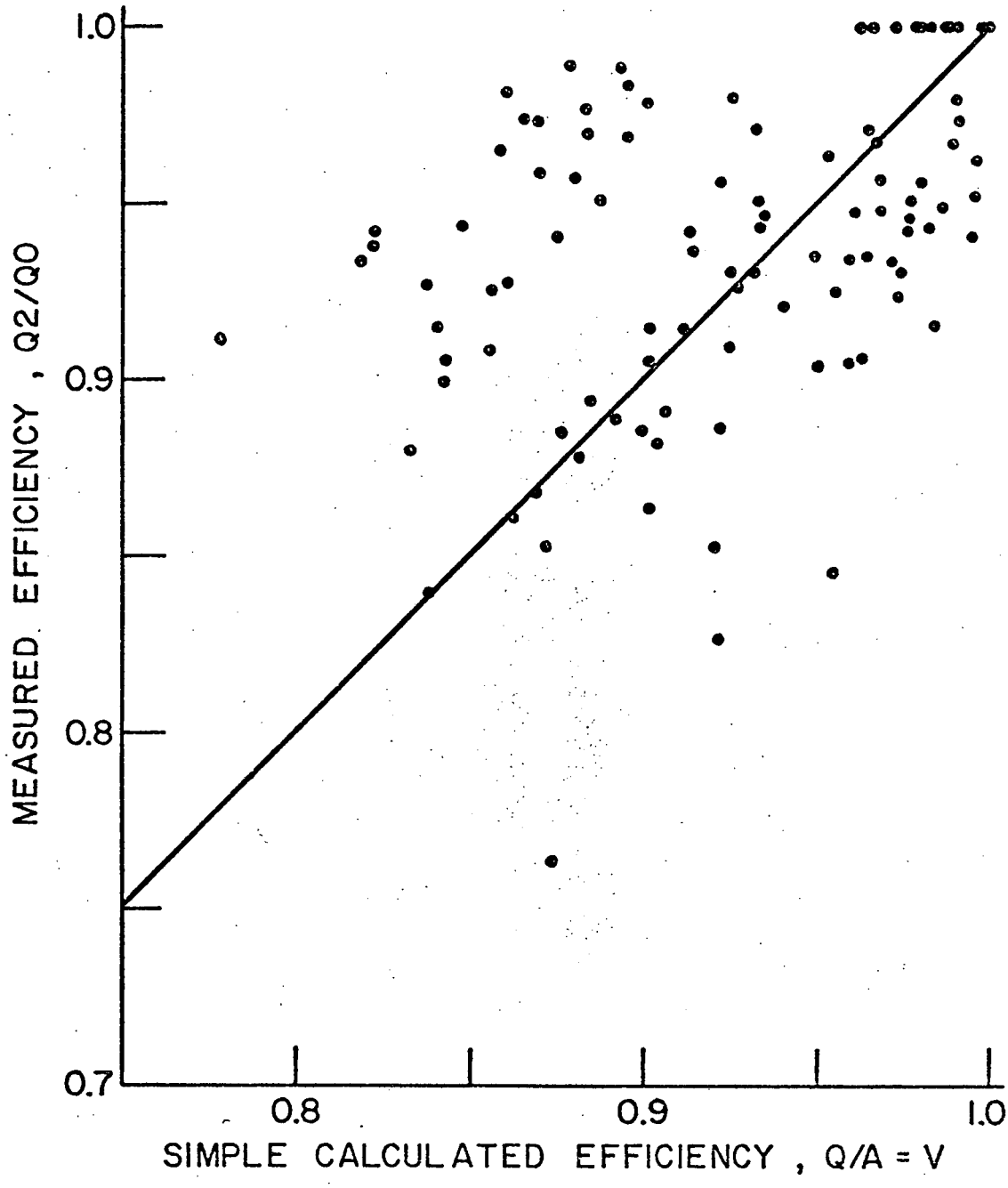

Fig. 2.5: Measured Efficiency Versus Simple Calculated Efficiency

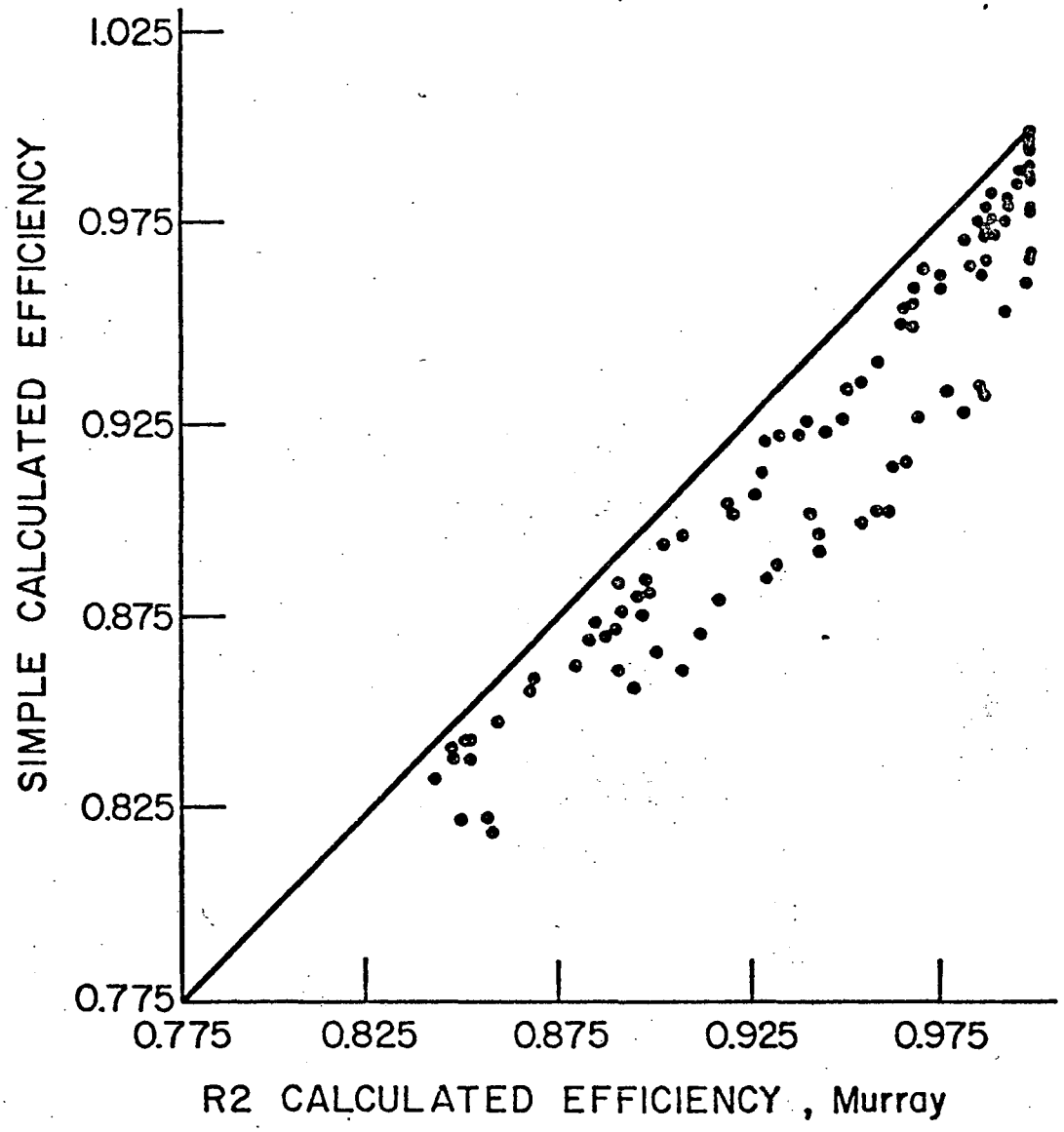

Fig. 2.6: Simple Calculated Efficiency Versus Murray's Calculated Efficiency

2.4.2 Linear Comparisons

Using Fig. 2.4 once again as a guide, the length parameters L' and L, and the depths D and D_o - depths at the invert and at the edge of the inlet respectively - which were utilized in the section, are indicated.

From trajectory theory, it is known that

$$L = v \left(\frac{2y}{g_s}\right)^{0.5} \qquad \text{Eq. 2.15}$$

where $g_s = g/S_s$ for relatively flat swale slopes, the swale slope equals $1/S_s$, and y is the width of flow beyond the edge of the inlet. With a bypassing flow situation, L equals L', and with a maximum critical efficiency situation L equals L_o or the length of the drain. If the two lengths are compared:

$$\frac{L_o}{L'} = \left(\frac{y_1}{y_1 + y_2}\right)^{0.5} \qquad \text{Eq. 2.16}$$

y is equal to the depth D times S_s which allows the conversion of L to a function of depth. If D_o is the depth at point o, D_o will equal the depth at the invert minus the width of the drain, w, divided by S_s. Thus:

$$\frac{L_o}{L'} = \left(\frac{D - \frac{W}{S_s}}{D' - \frac{W}{S_s}}\right)^{0.5} \qquad \text{Eq. 2.17}$$

where D' is the depth at the invert when there is a bypassing flow. D is the value of interest here. If the depth of flow can be calculated for the critical situation (see Eq. 2.18) where $L = L_o$ and all flow is intercepted, then through a flow rate equation, such as $Q = vA$, it would be possible to calculate a maximum allowable flow rate for the drainage system in use.

$$D = (D' - \frac{w}{S_s}) \left(\frac{L_o}{L'}\right)^2 + \frac{w}{S_s} \qquad \text{Eq. 2.18}$$

Data was fed into the computer. Depths derived from the observed maximum flow cases when $L_o = L'$ were inconsistent, but depths calculated using data when $L = L'$ (less than 100% efficient flow) were consistent for each channel and inlet configuration; that is the $D_{crit.}$ calculated from flows 1.5 and 2.0 times the observed maximum flow rate for a channel configuration yielded similar values. Unfortunately not all these calculated critical depths matched those that were measured during the actual testing. (The results of this work are not included here since more refinements were added to the calculations.)

In the original equation (Eq. 2.18), the velocity was assumed to be constant, however, in reality, the velocity of flow is not a constant for different flow rates. Thus it was decided to try to refine Eq. 2.18 by adding a velocity term. Manning's velocity equation was chosen for use in this expression.

$$v_m = \frac{1.49}{n} \left(\frac{A}{W}\right)^{0.667} (S_o)^{0.5} \qquad \text{Eq. 2.19}$$

with n equal to the Manning roughness coefficient (0.012), A, the cross-sectional area, W, the wetted perimeter, and S_o, the longitudinal slope.

$$\frac{v_m}{v_m'} = \frac{A/W}{A/W}^{0.667} = \frac{D}{D'}^{0.5} \qquad \text{Eq. 2.20}$$

now inserting the velocity ratio into Eq. 2.18,

$$\frac{L_o}{L'} = \frac{D}{D'}^{0.667} \left(\frac{D - \frac{W}{S_s}}{D' - \frac{W}{S_s}}\right)^{0.5} \qquad \text{Eq. 2.21}$$

The results of this modification are contained in Table 2.2, along with the measured depth values. Also contained in Table 2.2, are measured flow rates versus calculated flow rates using the Manning equation and this newly acquired depth value. It can be seen that while some values coincide, the majority of them do not.

An attempt was made at this juncture to find a relationship between the measured and calculated depth readings. Since the calculated depths were based upon the L' value, it seemed plausible that if a constant of proportionality or even a variable existed, perhaps it would show up in an L' ratio. The ratio chosen was an L' measured over an L' calculated using Eq. 2.15. This ratio was neither constant for similar channel configurations nor for similar

	Inlet Length						
	22.9cm	26.7cm	30.5cm	34.3cm	38.1cm		
S_s=12:1	9 in.	10.5 in.	12.0 in.	13.5 in.	15.0 in.	S_B	SO
$D_c$meas.(M)	.0162	0.0195	0.0213	0.0238	0.0290	1/8:1	0.04
$D_c$calc.(M)	.0293	0.0326	0.0363	0.0387	0.0445		
$Q_m$meas.(CMS)	.0020	0.0027	0.0035	0.0043	0.0061		
$Q_m$calc.(CMS)	.0050	0.0067	0.0087	0.0105	0.0151		
$D_c$meas.(M)	0.0152	0.0174	0.0213	0.0213	0.0226	3:1	0.04
$D_c$calc.(M)	0.0262	0.0299	0.0323	0.0351	0.0363		
$Q_m$meas.(CMS)	0.0020	0.0027	0.0034	0.0042	0.0045		
$Q_m$calc.(CMS)	0.0048	0.0066	0.0083	0.0102	0.0112		
$D_c$meas.(M)	.0260	0.0320	0.0340	0.0369	0.0384	1/8:1	0.02
$D_c$calc.(M)	.0399	0.0405	0.0408	0.0411	0.0421		
$Q_m$meas.(CMS)	.0045	0.0062	0.0071	0.0088	0.0099		
$Q_m$calc.(CMS)	.0080	0.0082	0.0084	0.0087	0.0092		
$D_c$meas.(M)	0.0238	0.0241	0.0296	0.0296	0.0326	3:1	0.02
$D_c$calc.(M)	0.0381	0.0393	0.0408	0.0411	0.0415		
$Q_m$meas.(CMS)	0.0037	0.0044	0.0060	0.0064	0.0079		
$Q_m$calc.(CMS)	0.0092	0.0099	0.0109	0.0112	0.0114		
$D_c$meas.(M)	0.0466	0.0494	0.0491	0.0500	0.0518	1/8:1	.005
$D_c$calc.(M)	0.0411	0.0421	0.0430	0.0439	0.0448		
$Q_m$meas.(CMS)	0.0074	0.0087	0.0089	0.0092	0.0105		
$Q_m$calc.(CMS)	0.0043	0.0046	0.0048	0.0052	0.0054		
$D_c$meas.(M)	0.0347	0.0408	0.0424	0.0460	0.0500	3:1	.005
$D_c$calc.(M)	0.0421	0.0424	0.0439	0.0451	0.0460		
$Q_m$meas.(CMS)	0.0055	0.0080	0.0090	0.0101	0.0126		
$Q_m$calc.(CMS)	0.0059	0.0061	0.0066	0.0072	0.0076		

Table 2.2 Critical Depths and Maximum Flow Rates (Measured and Calculated)

	Inlet Length						
	22.9cm	26.7cm	30.5cm	34.3cm	38.1cm		
S_s=48:1	9 in.	10.5 in.	12.0 in.	13.5 in.	15.0 in.	S_B	SO
$D_c$meas.(M)	0.0104	0.0101	0.0098	0.0104	0.0101	1/8:1	0.04
$D_c$calc.(M)	0.0098	0.0098	0.0098	0.0098	0.0101		
$Q_m$meas.(CMS)	0.0013	0.0014	0.0014	0.0015	0.0019		
$Q_m$calc.(CMS)	0.0011	0.0011	0.0011	0.0011	0.0012		
$D_c$meas.(M)	0.0122	0.0125	0.0131	0.0137	0.0140	3:1	0.04
$D_c$calc.(M)	0.0101	0.0104	0.0107	0.0104	0.0113		
$Q_m$meas.(CMS)	0.0024	0.0025	0.0028	0.0030	0.0032		
$Q_m$calc.(CMS)	0.0013	0.0013	0.0014	0.0014	0.0017		
$D_c$meas.(M)	0.0094	0.0098	0.0110	0.0125	0.0125	1/8:1	0.02
$D_c$calc.(M)	0.0098	0.0098	0.0098	0.0104	0.0104		
$Q_m$meas.(CMS)	0.0015	0.0019	0.0020	0.0021	0.0022		
$Q_m$calc.(CMS)	0.0008	0.0008	0.0008	0.0009	0.0009		
$D_c$meas.(M)	0.0104	0.0088	0.0104	0.0098	0.0140	3:1	0.02
$D_c$calc.(M)	0.0098	0.0098	0.0101	0.0101	0.0104		
$Q_m$meas.(CMS)	0.0010	0.0011	0.0017	0.0016	0.0022		
$Q_m$calc.(CMS)	0.0008	0.0008	0.0009	0.0009	0.0010		
$D_c$meas.(M)	0.0131	0.0140	0.0137	0.0137	0.0146	1/8:1	.005
$D_c$calc.(M)	0.0119	0.0119	0.0119	0.0116	0.0125		
$Q_m$meas.(CMS)	0.0008	0.0008	0.0009	0.0010	0.0011		
$Q_m$calc.(CMS)	0.0007	0.0007	0.0006	0.0006	0.0007		
$D_c$meas.(M)	0.0134	0.0137	0.0149	0.0140	0.0140	3:1	.005
$D_c$calc.(M)	0.0122	0.0125	0.0134	0.0131	0.0137		
$Q_m$meas.(CMS)	0.0012	0.0013	0.0017	0.0014	0.0014		
$Q_m$calc.(CMS)	0.0007	0.0008	0.0009	0.0009	0.0010		

Table 2.2 (Continued)

flow rates. No relationship was readily discernible.

The question now arose: if, given an initial calculated critical depth, say at L = 22.9 cm (9.0 in.) can we derive a critical depth at L = 26.7 cm (10.5 in.) just by inserting the two lengths into Eq. 2.21. If so, we can then compute a Q_{max} from the new D_c using the Manning equation and compare it to the measured values for Q_{max}. Table 2.3 gives these computed and measured Q_{max} values. The corresponding values in most cases are not in close relationship to one another.

Similar work was done comparing critical depths for backslope variations with all other factors held constant. Theory indicates that situations with back slopes of 3:1 should have higher critical depths and higher corresponding flow rates than channels with the 1/8:1 back slopes. The equation used for this comparison was derived from two flow rate ratios. The first was a comparison of two Manning equations (Eq. 2.19) which reduced to:

$$\frac{Q_{3:1}}{Q_{1/8:1}} = \frac{D_{3:1}}{D_{1/8:1}} \times K^{8/3} \qquad \text{Eq. 2.21}$$

K is equal to 0.9358 for 48:1 swale slopes and 0.7726 for 12:1 swale slopes. The second flow rate ratio is based upon, first Eq. 2.15:

$$\frac{L_{3:1}}{L_{1/8:1}} = \frac{V_{3:1}}{V_{1/8:1}} \quad \frac{D_{3:1} - \frac{W}{S_s}}{D_{1/8:1} - \frac{W}{S_s}}^{0.5} \qquad \text{Eq. 2.22}$$

	LENGTH OF INLET					
	22.9cm	26.7cm	30.5cm	34.3cm	38.1cm	
S_s=48:1	9"	10.5"	12"	13.5"	15"	
Qmeas.	0.0013	0.0014	0.0014	0.0015	0.0019	SO=0.04
Qcalc.	0.0013	0.0013	0.0014	0.0014	0.0015	S_B=1/8:1
Qmeas.	0.0024	0.0025	0.0028	0.0030	0.0032	SO=0.04
Qcalc.	0.0024	0.0027	0.0031	0.0036	0.0040	S_B=3:1
Qmeas.	0.0015	0.0019	0.0020	0.0021	0.0022	SO=0.02
Qcalc.	0.0011	0.0012	0.0012	0.0013	0.0014	S_B=1/8:1
Qmeas.	0.0010	0.0010	0.0017	0.0016	0.0022	SO=0.02
Qcalc.	0.0018	0.0021	0.0024	0.0027	0.0031	S_B=3:1
Qmeas.	0.0008	0.0008	0.0009	0.0010	0.0011	SO=0.005
Qcalc.	0.0008	0.0009	0.0010	0.0012	0.0013	S_B=1/8:1
Qmeas.	0.0012	0.0013	0.0017	0.0014	0.0014	SO=0.005
Qcalc.	0.0012	0.0015	0.0018	0.0021	0.0024	S_B=3:1
S_s=12:1						
Qmeas.	0.0074	0.0087	0.0089	0.0092	0.0105	SO=0.005
Qcalc.	0.0076	0.0088	0.0101	0.0115	0.0131	S_B=1/8:1
Qmeas.	0.0055	0.0080	0.0090	0.0101	0.0126	SO=0.005
Qcalc.	0.0071	0.0077	0.0083	0.0090	0.0098	S_B=3:1

All Readings in M^3/sec.

Table 2.3: Measured Maximum 100% Efficient Flow Rates and Calculated Maximum 100% Efficient Flow Rates Based Upon Calculated Critical Depths. (Flow Around)

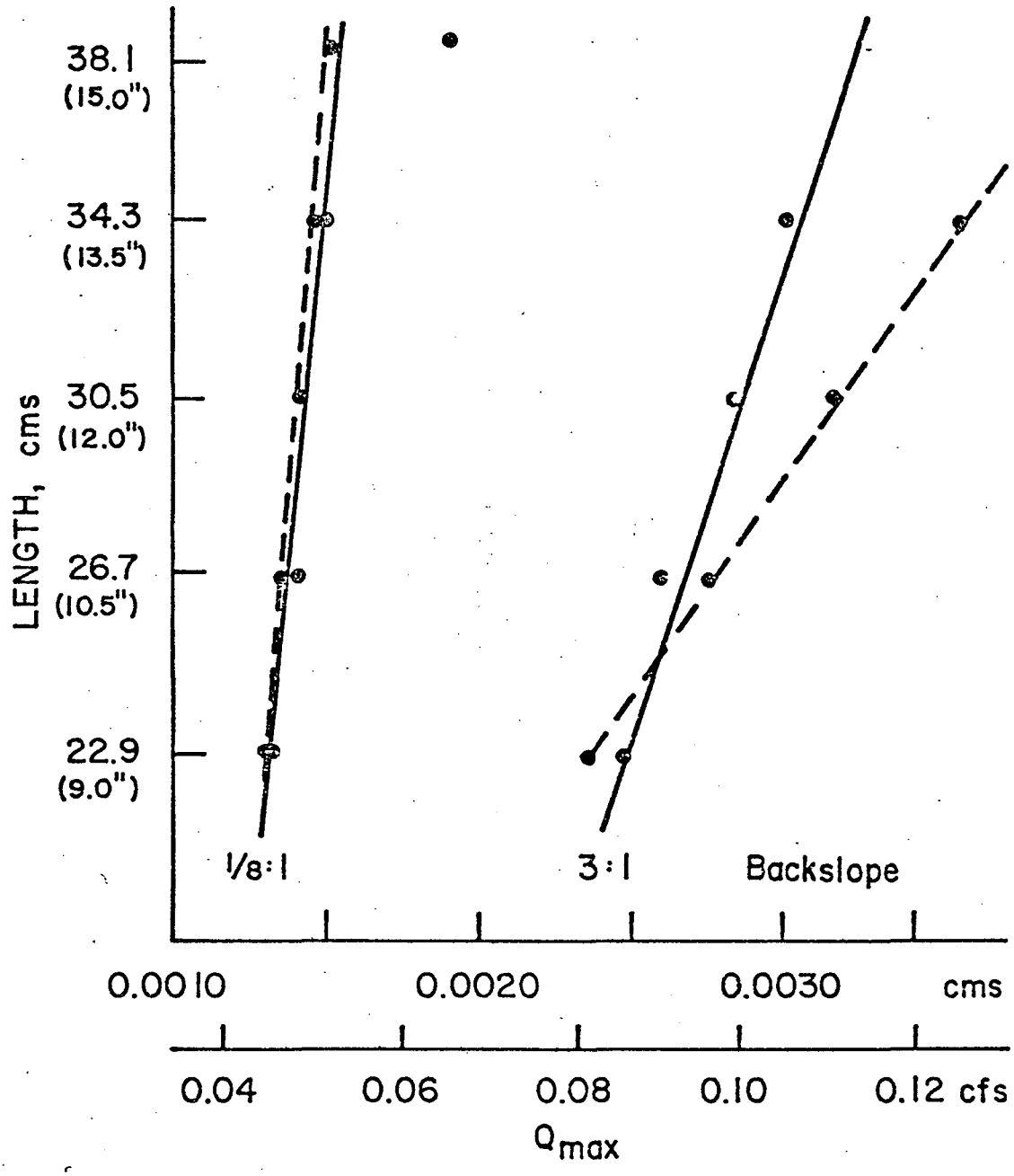

Fig. 2.7: Measured and Calculated Q_{max} Versus Length (Long. Slope = 4%; Swale = 48:1)

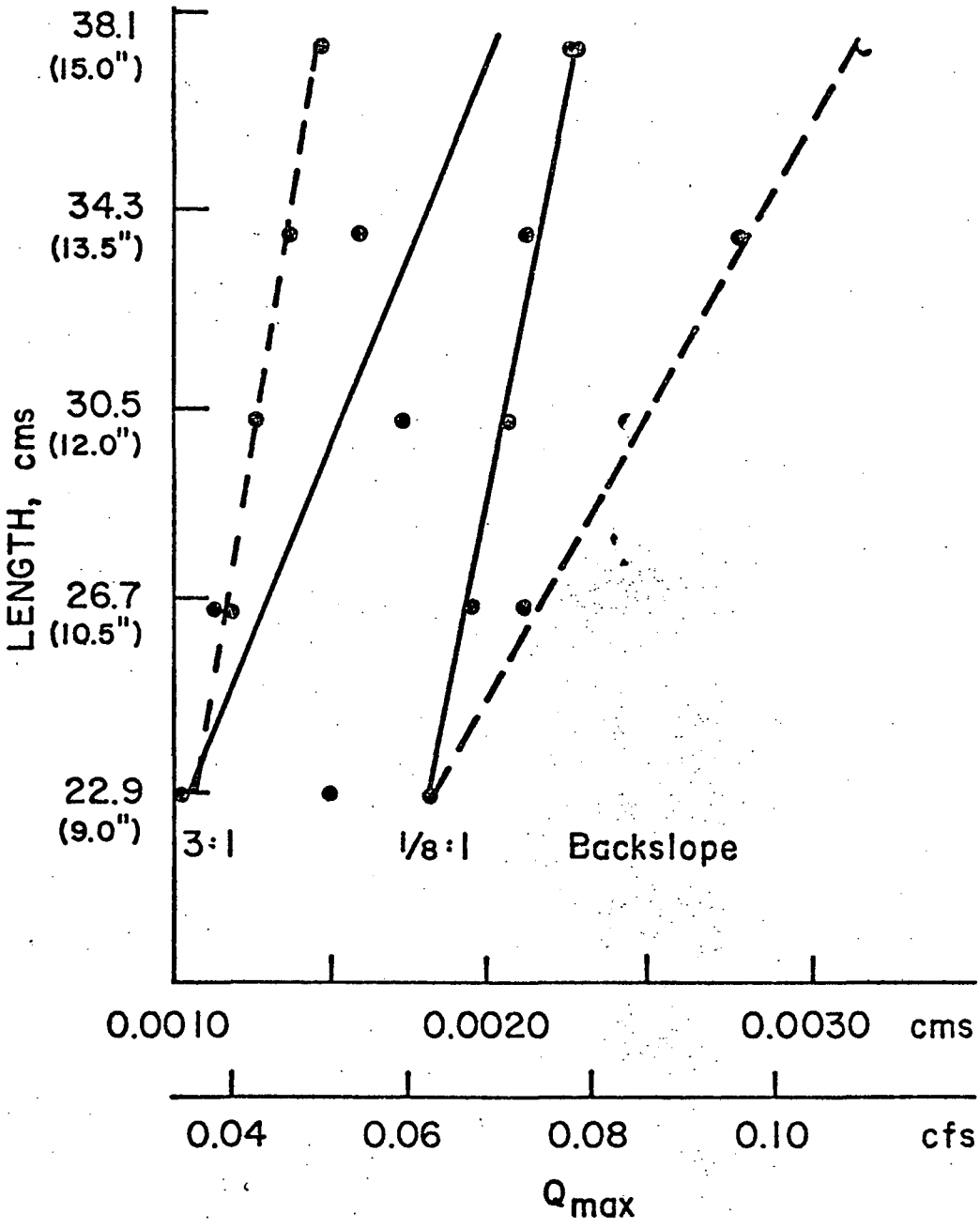

Fig. 2.8: Measured and Calculated Q_{max} Versus Length (Long. Slope = 2%; Swale = 48:1)

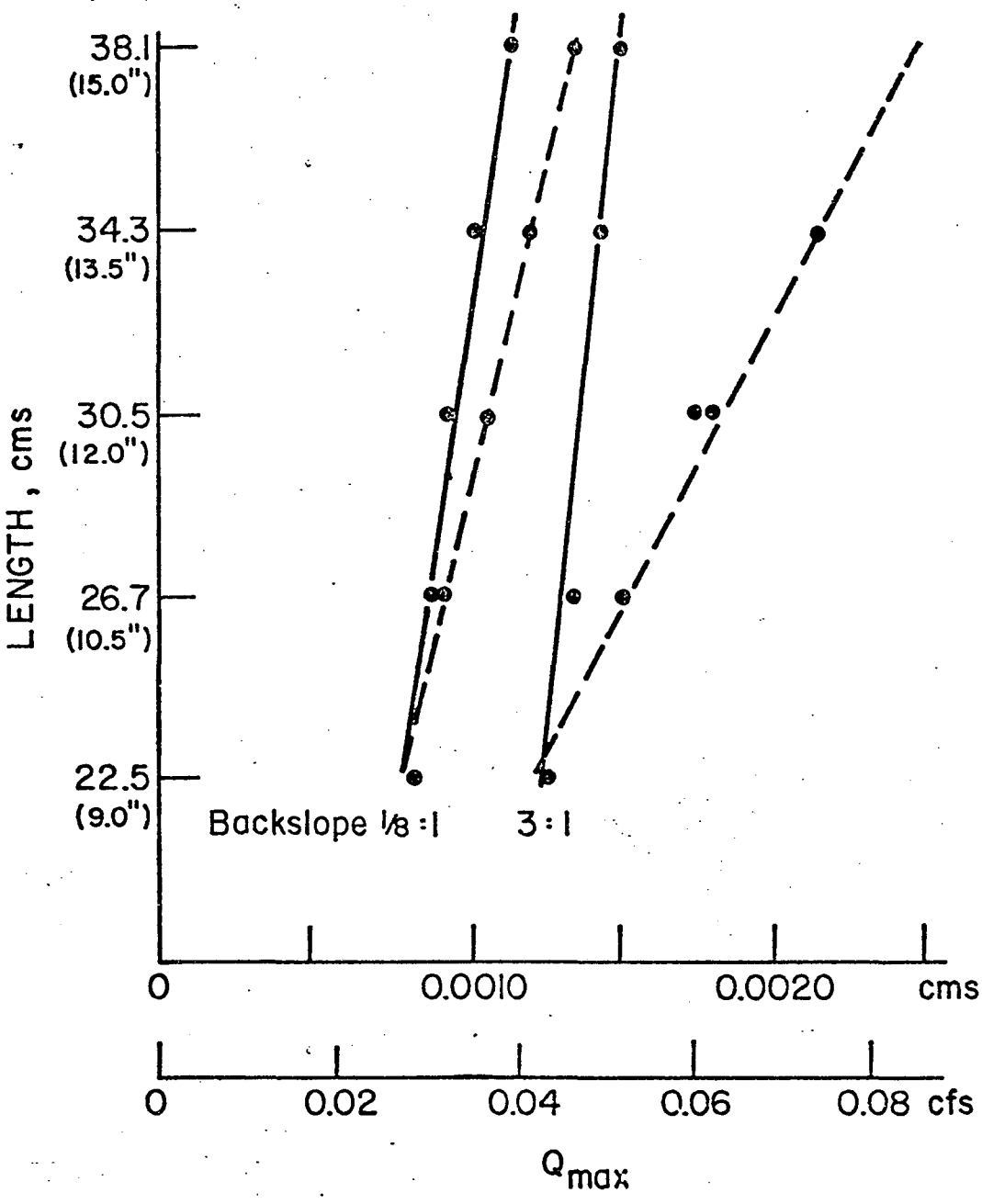

Fig. 2.9: Measured and Calculated Q_{max} Versus Length (Long. Slope = 1/2%; Swale = 48:1)

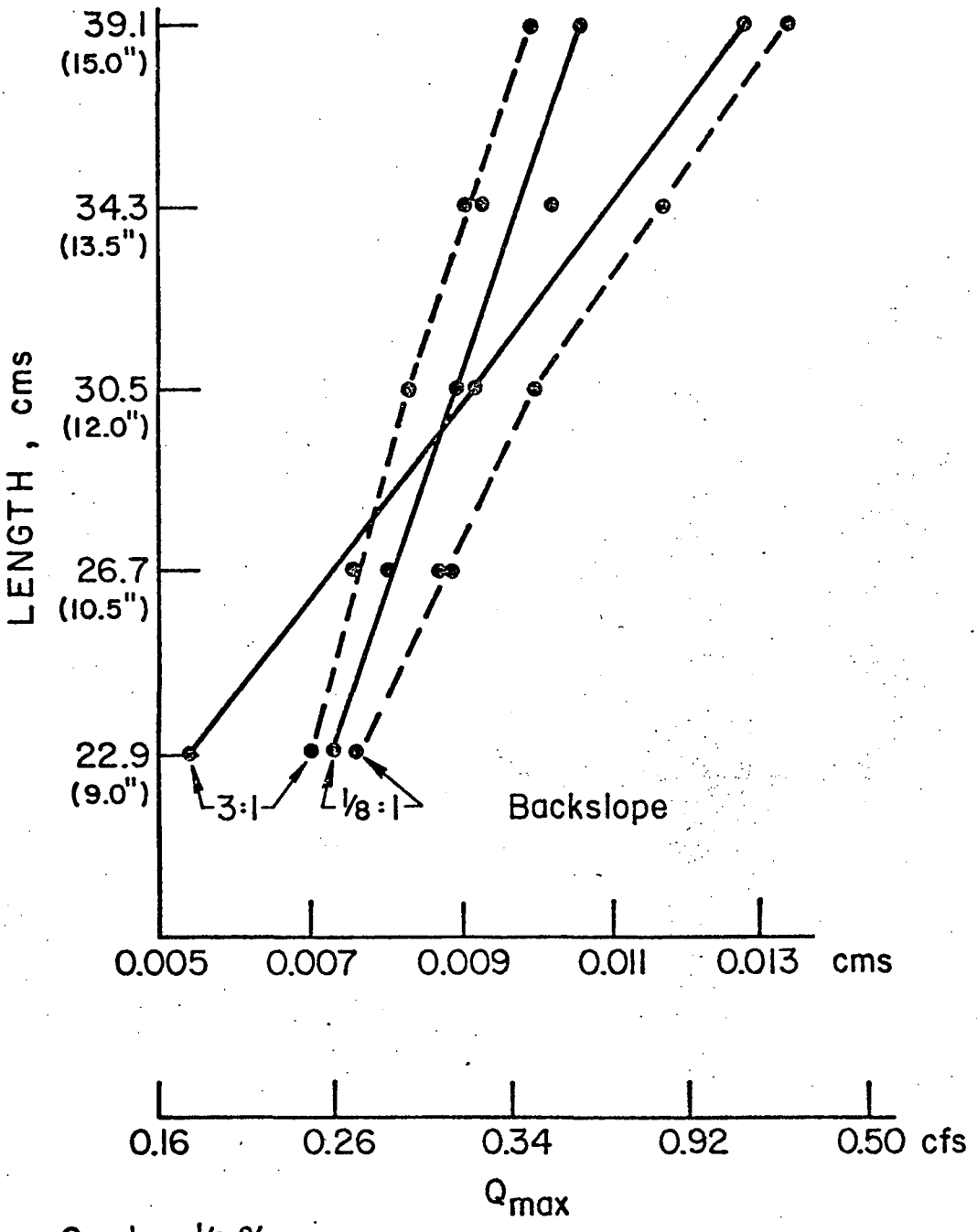

Fig. 2.10: Measured and Calculated Q_{max} Versus Length (Long. Slope = 1/2%; Swale = 12:1)

and upon the Wasley velocity expression. (Eq. 2.4)

$$\frac{V_{3:1}}{V_{1/8:1}} = \frac{Q_{3:1}}{Q_{1/8:1}} \quad \frac{D_{3:1} - \frac{w}{S_s}}{D_{1/8:1} - \frac{w}{S_s}}^{0.5} \quad \frac{D_{1/8:1}}{D_{3:1}}^{2.5} \qquad \text{Eq. 2.23}$$

combining equations 2.21, 2.22, and 2.23:

$$D_{3:1} = \frac{D_{1/8:1} - \frac{w}{S_s}}{(K)^{2.667}} \quad \frac{D_{1/8:1}}{D_{3:1}}^{1.0667} + \frac{w}{S_s} \qquad \text{Eq. 2.24}$$

Table 2.4 gives the calculated and measured values for the two backslope situations converted to flow rates by the Manning equation. Figures 1.6 to 1.11 and Table 2.4 show that although theory indicates that 3:1 backslopes should give higher values in all cases, this was not the case. The 48:1 S_s tests run on 0.5 and 4 percent longitudinal slopes agreed with the theory but the 2 percent longitudinal slope tests indicated that the 1/8:1 S_B (backslope inverse) yielded higher critical depths and flow rates. No explanation for this relationship was found. However, for the 12:1 S_s tests, all tests showed that the 1/8:1 S_B had higher critical values than the 3:15 S_B. Reasons for this phenomenon will be discussed in Section 2.8.

	Q(1/8:1)	Q(3:1)	
*			
Calc 1	0.0013	0.0024	SO=0.04
Calc 2		0.0014	S_s=48:1
Calc 1	0.0010	0.0018	SO=0.02
Calc 2		0.0011	S_s=48:1
Calc 1	0.0008	0.0012	SO=0.005
Calc 2		0.0009	S_s=48:1
Calc 1	0.0076	0.0071	SO=0.005
Calc 2		0.0140	S_s=12:1

Readings in M^3/sec L=22.9cm(9")

*All Calc 1 are calculated flows found for Table 2.3

Table 2.4 Comparison Between Calculated Flow Relationship for 3:1 and 1/8:1 Backslopes from Computed Values with Calculated Flow from Theory for 3:1 Backslope.

2.5 PASSING FLOW OVER THE DRAIN

Very little analytical work has been done on passing flow over the drain. The only attempt made as far as the author knows was by Li. His work is contained in the Appendix. He devised an efficiency equation based upon overflow which was checked using the pertinent data from this study. The results were not satisfactory. Also a separate analysis was made using a calculated critical depth as was done with flow around the drain.

Li's efficiency equation:

$$\frac{Q_3}{Q} = 1 - \frac{L^2}{L'^2}^2 \qquad \text{Eq. 2.25 (A1.6)}$$

was modified slightly by adding the relationship:

$$\frac{L}{L'}^2 = \frac{D}{D'} \qquad \text{Eq. 2.26 (A1.1)}$$

and $Q_3 = Q - Q_1$ (Q_1 is intercepted flow), to get:

$$D = D' \left[1. - \frac{Q - QI}{Q}\right]^2 \qquad \text{Eq. 2.27}$$

Placing the data directly into this equation did not yield satisfactory results. It was then decided to put D' in terms of Q by using the Manning equation in a similar way to that used in the flow around situation.

$$Q = \frac{1.49}{n} \frac{(A)^{1.667}}{(W)^{0.667}} (S_o)^{0.5} \qquad \text{Eq. 2.28}$$

where $$A = 0.5\ [S_s + S_B]\ D^2$$

and $$W = (S_B^{\ 2} + 1)^{0.5} + (S_s^{\ 2} + 1)^{0.5}$$

thus:

$$D' = \frac{Q_n}{1.49} \frac{[(S_B^{\ 2} + 1)^{0.5} + (S_s^{\ 2} + 1)^{0.5}]^{0.667}}{[1.49\ [0.5\ [S_s + S_B]]^{1.667} (S_o)^{0.5}}^{0.375}$$

Eq. 2.29

which was inserted into Eq. 2.27. S_B are the inverse of the back and swale slopes respectively.

Inserting the pertinent data (12:1 S_s only) gave consistent results; however, a constant factor had to be added to make the results conform to the measured results. Eq. 2.27 now reads

$$D_{crit.} = Z\ D'\ 1. - \frac{Q-QI}{Q}^{\ 2} \qquad \text{Eq. 2.27}$$

Z was found consistently to be 0.667 for all data of 12:1 S_s when Eq. 2.29 was used for D'. 48:1 S_s data were not here because flow did not go over the inlet with that configuration.

Fig. 2.11, 2.12, 2.13 present the calculated and measured depths from these tests.

2.6 CRITICAL DEPTHS FOR FLOW-OVER VERSUS FLOW-AROUND SITUATIONS

2.6.1 Theory

A comparison of flow around and flow over the inlet, and measured critical depths is best displayed in graphic form. (See Figs. 2.11-2.22) The boundary between flow-over and flow-around situations is illustrated when the S_s = 12.1 and the longitudinal slope is 2 percent. (Fig. 2.13, 2.14) The flow-over graphs are presented with and without the addition of the Z - factor, as discussed in Section 2.5, to illustrate the validity of the calculated Z - value of 0.667. The terms, flow-over and flow-around, indicate how flow will bypass the inlet after the critical depth is reached.

2.6.2 Data

An effort was made to derive a pair of dimensionless numbers which could be used to differentiate between flow situations over and around the inlet. These numbers would be placed upon coordinate axes and the data from the tests would be placed in these dimensionless numbers and plotted in the coordinate system.

Many combinations were tried. The Froude number was thought to be significant because of its importance with channel flow. This, unfortunately, was not the case. The best parameter found was a simple width of flow parameter:

$$Y = \frac{BS(S_s + S_B)}{L} \qquad \text{Eq. 2.28}$$

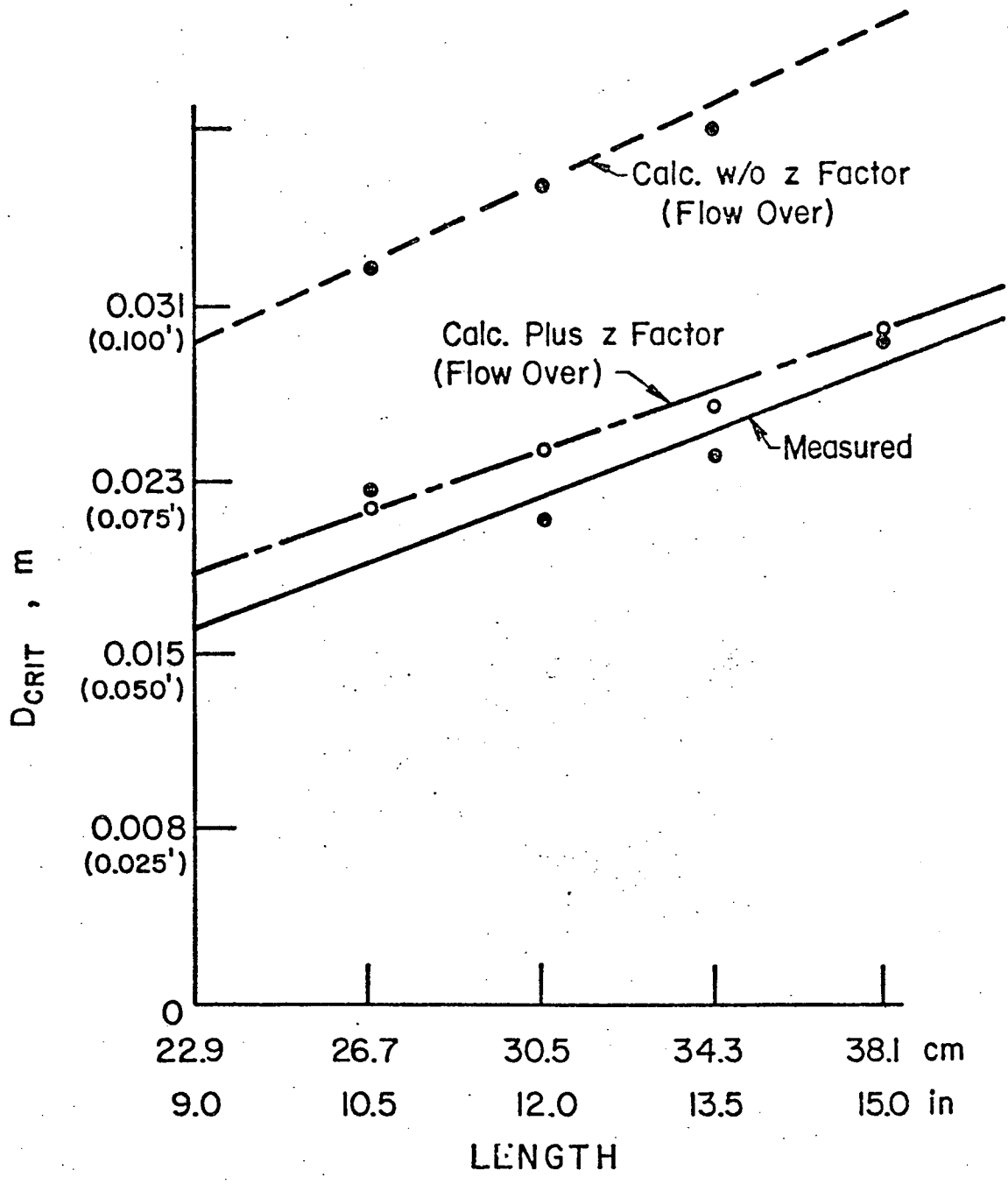

S_S = 12 : 1

S_B = 1/2 : 1

SO = 0.04

Fig. 2.11: Measured and Calculated D_{crit} Versus Length (Long. Slope = 4%; Swale = 12:1; Back.= 1/8:1)

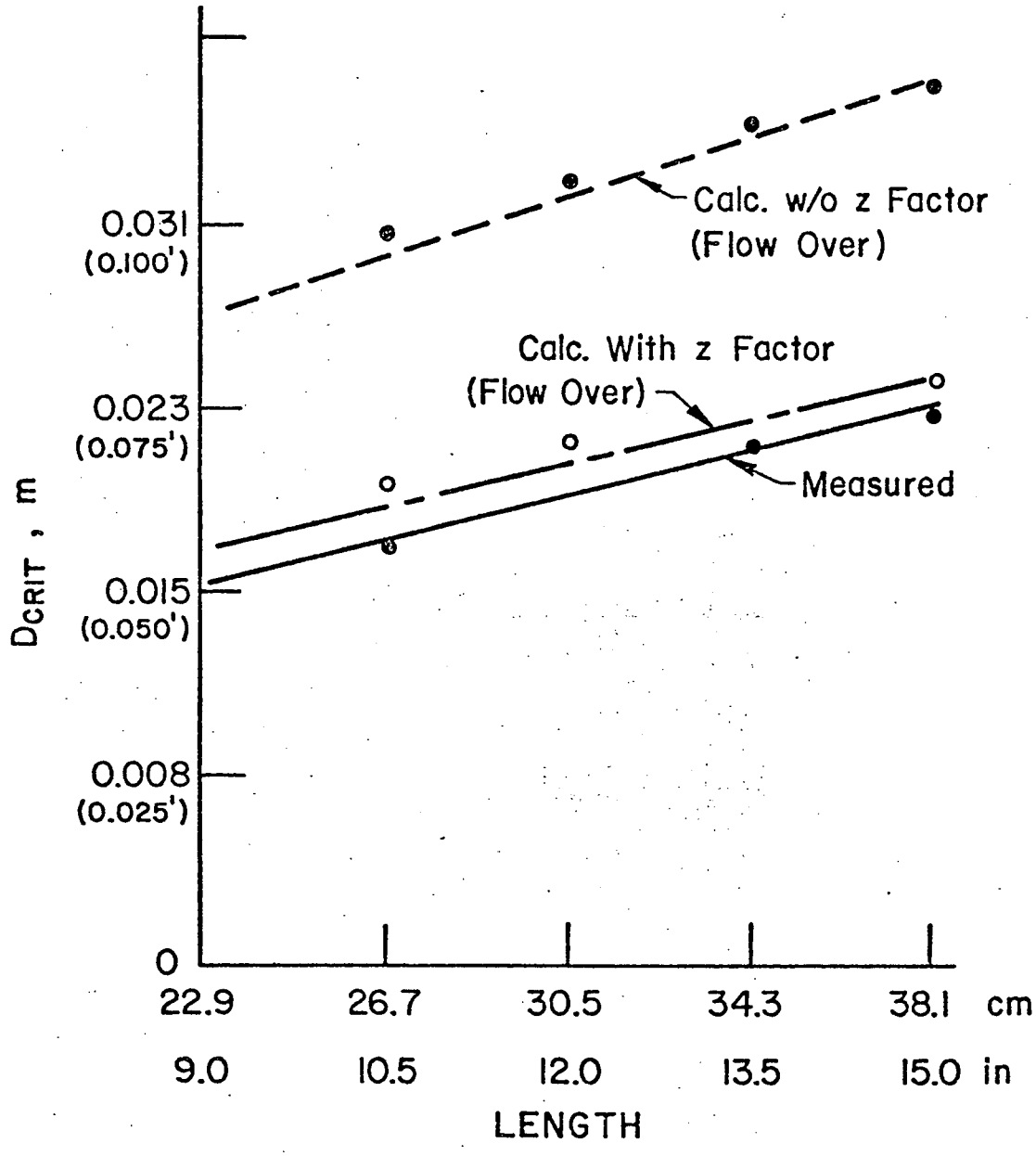

$S_S = 12:1$

$S_B = 3:1$

SO = 0.04

Fig. 2.12: Measured and Calculated $D_{crit.}$ Versus Length (Long. Slope = 4%; Swale = 12:1; Back = 3:1)

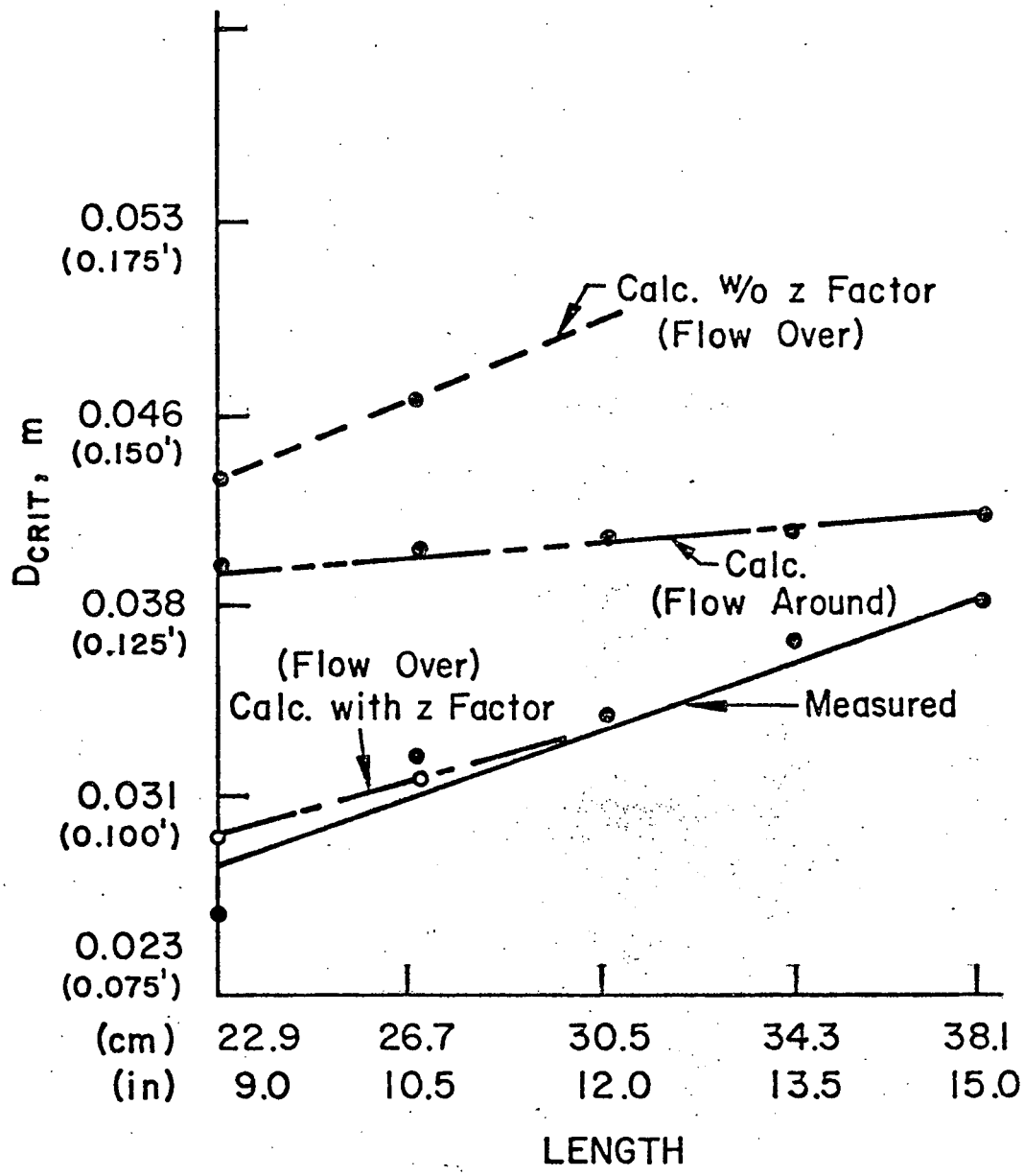

$S_S = 12:1$

$S_B = 1/8:1$

$SO = 0.02$

Fig. 2.13: Measured and Calculated $D_{crit.}$ Versus Length (Long. Slope = 2%; Swale = 12:1; Back 1/8:1)

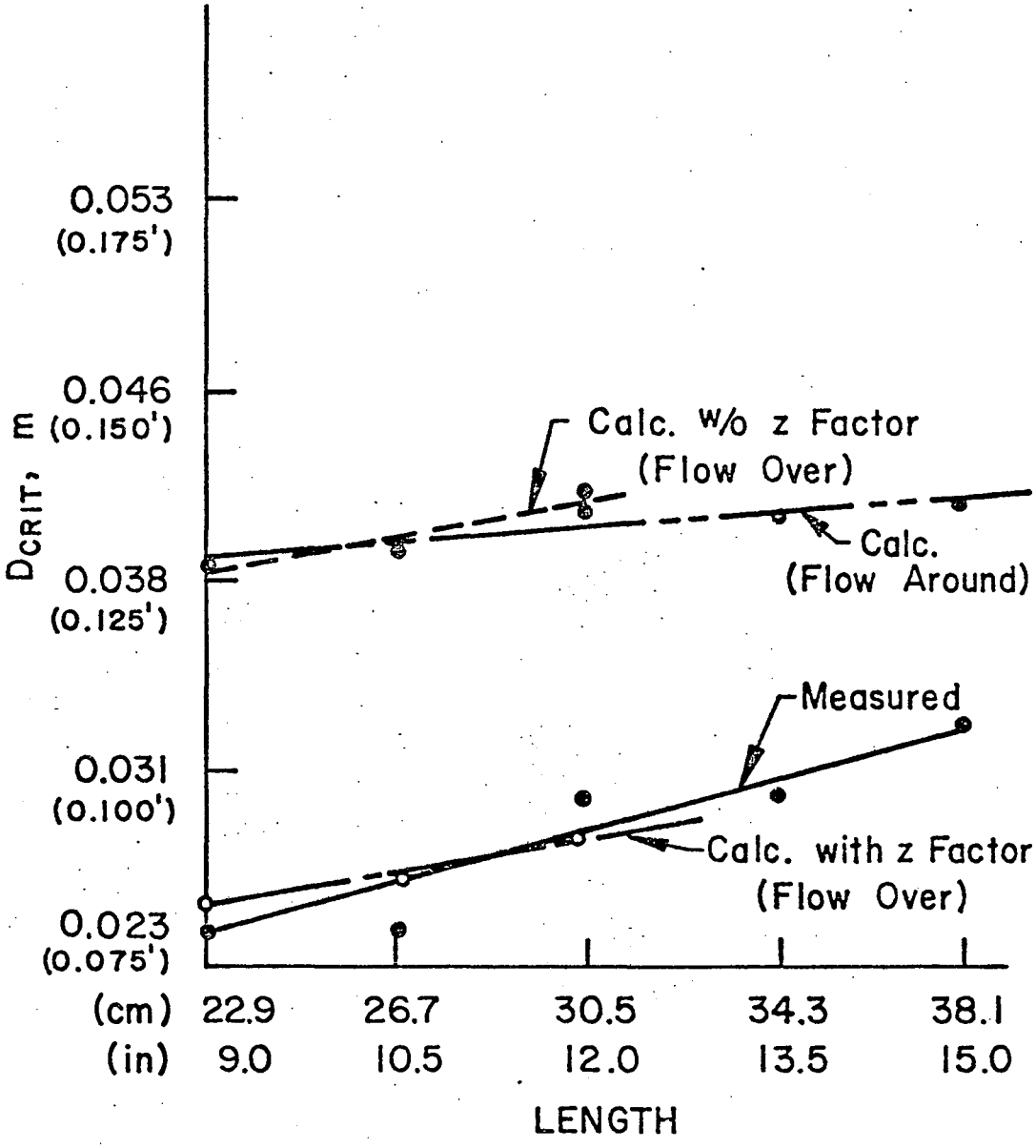

$S_S = 12:1$

$S_B = 3:1$

$SO = 0.02$

Fig. 2.14: Measured and Calculated $D_{crit.}$ Versus Length (Long. Slope = 2%; Swale = 12:1, Back = 3:1)

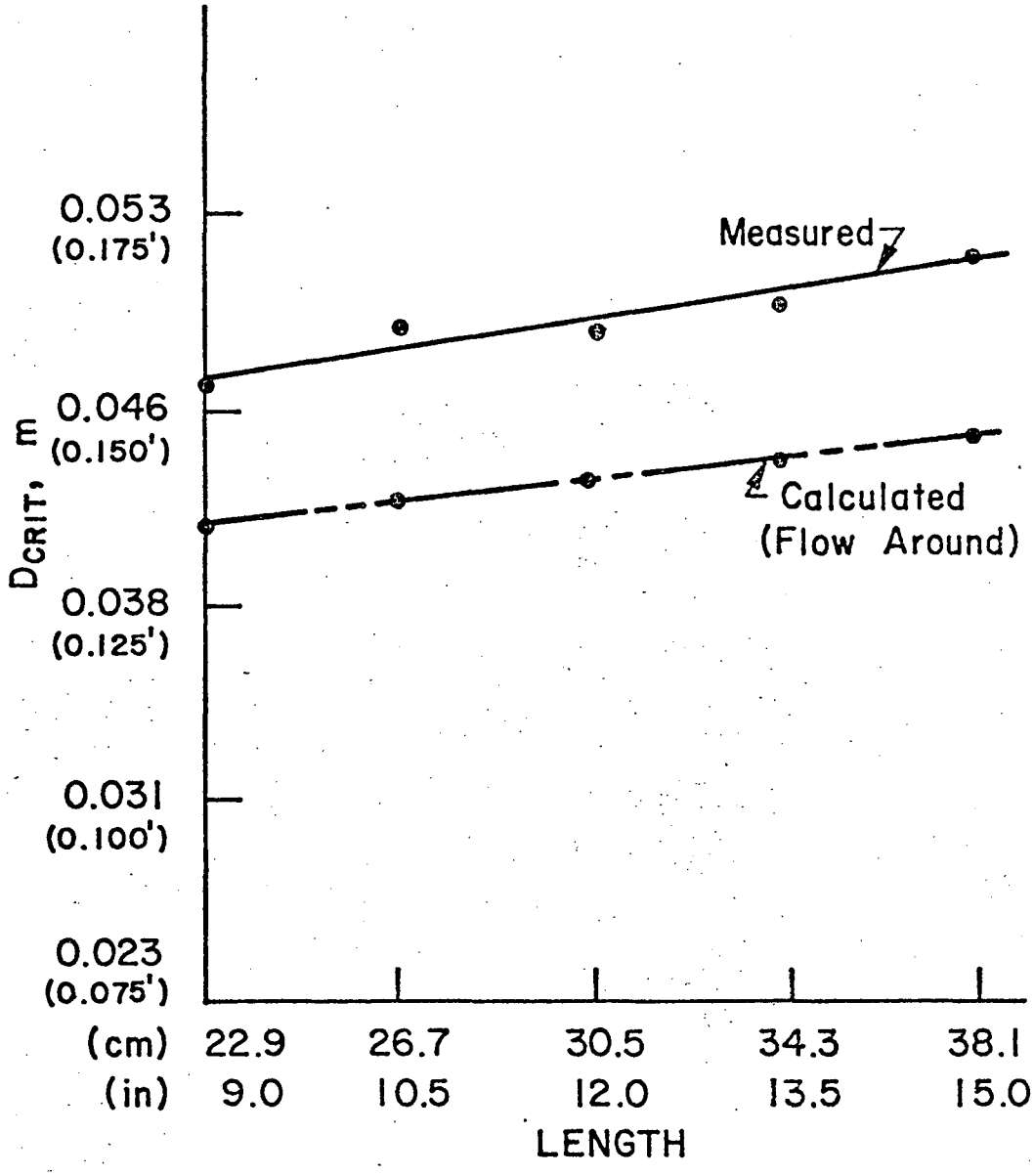

$S_S = 12:1$

$S_B = 1/8:1$

$SO = 0.005$

Fig. 2.15: Measured and Calculated D_{crit} Versus Length (Long. Slope = 1/2%; Swale = 12:1; Back = 1/8:1)

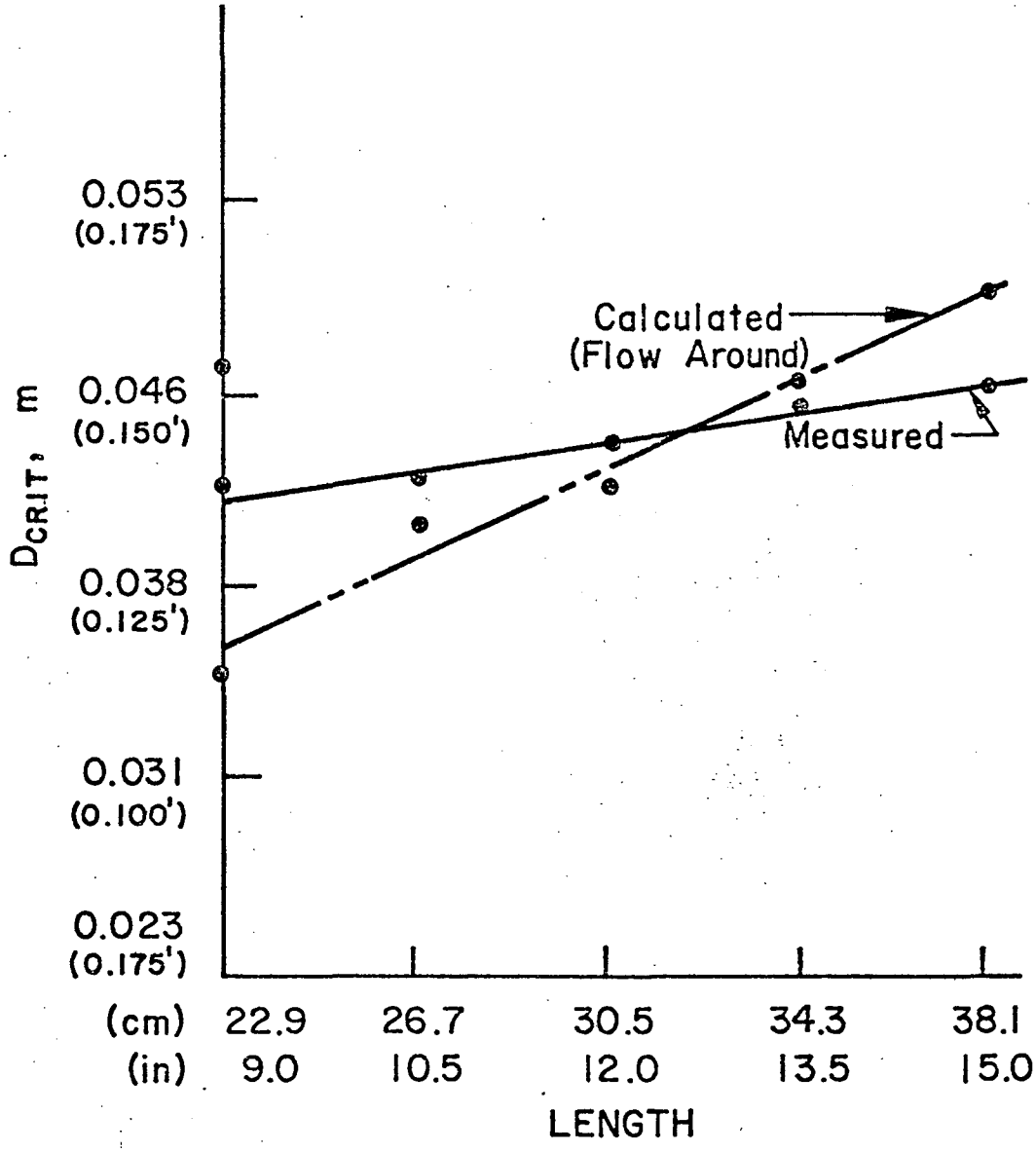

$S_S = 12:1$

$S_B = 3:1$

SO = 0.005

Fig. 2.16: Measured and Calculated $D_{crit.}$ Versus Length
(Long. Slope = 1/2%, Swale = 12:1, Back = 3:1)

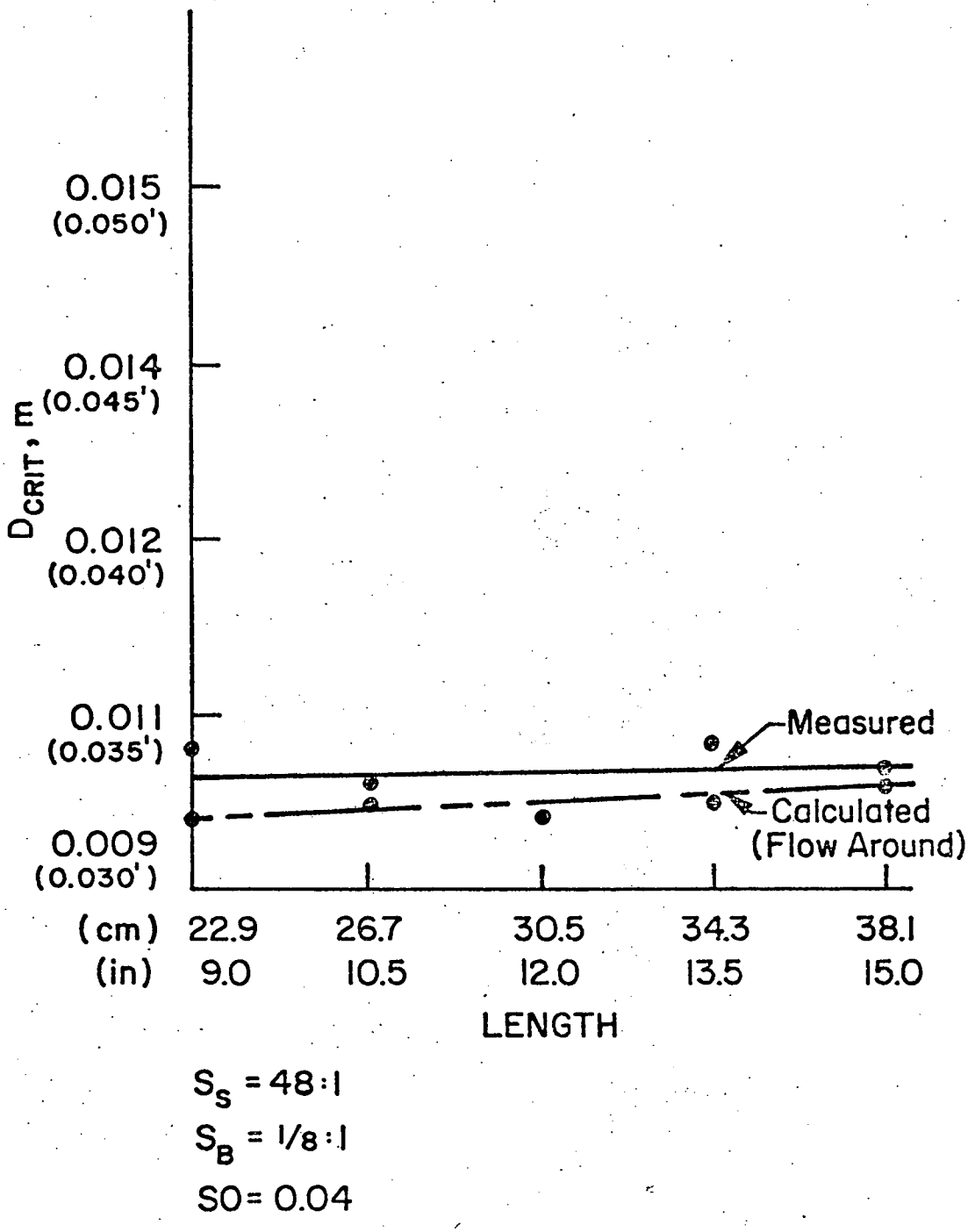

Fig. 2.17: Measured and Calculated $D_{crit.}$ Versus Length
(Long. Slope = 4%; Swale = 48:1; Back = 1/8:1)

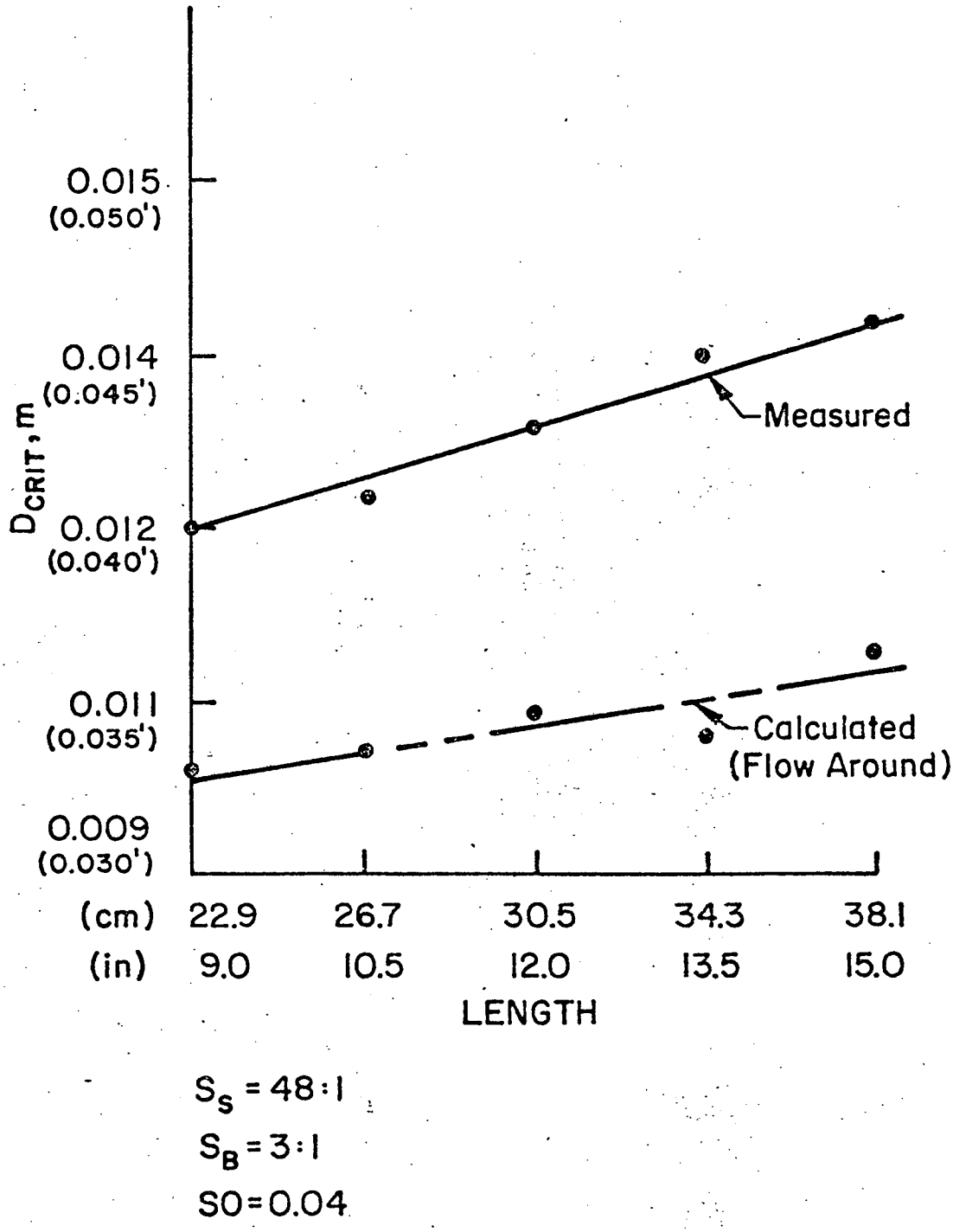

Fig. 2.18: Measured and Calculated $D_{crit.}$ Versus Length
(Long. Slope = 4%; Swale = 48:1; Back = 3:1)

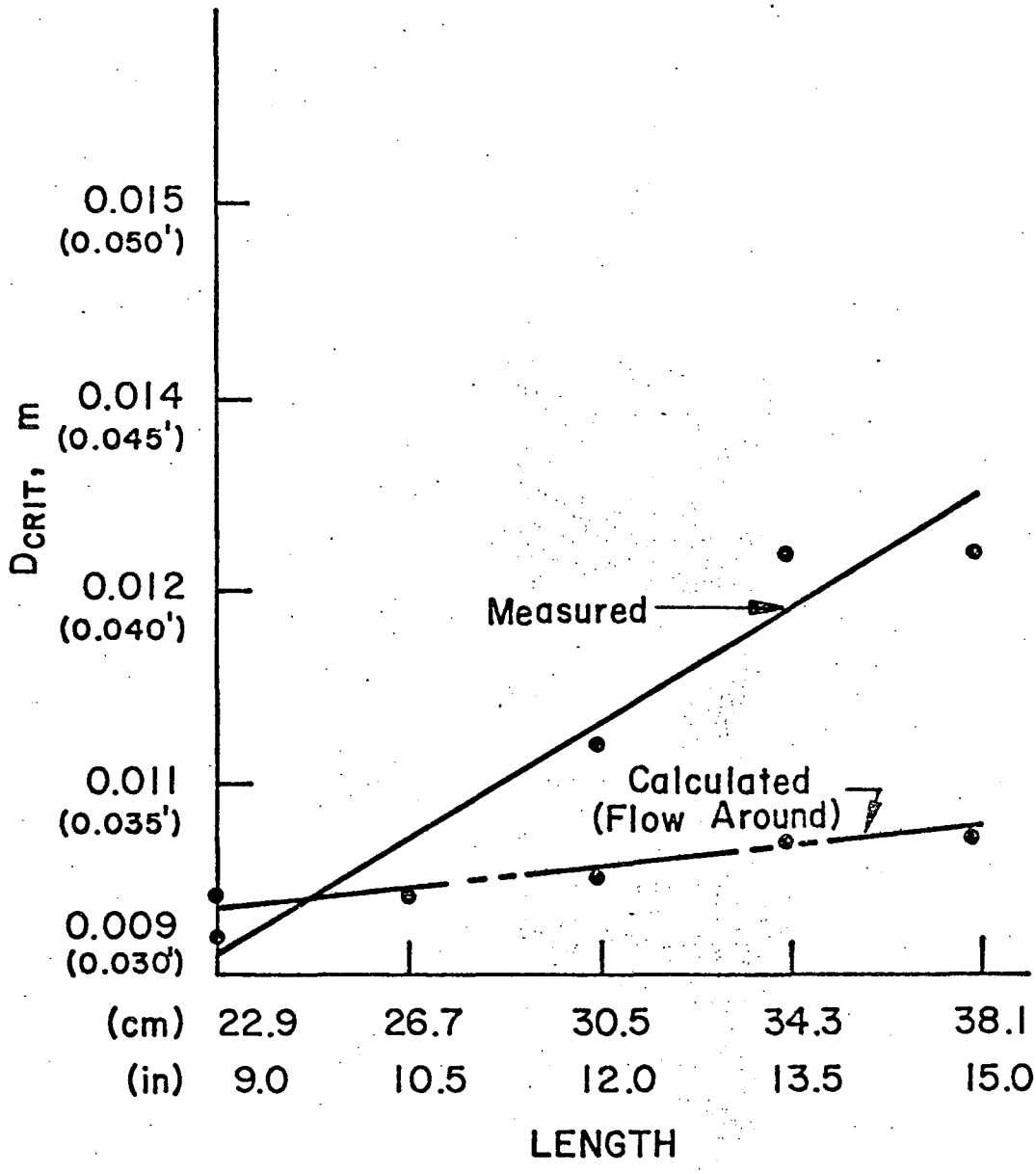

$S_S = 48:1$

$S_B = 1/8:1$

$SO = 0.02$

Fig. 2.19: Measured and Calculated $D_{crit.}$ Versus Length
(Long. Slope = 2%, Swale = 48:1; Back = 1/8:1)

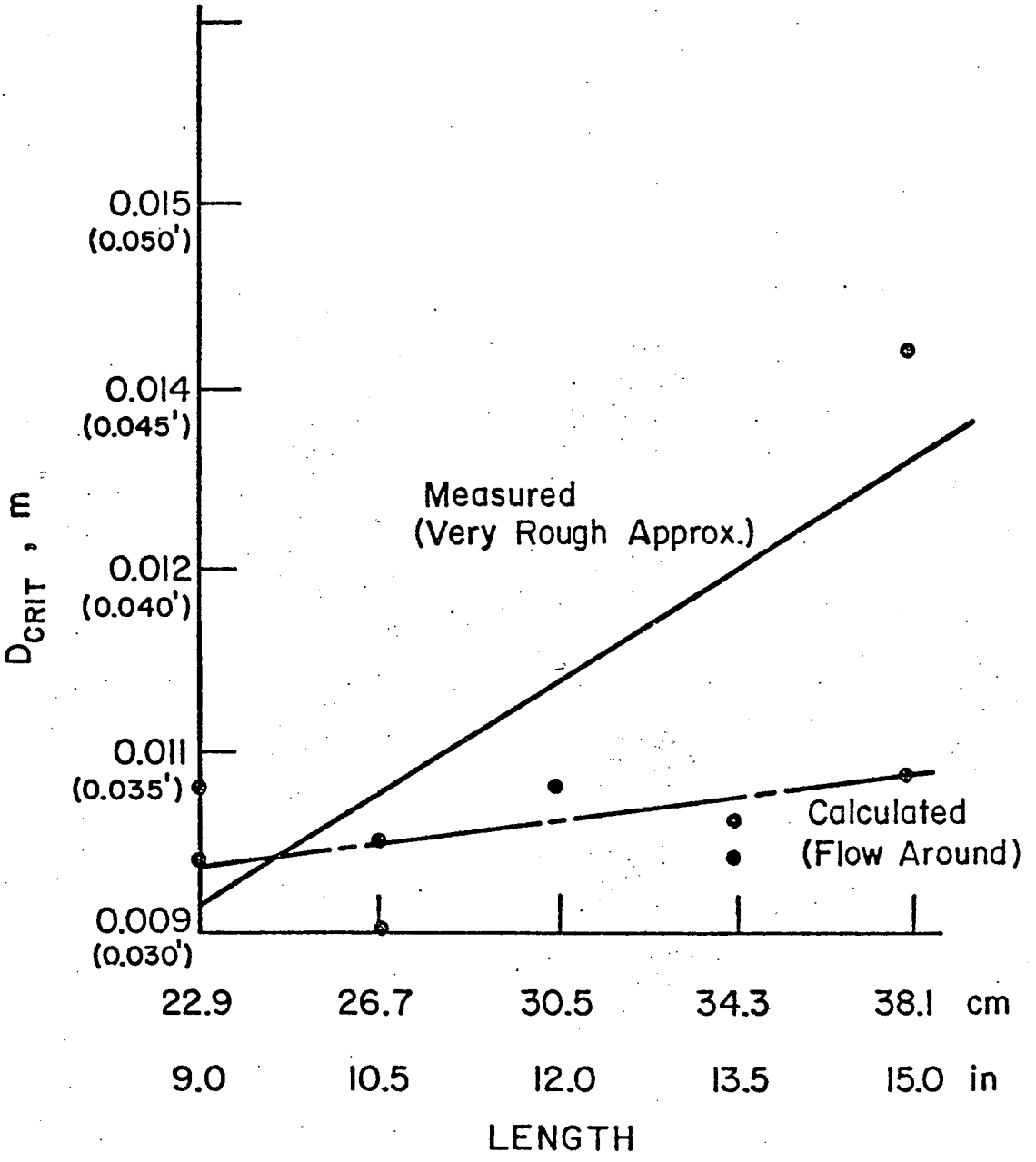

S_S = 48:1

S_B = 3:1

SO = 0.02

Fig. 2.20: Measured and Calculated $D_{crit.}$ Versus Length (Long. Slope = 2%; Swale = 48:1, Back = 3:1)

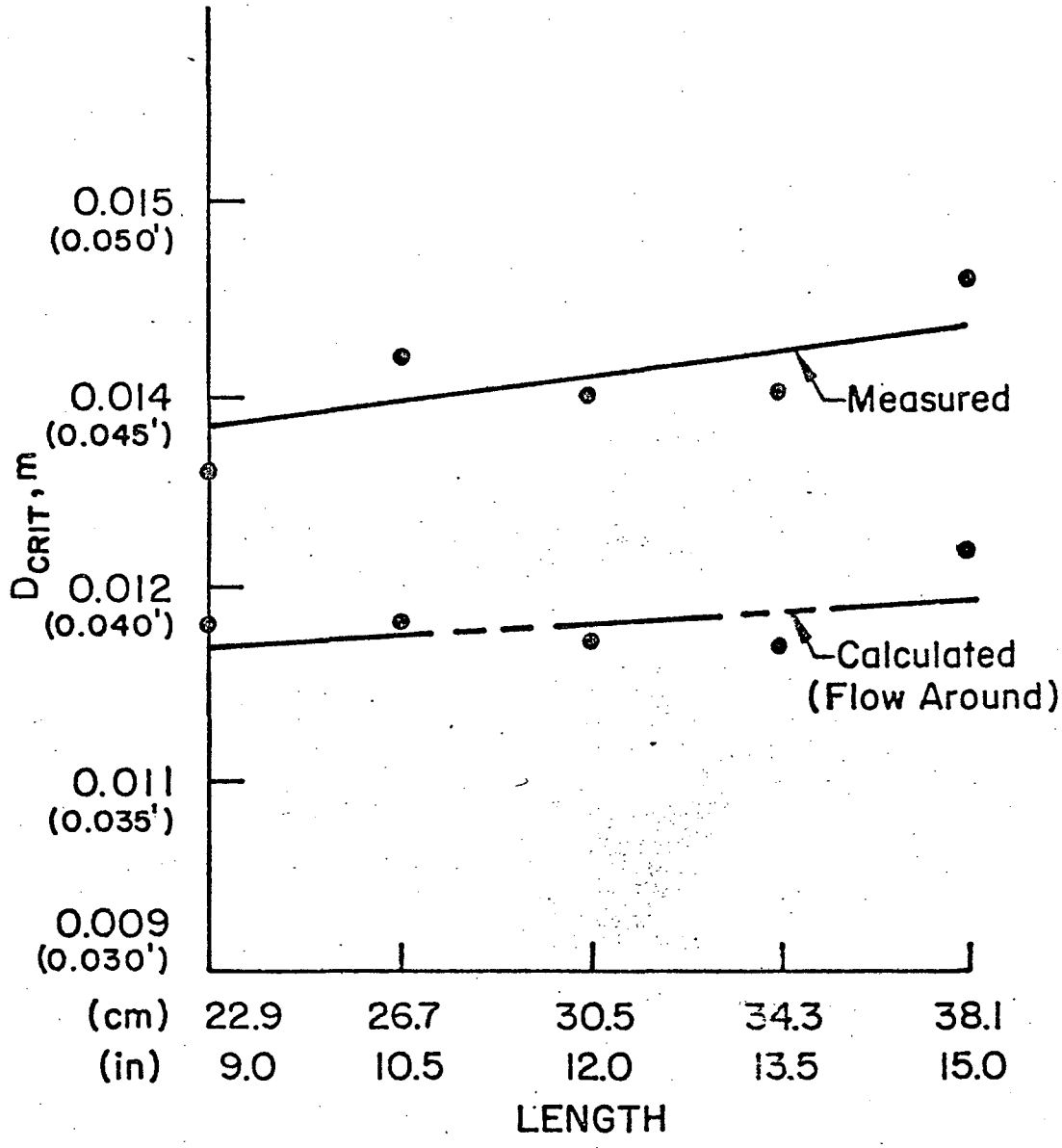

$S_S = 48:1$

$S_B = 1/8:1$

SO = 0.005

Fig. 2.21: Measured and Calculated $D_{crit.}$ Versus Length (Long. Slope = ½%; Swale = 48.1; Back = 1/8:1)

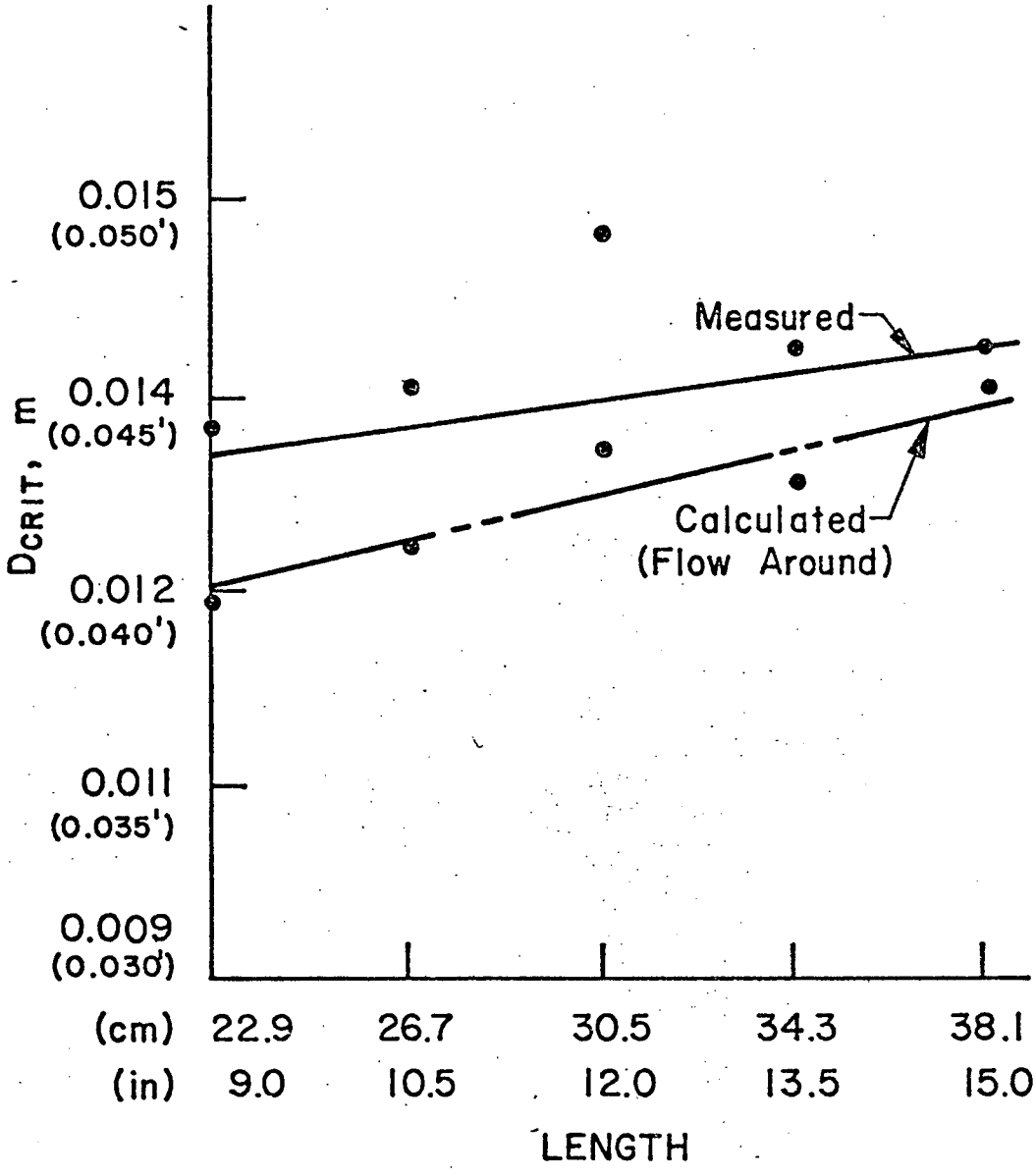

$S_S = 48:1$

$S_B = 3:1$

$SO = 0.005$

Fig. 2.22: Measured and Calculated $D_{crit.}$ Versus Length
(Long. Slope = ½%; Swale = 48:1; Back 3:1)

where BS is the width of flow on the swale slope side of the inlet and L is the length of the inlet. The purpose of the S_s is to help distinguish between the 12:1 and the 48:1 S_s tests. The S_B term is considered important because of the difference in flow characteristics observed when the backslope is varied. The $\frac{BS}{L}$ term is, of course, dimensionless. Fig. 2.19 is a plot of the data on a graph of:

$$X = \frac{(v)(D)(S_s)}{[(g)(L)]^{0.5}(BB)} \quad \text{vs} \quad Y = \frac{BS\ (S_s + S_B)}{L}$$

where X is a function of the Froude number, $\frac{v}{\sqrt{gL}}$, with g equal to the gravitational constant and BB equal to the backslope width of flow from the invert. Fig. 2.20 is a similar plot for the 12:1 S_s tests only. The division between flow over and both types of flow is vague.

2.7 FURTHER RESEARCH

It was hoped that a critical Froude number could be found, which would arise everytime time flow passed by the inlet. Also, an effort was made to calculate a Froude number using the derived critical depths and velocities and to compare it to a Froude number found using the measured data. The results of this work were insignificant. No relationships were found in either case.

The expression for the critical depth of flow around the drain was modified to include a velocity ratio using Manning's

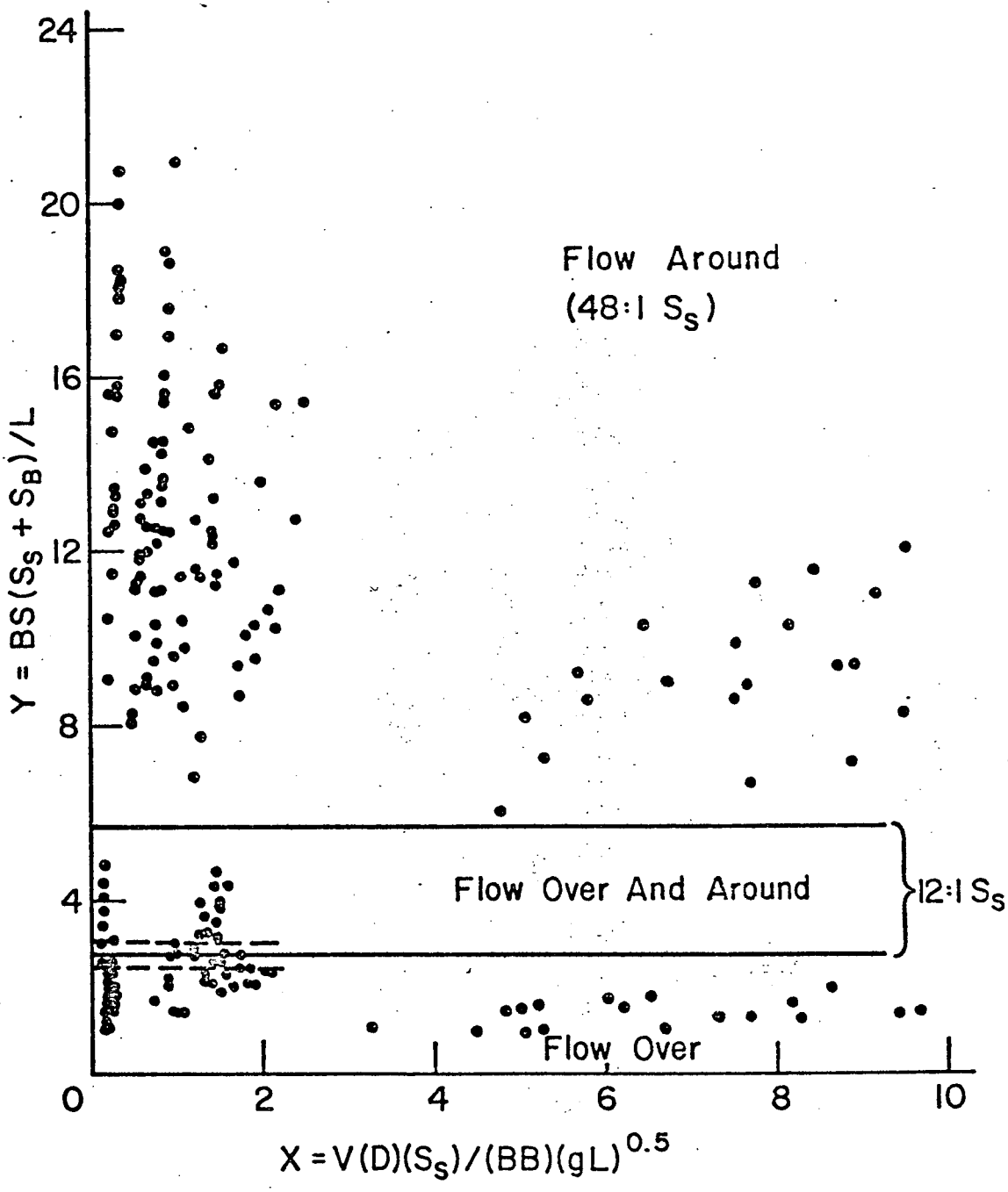

Fig. 2.23: Dimensionless Plot to Illustrate Flow Over Versus Flow Around. (All points)

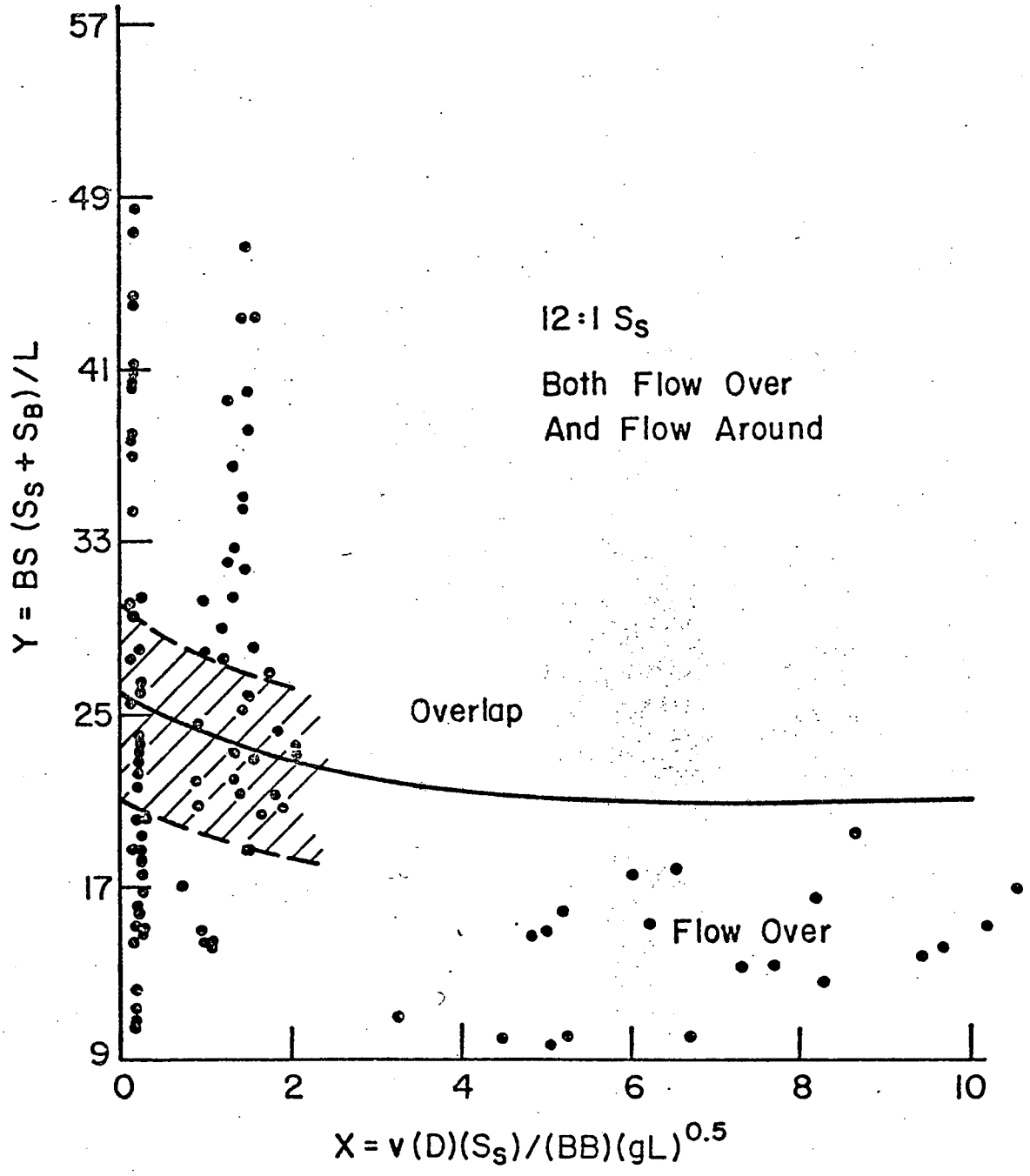

Fig. 2.24: Dimensionless Plot to Illustrate Flow Over Versus Flow Over and Around. (12:1 Swale Slope)

velocity term. It has since been discovered that the Wasley velocity term may also be inserted. A computer program was written in an attempt to use this new ratio, although, at this time, a successful solution has not yet been found. Work is continuing on this idea.

2.8 POSSIBLE REASONS FOR NONCONFORMITY BETWEEN THEORETICAL AND CALCULATED MEASUREMENTS

The first tendency for a researcher when the measured results do not conform to theory is to suspect the data of being faulty. Fig. 2.21 is a plot of the measured flow rates versus the calculated flow rates using the measured depths and the Manning velocity equation. Fig. 2.22 and Fig. 2.23 are plots of the width of flow on the swale side of the invert (measured versus calculated) for 12:1 S_s and 48:1 S_s respectively. These figures show an agreement between measured and calculated values, with the most scatter appearing in the 48:1 S_s situation. From these plots, it can be assumed that the data are consistent within itself; that is, the depth, width, area, and flow rates all vary in the proportion indicated by theoretical equations.

Fortunately, throughout the testing procedure, a careful photographic study was kept of each flow situation. It was thought that, since the maximum flow reached before overflow for an inlet set-up was visually estimated, perhaps the photographs would show

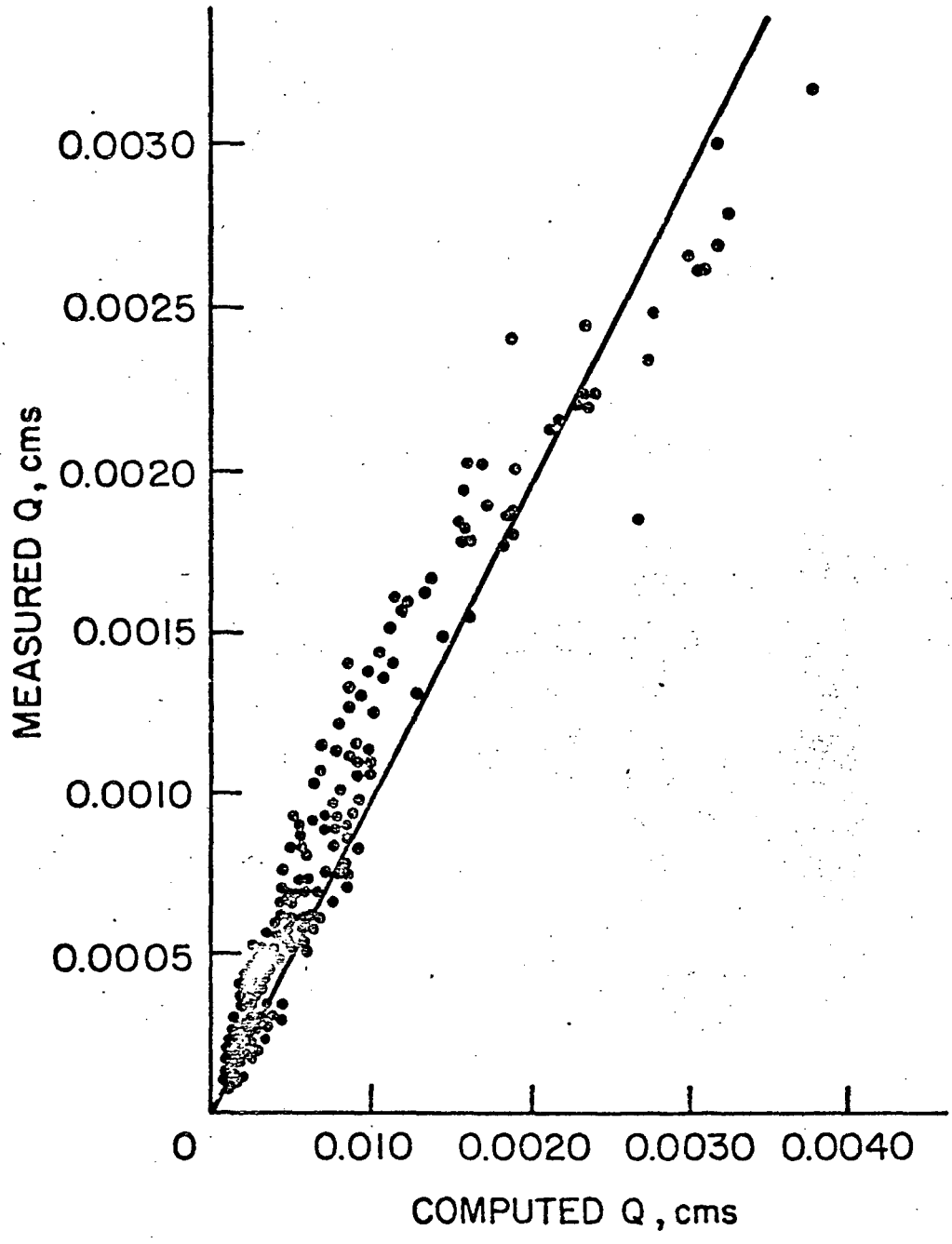

Fig. 2.25: Measured Q vs Computed Q (Manning)

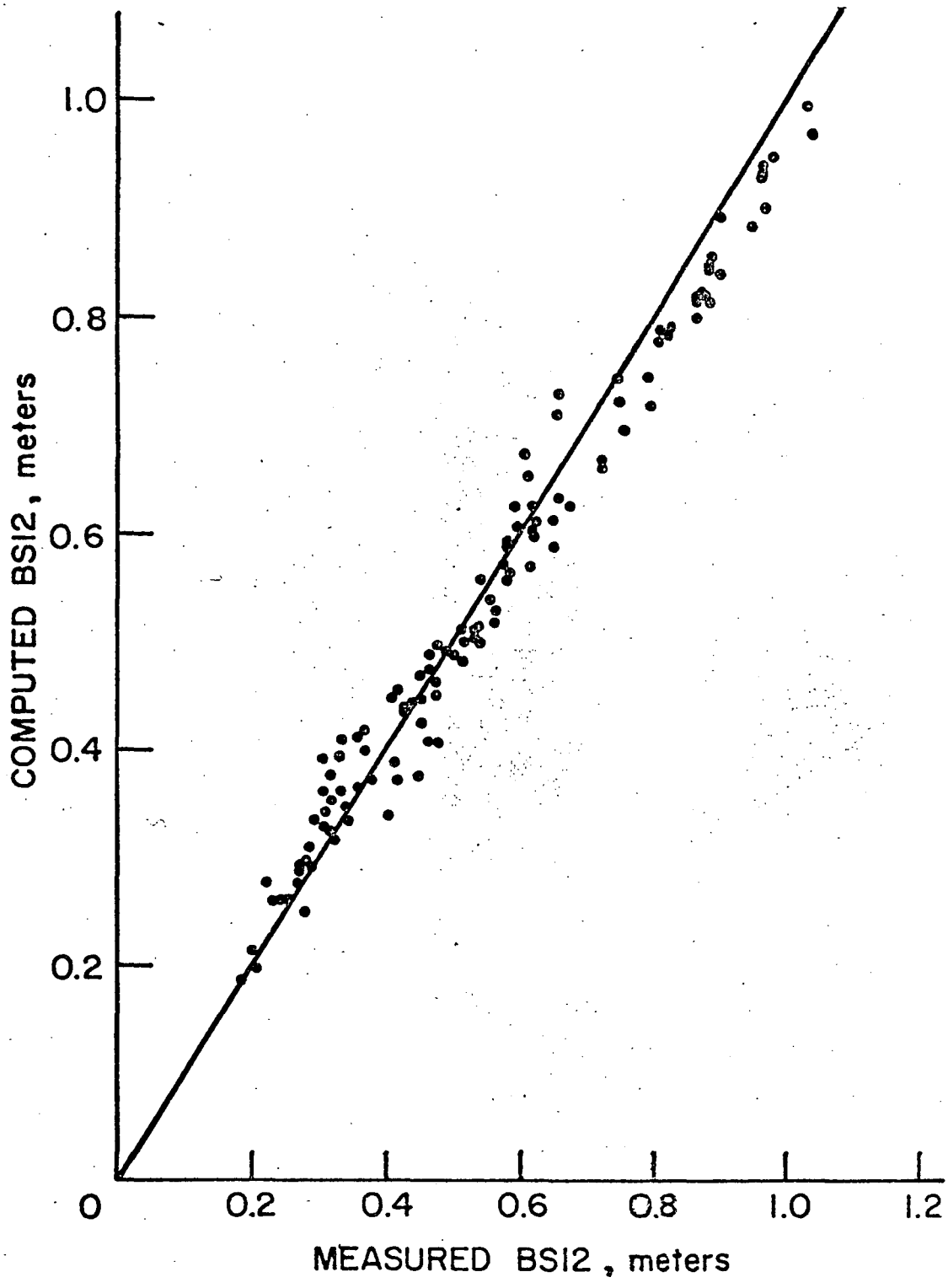

Fig. 2.26: Computed BS Versus Measured BS (12:1 Swale Slope)

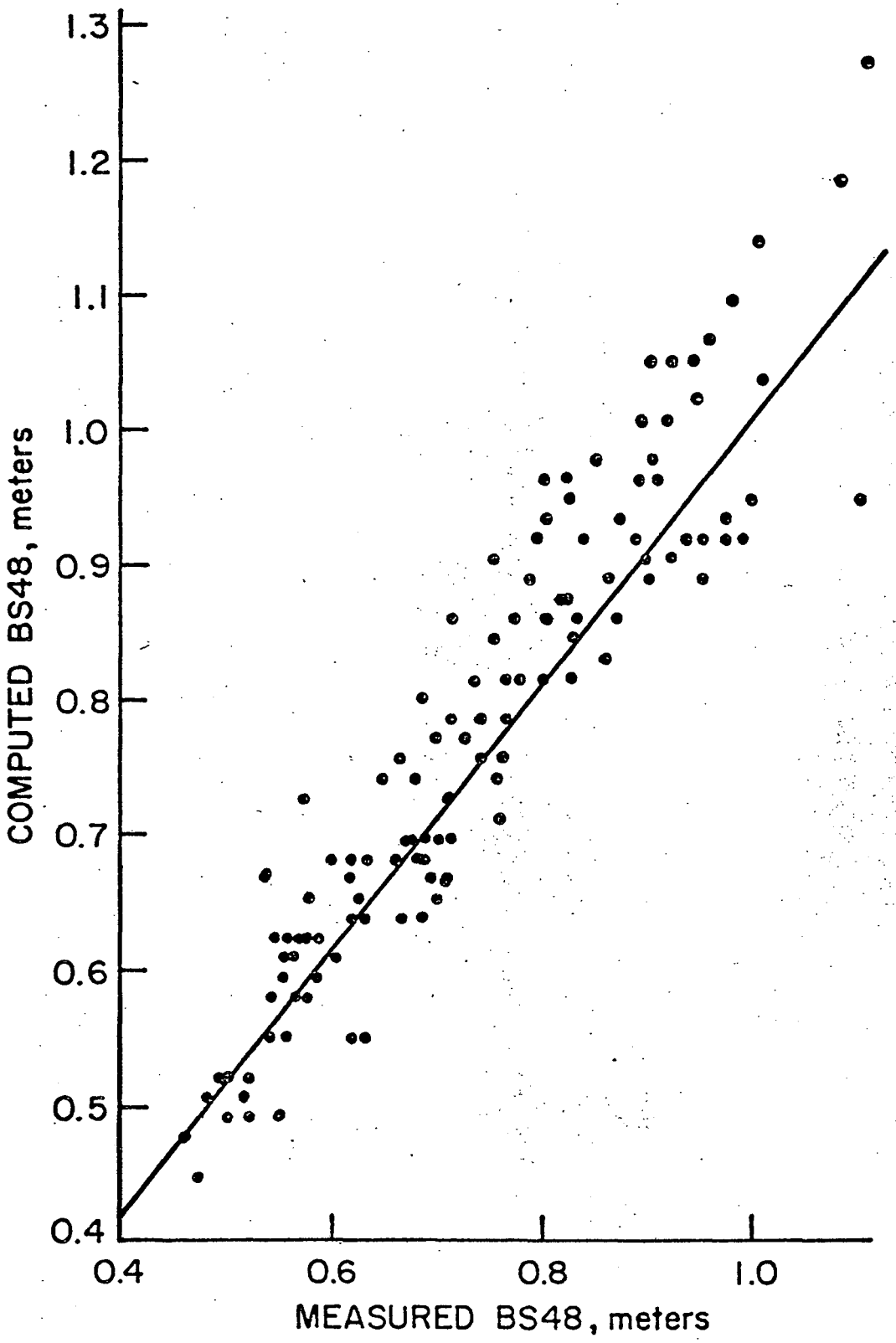

Fig. 2.27: Computed BS Versus Measured BS (48:1 Swale Slope)

that some tests were above or below the actual critical flow rate. This would have presented a reason for some minor non-conformities between measured values and theory. Although some of the photos did indicate some over or under estimation, the resulting additions or subtractions were not all in the appropriate direction, and none of them were deemed significant.

One enlightening factor learned from the photographic study involved the 12:1 S_s tests with the two different backslopes. In section 2.4, it was mentioned that all of the 12:1 S_s data with the 3:1 S_B was continually less than the data from the 1/8:1 S_B tests with the same S_s. This relationship is opposite to what theory indicates. Photographs showed that when 3:1 backslope was in place, water bypassed the inlet on that side before it actually flowed over the drain. This was not the case with the 1/8:1 backslope; thus, the inlet was able to intercept more water with the steeper backslope.

2.9 CONCLUSION AND SUMMARY

Even after checking and rechecking calculations, testing the validity of the data and studying photographs, few of the non-conformities between measurements and theory can be explained. There is always the human error aspect which plagues all research projects. These tests were not originally performed to be used in an analytical study. The only parameter of immediate interest to the sponsor was the maximum obtainable flow rate before bypassing

flow occurred. Even though extreme care was not used in taking the various other measurements, they were not found to be significantly erroneous.

Perhaps the best reason for not achieving uniformity between theory and reality, is that much of the analytical work was done using data from tests with efficiencies less than 100 percent; yet, none of the efficiencies were below 85 percent. This small range of flow rates caused a minimal variation in depth and width relationships, and forced a necessary precision of the data and calculations which may have been above that obtainable from the model set-up. The pumps used in the tests were run at capacity on several occasions, and greater flow rates were not available; thus necessitating this small flow rate range. The model was ideal for investigating the optimal dimensions of an inlet grating through visual analysis, but perhaps it did not lend itself to theoretical study.

This analysis is not without merit, however. The theoretical work is based upon proven concepts and should prove to be useful in further studies. Perhaps using this work as a basis, a complete set of analytical relationships can be formulated at a later date, which will exactly duplicate the field situations and thus make highway inlet grating design less complicated.

APPENDIX

A1 ANALYSIS BY LI

The following is a synopsis of work done by Dr. Wen-Hsiung Li at Johns Hopkins University in 1954. His work is based largely upon trajectory theory and algebraic relationships which require little explanation.

A1.1 Free Drop at End of Channel

$$L_o = vt \qquad \text{(See Fig. A1.1)}$$

$$d = gt^2/2$$

$$L_o = v\sqrt{2d}/g$$

$$L = v\sqrt{2d_1}/g$$

$$\frac{d_1}{d} = \left(\frac{L}{L_o}\right)^2 \qquad \text{(Eq. A1.1)}$$

where L_o, L are lengths of flow trajectory; d, d_1 are corresponding depths; v is the velocity of flow; and g is the gravitational constant.

A1.2 Curb Opening Required to Capture Entire Gutter Flow

$$L' = v\left(\frac{2d}{a}\right)^{1/2} = v'\left(\frac{2y'\tan\theta}{g\cos\theta}\right)^{1/2} \qquad \text{(See Fig. A1.2)}$$

$$Q' = v_{oy'}^2 \left(\tan\frac{\theta}{2}\right) \qquad \text{(Eq. A1.2)}$$

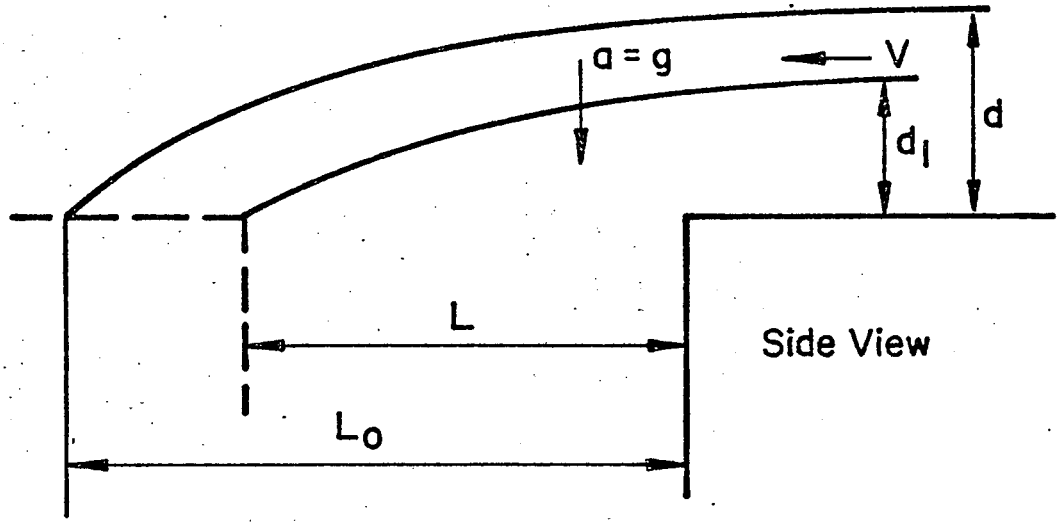

Fig. A1.1: Li's Diagram For Basic Trajectory Theory of Flow into an Opening

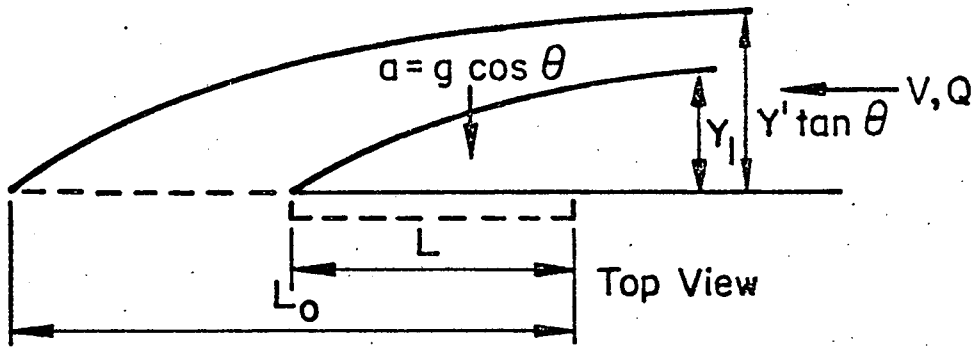

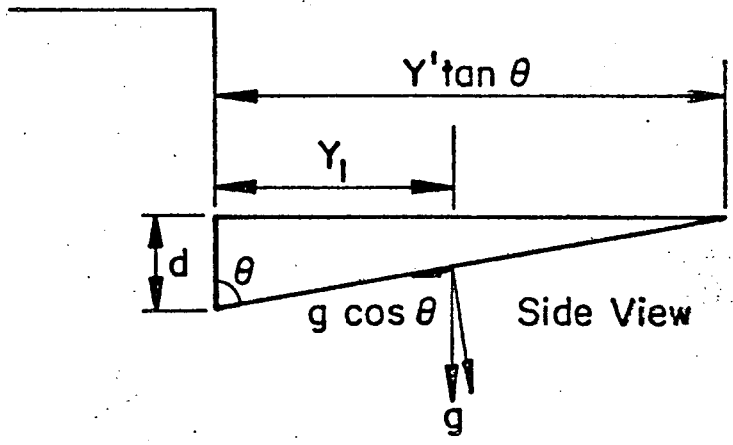

Fig. A1.2: Flow into Curb Opening

$$\frac{Q'}{L_o y' \sqrt{gy}} = \left(\frac{\sin\theta}{8}\right)^{1/8}$$

if $\theta = 90^{\circ}$, with no friction, $\left(\frac{\sin\theta}{8}\right)^{1/2} = 0.35$

$$K = Q'/L'y' \sqrt{gy'} \qquad \text{Eq. A1.3}$$

where θ is the angle that the pavement makes with the curb; K is a constant; and Q_o is the flow rate. Li found experimentally that for pavement swale slopes of 12:1, K = 0.23, and for 24:1 and 48:1 pavement swale slopes, K = 0.20. Also he found that for $L \geq 0.6\ L_o$, Q/Q_o is approximately equal to L/L_o.

A1.3 Grate Inlet with Longitudinal Bars

- Combining Eq's A1.2 and A1.3, (See Fig. A1.3)

$$\frac{\tan\theta}{2k} = \frac{L' \sqrt{g}}{v' \sqrt{y'}}$$

multiplying by 1/v

$$\frac{\tan\theta v'}{2k} = \frac{L' \sqrt{g}}{v' \sqrt{y'}} = m \qquad \text{(Eq. A1.4)}$$

Li found v/2k to be approximately 1.2 for longitudinal bars.

A1.4 Carry Around Flow (Q_2)

$$Q/Q' = L/L'$$

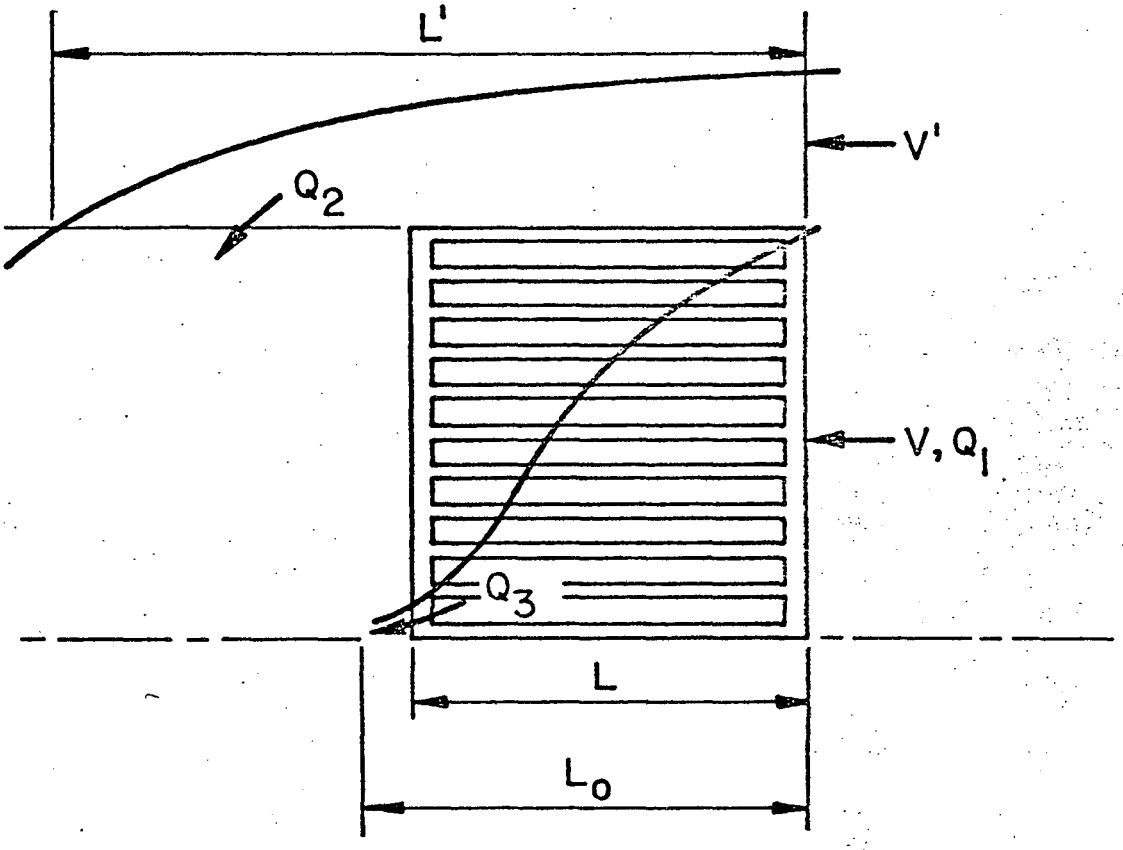

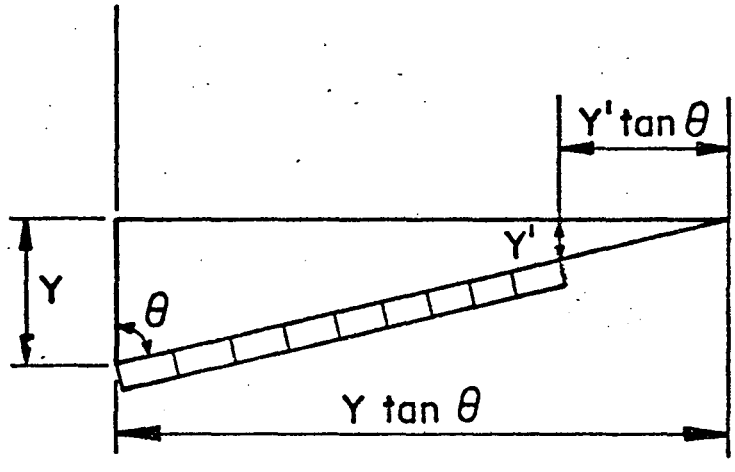

Fig. A1.3: Methods of Bypassing Flow

From Eq. A1.3, $Q'/L' = Ky' \sqrt{gy'}$

$$Q' - Q = K(L'-L)\ Y' \sqrt{gy'}$$

$$Q_2 = K(L'-L)\ y' \sqrt{gy'} \qquad \text{(Eq. A1.5)}$$

A1.5 Carry Over Flow (Q_3)

With flow over the inlet (with no grate), m from Eq. A1.4 = $\sqrt{2}$ by trajectory theory. With a grating present, Li found experimentally that m varied from $\sqrt{2}$ to 10. To trap all flow, L must equal L_3.

$$L_3 = mv\ (y'/g)^{1/2}$$

$$L_3 = mv\ [y\ (1 - \frac{x}{y\tan\theta})/g]^{1/2}$$

$$d - d_1 = y(1 - L^2/L_3^2) - x/\tan\theta$$

setting $d-d_1 = 0$ and integrating as x 0 (See Fig. A1.3)

$$Q_3 = Q_1\ (1 - (L^2/L_3^2))^2 \qquad \text{(Eq. A1.6)}$$

A2 ANALYSIS BY WASLEY

Wasley's work was only concerned with passing flow around the drain as opposed to passing flow over the drain. This information was taken from his doctoral dissertation presented at Stanford University in 1961.

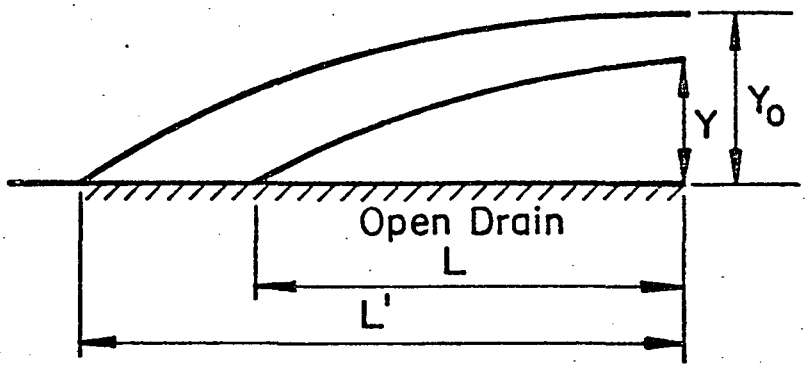

Fig. A2.1: Flow into an Open Drain (Wasley)

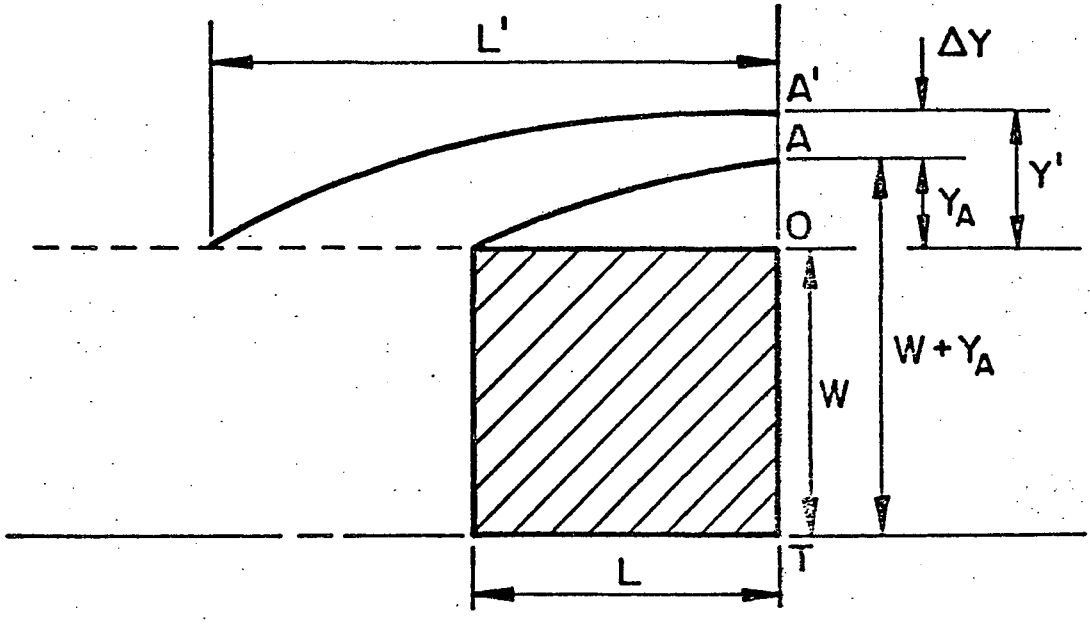

Fig. A2.2: Bypassing Flow Around Inlet (Wasley)

A2.1 Gutter Flow Into Curb Opening

(See Fig. A2.1)

Wasley showed that

$$L' = \frac{C'y'}{\sqrt{g}} \quad (1 + 1/\ \ 2) \qquad \text{(Eq. A2.1)}$$

where C' = Chezy's C.

$$C' = \frac{8gS_o}{f}^{1/2}$$

where S_o = longitudinal slope, and f = Darcy's friction factor

$$f = \frac{8gR_H S_o}{v_a^2}$$

where R_H is the hydraulic radius and v_a the average flow velocity.

A2.2 Flow into a Drainage Inlet

Eq. A2.1 can be applied to the region outside of the grating in a channel inlet. (See Fig. A2.2)

$$L = \frac{C_o y_a}{\sqrt{g}} \ (1.707) \qquad \text{(Note } C_o = V_a / \sqrt{R_H}\text{)}$$

$$W + y' = D_T/\cos\theta = D_T(S_s)$$

where D_T = depth of flow at point T, and S_s is the inverse of the swale slope. S_s is large allowing for the approximation, $\cos\theta = 1/S_s$.

$$S_s = \frac{W + y'}{D_t}$$

when flow is at A'

$$D_a = D_t - \frac{(W + Y_a)}{S_s} = \frac{y' - y_a}{S_s} = \frac{\Delta y}{S_s} \quad \text{(Eq. A2.2)}$$

$$y_a = S_s D_t - W - D_a S_s \quad \text{(Eq. A2.3)}$$

$$L = \frac{C_o\ (1.707)}{\sqrt{g}}\ [(S_s)\ (D_t - D_a) - W] \quad \text{(Eq. A2.4)}$$

$$D_a = D_t - \frac{L\ \sqrt{g}}{C_o S_s\ (1.707)} - \frac{W}{S_s} \quad \text{(Eq. A2.5)}$$

A2.3 Velocity Distribution

Wasley begins with the assumption that the velocity of flow in a triangular channel is a function of the square root of the depth of flow. (See Fig. A2.3)

$$v(x) = cy^{1/2} \quad \text{(Eq. A2.6)}$$

Therefore:

$$Q = \int_{0}^{S_s D} v \, dA \quad \text{where } dA = y\,dx$$

$$Q = \int_{0}^{S_s D} cy^{3/2} \, dx \quad \text{where } -dx = S_s\,dy$$

$$\text{Therefore } Q = cS_s \int_{D}^{0} -y^{3/2} \, dy$$

$$Q = \frac{2}{5} cS_s D^{5/2}$$

$$c = \frac{5}{2} \frac{Q}{S_s D^{5/2}} \qquad \text{(Eq. A2.7)}$$

$$\text{and } v(x) = \frac{5}{2} \frac{Q}{S_s D^{5/2}} (y)^{1/2} \qquad \text{(Eq. A2.8)}$$

A3 ANALYSIS BY MURRAY

Dr. Willard A. Murray performed some preliminary theoretical work using data from Fritz Engineering Laboratory Project 364 (Lehigh University, Bethlehem, Pa. 1972). His primary goal was to establish an equation which would represent the efficiency of a drain that was subject to bypassing flow going around the drain on the swale slope side. Dr. Murray's work was based extensively on Wasley's analysis.

A3.1 Establishing an Equation for Bypass Flow (Q_2)

(See Fig. A3.1)

$$T = D_B S_s$$

$$T_A = D_A S_s$$

$$Q_2 = v_A A_{T-W}$$

v_A = average velocity of flow between points "O" and "A".

First, Dr. Murray established a v_A based upon trajectory theory. (See. Fig. A3.2)

g = travitational constant

$g_s = g \cos\theta$

θ is small, $\cos\theta = 1/S_s$

$g_s = g/S_s$

$L = vt$

$$z = \frac{gt^2}{2S_s}; \quad t = \frac{2z(S_s)}{g}$$

$$L = v_A \frac{2z(S_s)}{g} \qquad \text{(Eq. A3.1)}$$

Next, he found an expression for "D_A" in terms of v_A.

$z = Y_A$

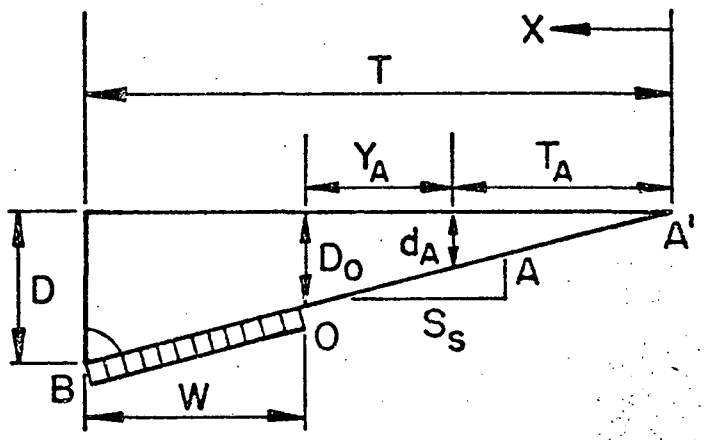

Fig. 3.1: Diagram for Murray Calculations

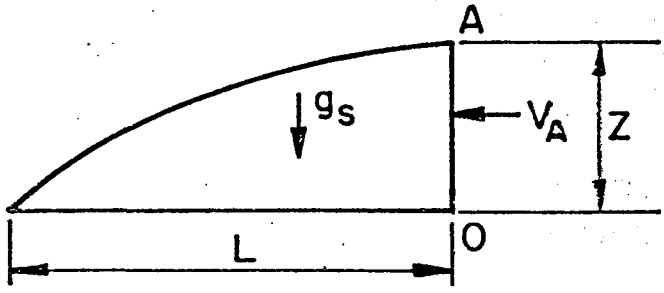

Fig. 3.2: Flow Trajectory Theory Down a Swaleslope (Murray)

From Eq. A3.1:

$$y_A = \frac{1}{2} \frac{L^2 g}{S_s v_A^2} \qquad \text{(Eq. A3.2)}$$

$$y_A = S_s (D_B - D_A) - w$$

$$D_A = D_B - \frac{w}{S_s} - \frac{1}{2} \frac{L^2 g}{v_A^2 S_s^2} \qquad \text{(Eq. A3.3)}$$

$$Q_2 = \int_{T_A} v(x)\, dy$$

$$dy = -S_s dx$$

Using Wasley's velocity distribution:

$$v = \frac{5}{2} \frac{Q}{S_s D_B^{2.5}} (x_i)^{1/2} \qquad \text{(Eq. A2.8)}$$

$$Q_2 = \int_{D_A}^{o} -\frac{5}{2} \frac{Q}{S_s D_B^{2.5}} (x)^{1/2} (x)\, dx$$

$$Q_2 = \frac{Q}{D_B^{2.5}} (D_A)^{2.5}$$

$$\frac{Q_2}{Q} = \left(\frac{D_A}{D_B}\right)^{2.5} \qquad \text{(Eq. A3.4)}$$

Combining this with Eq. A3.3 to get an expression for Q_2 gives:

$$Q_2 = \frac{Q}{D_B^{2.5}} \left(D - \frac{w}{S_s} - \frac{L^2}{2v_A^2} \frac{g}{S_s^2}\right)^{2.5} \quad \text{(Eq. A3.5)}$$

A3.2 Establishing Efficiency Equations

First Dr. Murray found an efficiency expression using a Wasley average velocity determined between points A and A' and then he established an expression using a similar average velocity for the flow between points O and A'. (See Fig. A3.1)

A3.2.1 Efficiency Using $v_{A-A'}$

$$v_A = \frac{5}{2} \frac{Q}{S_s D_B^{2.5}} (D_A)^{0.5} \quad \text{(Eq. A2.8)}$$

$$D_A = D_B - \frac{w}{S_s} - \frac{1}{2} \frac{L^2 g}{v_A^2 S_s^2} \quad \text{(Eq. A3.3)}$$

$$\text{therefore } D_A = D_A - \frac{w}{S_s} \frac{2L^2 g D_B^5}{25Q^2 D_A}$$

$$\text{or } D_A^2 - \left(D_B - \frac{w}{S_s}\right) D_A - \frac{2L^2 g D_B^5}{25Q^2} = 0$$

Solving the quadratic equation:

$$D_A = \frac{(D_B - \frac{w}{S_s}) \pm \left[(D_B - \frac{w}{S_s})^2 - \frac{8gL^2D_B^5}{25Q}\right]^{1/2}}{2} \quad \text{(Eq. A3.6)}$$

$$\text{Set } R' = \frac{8gL^2D_B^3}{25Q^2(1 - \frac{w}{D_o S_s})^2}$$

$$\text{Then } \frac{Q_2}{Q} = \frac{D_A}{D_B}^{2.5} = \frac{1 - \frac{w}{D_B S_s}}{2}^{2.5} [1 \pm \sqrt{1 - R'}] \quad \text{(Eq. A3.7)}$$

The efficiency, η, then equals $1 - \frac{Q_2}{Q}$.

A3.22 Efficiency Using $v_{o-A'}$

$$v_{o-A'} = \frac{1}{A_{\Delta y}} \int_{\Delta y} v dA; \quad dA = xS_s dx$$

$$v_{o-A'} = \frac{2}{(D_B - \frac{w}{S_s})^2 S_s} \int_{\Delta D} -\frac{5}{2} \frac{Q_o}{S_s} x \, (xS_s dx)$$

$$v_{o-A'} = \frac{2}{(D_B - \frac{w}{S_s})^2 S_s} \frac{Q_o}{D_B^{2.5}} [D_o]^{2.5}$$

$$D_o = D_B - \frac{w}{S_s}$$

$$v = \frac{2}{S_s} \frac{Q_o}{D_B 2.5} (D_o - \frac{w}{S_s})^{0.5}$$

Combining this with Eq.s A3.3 and A3.4:

$$Q_2 = \frac{Q_o}{D_B^{2.5}} \left(D_B - \frac{w}{S_s} \right)^{2.5} - \frac{gL^2 D_B^5}{8Q^2 (D_B - \frac{w}{S_s})}$$

(Eq. A3.8)

$$\frac{Q_2}{Q} = \left(1 - \frac{w}{D_B S_s}\right)^{2.5} \left[1 - \frac{gL^2 D_B^5}{8Q^2 (D_B - \frac{w}{S_s})^2}\right]^{2.5}$$

Make $R'' = \dfrac{gL^2 D_B^5}{8Q^2 (D_B - \frac{w}{S_s})^2}$

Then $\dfrac{Q_2}{Q} = \left(1 - \dfrac{w}{DS_s}\right)^{2.5} [1 - R'']^{2.5}$ (Eq. A3.9)

With efficiency, $\eta = 1 - \dfrac{Q_2}{Q}$

Length	Test	S_o	S_S	S_B	Q_T	Q_I	Depth	B_B	B_S	L'*
WCL09	85	.040	12.	.125	.071	.071	.053	.01	.68	0
WCL09	85	.040	12.	.125	.142	.139	.067	.01	.92	0
WCL09	85	.040	12.	.125	.178	.170	.078	.01	.95	0
WCL09	85	.040	12.	.125	.215	.204	.092	.01	1.02	0
WCL10	97	.040	12.	.125	.096	.096	.074	.01	.73	0
WCL10	97	.040	12.	.125	.192	.187	.090	.01	.96	0
WCL10	97	.040	12.	.125	.240	.229	.105	.01	1.00	0
WCL10	97	.040	12.	.125	.288	.265	.110	.01	1.10	0
WCL12	109	.040	12.	.125	.124	.124	.070	.01	.83	0
WCL12	109	.040	12.	.125	.252	.247	.101	.01	1.04	0
WCL12	109	.040	12.	.125	.311	.292	.111	.01	1.18	0
WCL12	109	.040	12.	.125	.372	.347	.117	.01	1.40	0
WCL13	121	.040	12.	.125	.151	.151	.078	.01	.90	0
WCL13	121	.040	12.	.125	.300	.288	.100	.01	1.24	0
WCL13	121	.040	12.	.125	.380	.353	.120	.02	1.48	0
WCL13	121	.040	12.	.125	.456	.415	.131	.02	1.64	0
WCL15	133	.040	12.	.125	.215	.215	.095	.01	1.04	0
WCL15	133	.040	12.	.125	.435	.416	.121	.02	1.55	0
WCL15	133	.040	12.	.125	.536	.492	.142	.02	1.85	0
WCL15	133	.040	12.	.125	.645	.567	.168	.02	2.02	0
WCL09	86	.040	48.	.125	.046	.046	.034	.01	1.61	0.75
WCL09	86	.040	48.	.125	.091	.088	.038	.01	1.76	2.08
WCL09	86	.040	48.	.125	.114	.109	.040	.01	1.80	3.08
WCL09	86	.040	48.	.125	.138	.129	.043	.01	1.88	3.83
WCL10	98	.040	48.	.125	.049	.049	.033	.01	1.68	0.88
WCL10	98	.040	48.	.125	.098	.093	.039	.01	1.80	2.38
WCL10	98	.040	48.	.125	.122	.115	.041	.01	1.87	3.30
WCL10	98	.040	48.	.125	.147	.133	.044	.01	2.00	4.46

Table A-1 Model Test Data (cfs, ft)

*Symbols defined in nomenclature

Length	Test	S_o	S_S	S_B	Q_T	Q_I	Depth	B_B	B_S	L'
WCL12	110	.040	48.	.125	.049	.049	.032	.01	1.70	1.00
WCL12	110	.040	48.	.125	.098	.096	.038	.01	1.87	2.75
WCL12	110	.040	48.	.125	.122	.116	.041	.01	1.85	3.42
WCL12	110	.040	48.	.125	.147	.136	.045	.01	1.95	4.67
WCL13	122	.040	48.	.125	.052	.052	.034	.01	1.70	1.13
WCL13	122	.040	48.	.125	.104	.099	.036	.01	2.01	4.30
WCL13	122	.040	48.	.125	.131	.121	.042	.01	2.01	4.55
WCL13	122	.040	48.	.125	.156	.141	.046	.01	2.19	4.84
WCL15	134	.040	48.	.125	.066	.066	.033	.01	1.57	1.25
WCL15	134	.040	48.	.125	.135	.131	.044	.01	1.74	3.17
WCL15	134	.040	48.	.125	.165	.152	.048	.01	1.86	4.42
WCL15	134	.040	48.	.125	.198	.180	.050	.01	2.15	6.00
WCL09	87	.040	12.	3.000	.069	.069	.050	.18	.61	0
WCL09	87	.040	12.	3.000	.138	.132	.070	.25	.80	0
WCL09	87	.040	12.	3.000	.173	.162	.077	.26	.89	0
WCL09	87	.040	12.	3.000	.205	.184	.083	.27	.94	0
WCL10	99	.040	12.	3.000	.096	.096	.057	.23	.66	0
WCL10	99	.040	12.	3.000	.196	.189	.080	.26	.92	0
WCL10	99	.040	12.	3.000	.241	.228	.087	.27	1.03	0
WCL10	99	.040	12.	3.000	.287	.247	.090	.29	1.13	0
WCL12	111	.040	12.	3.000	.120	.120	.070	.24	.76	0
WCL12	111	.040	12.	3.000	.240	.230	.088	.27	1.01	0
WCL12	111	.040	12.	3.000	.300	.280	.093	.30	1.12	0
WCL12	111	.040	12.	3.000	.360	.320	.098	.30	1.18	0
WCL13	123	.040	12.	3.000	.150	.150	.070	.25	.81	0
WCL13	123	.040	12.	3.000	.290	.280	.093	.28	1.11	0
WCL13	123	.040	12.	3.000	.370	.330	.100	.34	1.37	0
WCL13	123	.040	12.	3.000	.460	.410	.109	.34	1.52	0

Table A-1 Model Test Data (cfs, ft) (Continued)

Length	Test	S_o	S_S	S_B	Q_T	Q_I	Depth	B_B	B_S	L'
WCL15	135	.040	12.	3.000	.160	.160	.074	.26	.88	0
WCL15	135	.040	12.	3.000	.320	.310	.091	.29	1.32	0
WCL15	135	.040	12.	3.000	.400	.370	.101	.32	1.46	0
WCL15	135	.040	12.	3.000	.490	.450	.109	.36	1.56	0
WCL09	88	.040	48.	3.000	.086	.086	.040	.09	1.83	0.75
WCL09	88	.040	48.	3.000	.173	.171	.054	.15	2.59	3.25
WCL09	88	.040	48.	3.000	.212	.207	.055	.16	2.78	4.25
WCL09	88	.040	48.	3.000	.259	.237	.061	.17	3.08	5.75
WCL10	100	.040	48.	3.000	.090	.090	.041	.10	1.91	0.88
WCL10	100	.040	48.	3.000	.180	.177	.054	.15	2.68	3.01
WCL10	100	.040	48.	3.000	.228	.220	.059	.16	2.91	4.88
WCL10	100	.040	48.	3.000	.269	.242	.061	.17	3.20	6.01
WCL12	112	.040	48.	3.000	.099	.099	.043	.11	2.03	1.00
WCL12	112	.040	48.	3.000	.198	.192	.056	.15	2.68	3.25
WCL12	112	.040	48.	3.000	.247	.233	.061	.17	3.03	4.50
WCL12	112	.040	48.	3.000	.297	.269	.061	.17	3.15	5.25
WCL13	124	.040	48.	3.000	.105	.105	.045	.13	2.01	1.13
WCL13	124	.040	48.	3.000	.211	.202	.057	.16	2.69	4.38
WCL13	124	.040	48.	3.000	.262	.238	.060	.16	2.98	5.51
WCL13	124	.040	48.	3.000	.318	.267	.062	.17	3.15	7.63
WCL15	136	.040	48.	3.000	.114	.114	.046	.12	2.18	1.25
WCL15	136	.040	48.	3.000	.228	.222	.059	.16	3.08	3.50
WCL15	136	.040	48.	3.000	.288	.267	.063	.17	3.23	4.25
WCL15	136	.040	48.	3.000	.341	.300	.063	.18	3.56	5.50
WCL09	89	0.020	12.	0.125	0.160	0.160	.085	0.07	1.06	0.00
WCL09	89	0.020	12.	0.125	0.321	0.317	.122	0.07	1.37	0.00

Table A-1 Model Test Data (cfs, ft) (Continued)

Length	Test	S_o	S_S	S_B	Q_T	Q_I	Depth	B_B	B_S	L'
WCL09	89	0.020	12.	0.125	0.400	0.390	.132	0.07	1.60	0.50
WCL09	89	0.020	12.	0.125	0.480	0.440	.135	0.07	1.74	0.96
WCL10	101	0.020	12.	0.125	0.220	0.220	.106	0.07	1.08	0.00
WCL10	101	0.020	12.	0.125	0.440	0.430	.129	0.07	1.68	0.50
WCL10	101	0.020	12.	0.125	0.550	0.520	.144	0.08	1.82	1.46
WCL10	101	0.020	12.	0.125	0.660	0.600	.163	0.08	1.95	2.46
WCL12	113	0.020	12.	0.125	0.250	0.250	.112	0.07	1.20	0.50
WCL12	113	0.020	12.	0.125	0.500	0.480	.138	0.07	1.76	1.13
WCL12	113	0.020	12.	0.125	0.620	0.590	.159	0.08	1.90	2.13
WCL12	113	0.020	12.	0.125	0.750	0.700	.176	0.08	2.00	3.17
WCL13	125	0.020	12.	0.125	0.310	0.310	.121	0.07	1.35	0.50
WCL13	125	0.020	12.	0.125	0.620	0.600	.158	0.07	1.90	2.09
WCL13	125	0.020	12.	0.125	0.770	0.710	.181	0.08	1.98	3.30
WCL13	125	0.020	12.	0.125	0.930	0.840	.196	0.08	2.15	4.17
WCL15	137	0.020	12.	0.125	0.350	0.350	.126	0.07	1.47	1.25
WCL15	137	0.020	12.	0.125	0.700	0.670	.168	0.08	1.94	2.25
WCL15	137	0.020	12.	0.125	0.870	0.820	.191	0.08	2.14	3.50
WCL15	137	0.020	12.	0.125	1.050	0.940	.200	0.08	2.44	4.38
WCL09	90	.020	48.	0.125	0.052	0.052	.031	0.04	1.50	0.75
WCL09	90	.020	48.	0.125	0.101	0.095	.036	0.04	1.81	3.50
WCL09	90	.020	48.	0.125	0.130	0.119	.039	0.04	1.90	5.00
WCL09	90	.020	48.	0.125	0.156	0.133	.050	0.04	2.40	7.00
WCL10	102	.020	48.	0.125	0.067	0.067	.032	0.04	1.63	0.88
WCL10	102	.020	48.	0.125	0.136	0.115	.045	0.04	2.14	5.63
WCL10	102	.020	48.	0.125	0.167	0.138	.050	0.04	2.47	7.67
WCL10	102	.020	48.	0.125	0.203	0.155	.057	0.04	2.81	9.05
WCL12	114	.020	48.	0.125	0.071	0.071	.036	0.04	1.76	1.00

Table A-1 Model Test Data (cfs, ft) (Continued)

Length	Test	S_o	S_S	S_B	Q_T	Q_I	Depth	B_B	B_S	L'
WCL10	114	.020	48.	0.125	0.142	0.135	.049	0.04	2.10	4.42
WCL12	114	.020	48.	0.125	0.178	0.157	.053	0.04	2.22	6.00
WCL12	114	.020	48.	0.125	0.212	0.184	.058	0.04	2.65	7.42
WCL13	126	.020	48.	0.125	0.075	0.075	.041	0.04	1.81	1.13
WCL13	126	.020	48.	0.125	0.150	0.142	.049	0.04	2.20	3.21
WCL13	126	.020	48.	0.125	0.187	0.171	.052	0.04	2.40	4.92
WCL13	126	.020	48.	0.125	0.226	0.200	.057	0.04	2.60	6.51
WCL15	138	.020	48.	0.125	0.079	0.079	.041	0.04	1.78	1.25
WCL15	138	.020	48.	0.125	0.158	0.147	.051	0.04	2.26	3.67
WCL15	138	.020	48.	0.125	0.198	0.171	.054	0.04	2.48	5.58
WCL15	138	.020	48.	0.125	0.237	0.202	.058	0.04	2.66	7.33
WCL09	91	.020	12.	3.000	.131	.131	.078	.28	.94	0
WCL09	91	.020	12.	3.000	.262	.259	.098	.36	1.18	0
WCL09	91	.020	12.	3.000	.333	.317	.117	.41	1.40	0
WCL09	91	.020	12.	3.000	.394	.360	.127	.44	1.52	0
WCL10	103	.020	12.	3.000	.156	.156	.079	.27	.94	0
WCL10	103	.020	12.	3.000	.313	.302	.104	.35	1.35	0
WCL10	103	.020	12.	3.000	.393	.367	.118	.41	1.40	.40
WCL10	103	.020	12.	3.000	.476	.441	.131	.45	1.52	1.04
WCL12	115	.020	12.	3.000	.212	.212	.097	.33	1.01	0.00
WCL12	115	.020	12.	3.000	.422	.401	.119	.39	1.45	0.40
WCL12	115	.020	12.	3.000	.529	.489	.133	.45	1.56	1.08
WCL12	115	.020	12.	3.000	.636	.550	.149	.49	1.77	1.42
WCL13	127	.020	12.	3.000	.225	.225	.097	.33	1.09	0.20
WCL13	127	.020	12.	3.000	.451	.436	.124	.44	1.55	1.21
WCL13	127	.020	12.	3.000	.560	.522	.134	.46	1.68	1.29
WCL13	127	.020	12.	3.000	.673	.597	.149	.49	1.77	1.76

Table A-1 Model Test Data (cfs, ft) (Continued)

Length	Test	S_o	S_S	S_B	Q_T	Q_I	Depth	B_B	B_S	L'
WCL15	139	.020	12.	3.000	.280	.280	.107	.39	1.21	0.00
WCL15	139	.020	12.	3.000	.557	.545	.137	.47	1.68	0.50
WCL15	139	.020	12.	3.000	.706	.637	.150	.49	1.90	1.75
WCL15	139	.020	12.	3.000	.839	.748	.158	.52	2.13	2.92
WCL09	92	.020	48.	3.000	.035	.035	.034	.06	1.63	0.75
WCL09	92	.020	48.	3.000	.075	.073	.038	.07	1.84	2.17
WCL09	92	.020	48.	3.000	.088	.083	.040	.09	1.96	2.58
WCL09	92	.020	48.	3.000	.105	.098	.042	.10	2.05	3.25
WCL10	104	.020	48.	3.000	.039	.039	.029	.05	1.54	0.88
WCL10	104	.020	48.	3.000	.079	.076	.036	.08	2.05	2.09
WCL10	104	.020	48.	3.000	.101	.094	.042	.09	2.16	3.13
WCL10	104	.020	48.	3.000	.117	.106	.044	.11	2.25	4.17
WCL12	116	.020	48.	3.000	.060	.060	.034	.08	1.62	1.00
WCL12	116	.020	48.	3.000	.121	.113	.045	.12	2.21	4.16
WCL12	116	.020	48.	3.000	.150	.133	.051	.12	2.35	5.16
WCL12	116	.020	48.	3.000	.180	.158	.057	.16	2.50	6.25
WCL13	128	.020	48.	3.000	.055	.055	.032	.07	1.79	1.13
WCL13	128	.020	48.	3.000	.110	.104	.042	.10	2.22	3.51
WCL13	128	.020	48.	3.000	.138	.129	.047	.12	2.46	5.05
WCL13	128	.020	48.	3.000	.165	.147	.054	.14	2.52	5.71
WCL15	140	.020	48.	3.000	.079	.079	.046	.11	2.18	1.25
WCL15	140	.020	48.	3.000	.159	.152	.052	.14	2.48	3.58
WCL15	140	.020	48.	3.000	.201	.189	.059	.15	2.79	5.33
WCL15	140	.020	48.	3.000	.237	.204	.060	.16	2.90	8.33
WCL09	93	.005	12.	.125	0.260	0.260	.153	0.07	1.88	0.75
WCL09	93	.005	12.	.125	0.519	0.491	.194	0.08	2.45	2.33
WCL09	93	.005	12.	.125	0.649	0.582	.211	0.08	2.69	3.00
WCL09	93	.005	12.	.125	0.776	0.668	.228	0.09	2.89	3.58

Table A-1 Model Test Data (cfs, ft) (Continued)

Length	Test	S_o	S_S	S_B	Q_T	Q_I	Depth	B_B	B_S	L'
WCL10	105	.005	12.	.125	0.307	0.307	.162	0.07	2.02	0.88
WCL10	105	.005	12.	.125	0.616	0.575	.210	0.08	2.64	2.88
WCL10	105	.005	12.	.125	0.771	0.671	.227	0.08	2.89	3.55
WCL10	105	.005	12.	.125	0.916	0.755	.250	0.09	3.14	4.13
WCL12	117	.005	12.	.125	0.313	0.313	.161	0.07	2.03	1.00
WCL12	117	.005	12.	.125	0.627	0.582	.212	0.08	2.65	2.92
WCL12	117	.005	12.	.125	0.781	0.680	.230	0.08	2.90	3.83
WCL12	117	.005	12.	.125	0.939	0.790	.253	0.09	3.16	4.25
WCL13	129	.005	12.	.125	0.324	0.324	.164	0.07	2.04	1.13
WCL13	129	.005	12.	.125	0.654	0.606	.212	0.08	2.70	3.05
WCL13	129	.005	12.	.125	0.817	0.704	.240	0.08	2.95	3.76
WCL13	129	.005	12.	.125	0.974	0.813	.255	0.09	3.21	4.42
WCL15	141	.005	12.	.125	0.370	0.370	.170	0.07	2.15	1.25
WCL15	141	.005	12.	.125	0.744	0.663	.221	0.08	2.85	3.42
WCL15	141	.005	12.	.125	0.917	0.786	.251	0.09	3.15	4.17
WCL15	141	.005	12.	.125	1.110	0.886	.268	0.10	3.38	4.92
WCL09	94	.005	48.	.125	0.028	0.028	.043	.04	2.27	0.75
WCL09	94	.005	48.	.125	0.055	0.053	.052	.04	2.31	1.08
WCL09	94	.005	48.	.125	0.069	0.065	.060	.04	2.44	2.25
WCL09	94	.005	48.	.125	0.085	0.076	.062	.04	2.60	2.75
WCL10	106	.005	48.	.125	0.030	0.030	.046	.04	2.27	0.88
WCL10	106	.005	48.	.125	0.057	0.054	.057	.04	2.31	1.71
WCL10	106	.005	48.	.125	0.079	0.074	.061	.04	2.57	2.59
WCL10	106	.005	48.	.125	0.090	0.080	.064	.04	2.88	2.96
WCL12	118	.005	48.	.125	0.032	0.032	.045	.04	2.06	1.00
WCL12	118	.005	48.	.125	0.062	0.060	.054	.04	2.38	1.96
WCL12	118	.005	48.	.125	0.081	0.075	.064	.04	2.59	2.58
WCL12	118	.005	48.	.125	0.096	0.085	.065	.04	2.75	3.25

Table A-1 Model Test Data (cfs, ft) (Continued)

Length	Test	S_o	S_S	S_B	Q_T	Q_I	Depth	B_B	B_S	L'
WCL13	130	.005	48.	.125	0.035	0.035	0.045	0.04	2.23	1.13
WCL13	130	.005	48.	.125	0.069	0.066	0.056	0.04	2.44	2.71
WCL13	130	.005	48.	.125	0.088	0.083	0.063	0.04	2.67	3.01
WCL13	130	.005	48.	.125	0.106	0.096	0.067	0.04	2.89	3.71
WCL15	142	.005	48.	.125	0.039	0.039	0.048	0.04	2.30	1.25
WCL15	142	.005	48.	.125	0.077	0.073	0.059	0.04	2.55	2.75
WCL15	142	.005	48.	.125	0.101	0.094	0.070	0.04	2.92	3.33
WCL15	142	.005	48.	.125	0.117	0.107	0.070	0.04	2.98	3.83
WCL09	95	.005	12.	3.000	0.193	0.193	.114	0.37	1.48	0.75
WCL09	95	.005	12.	3.000	0.386	0.380	.153	0.49	2.01	1.08
WCL09	95	.005	12.	3.000	0.489	0.448	.168	0.55	2.20	1.54
WCL09	95	.005	12.	3.000	0.580	0.522	.179	0.61	2.37	1.96
WCL10	107	.005	12.	3.000	0.284	0.284	.134	0.45	1.76	0.88
WCL10	107	.005	12.	3.000	0.565	0.525	.178	0.59	2.36	1.92
WCL10	107	.005	12.	3.000	0.705	0.635	.193	0.65	2.59	2.46
WCL10	107	.005	12.	3.000	0.856	0.742	.215	0.72	2.83	2.96
WCL12	119	.005	12.	3.000	0.318	0.318	.139	0.47	1.84	1.00
WCL12	119	.005	12.	3.000	0.639	0.609	.187	0.63	2.47	2.17
WCL12	119	.005	12.	3.000	0.793	0.694	.109	0.68	2.73	2.67
WCL12	119	.005	12.	3.000	0.957	0.809	.226	0.74	2.94	3.21
WCL13	131	.005	12.	3.000	0.358	0.358	.151	0.50	1.91	1.13
WCL13	131	.005	12.	3.000	0.717	0.672	.200	0.67	2.59	2.42
WCL13	131	.005	12.	3.000	0.891	0.806	.220	0.72	2.83	3.01
WCL13	131	.005	12.	3.000	1.072	0.905	.238	0.78	3.10	3.46
WCL15	143	.005	12.	3.000	0.446	0.446	.164	0.54	2.13	1.25
WCL15	143	.005	12.	3.000	0.891	0.817	.220	0.70	2.87	3.00

Table A-1 Model Test Data (cfs, ft) (Continued)

Length	Test	S_o	S_S	S_B	Q_T	Q_I	Depth	B_B	B_S	L'
WCL15	143	.005	12.	3.000	1.099	0.954	.242	0.78	3.17	3.58
WCL15	143	.005	12.	3.000	1.322	1.103	.261	0.85	3.40	4.25
WCL12	120	.005	48.	3.000	0.060	0.060	.049	0.15	2.45	1.00
WCL12	120	.005	48.	3.000	0.120	0.115	.068	0.20	3.06	2.33
WCL12	120	.005	48.	3.000	0.150	0.140	.079	0.22	3.50	2.83
WCL12	120	.005	48.	3.000	0.181	0.165	.085	0.23	3.58	3.33
WCL10	108	.005	48.	3.000	0.046	0.046	.045	0.11	2.22	0.88
WCL10	108	.005	48.	3.000	0.093	0.091	.061	0.17	2.71	1.92
WCL10	108	.005	48.	3.000	0.116	0.113	.065	0.19	2.92	2.42
WCL10	108	.005	48.	3.000	0.138	0.130	.073	0.21	3.17	2.71
WCL09	096	.005	48.	3.000	0.043	0.043	.044	0.14	2.30	0.75
WCL09	096	.005	48.	3.000	0.090	0.089	.064	0.17	2.66	1.67
WCL09	096	.005	48.	3.000	0.108	0.106	.064	0.18	2.94	2.25
WCL09	096	.005	48.	3.000	0.129	0.121	.070	0.20	3.05	2.67
WCL15	144	.005	48.	3.000	0.051	0.051	.046	0.13	2.23	1.25
WCL15	144	.005	48.	3.000	0.104	0.101	.062	0.18	2.82	2.50
WCL15	144	.005	48.	3.000	0.128	0.124	.071	0.20	3.10	2.92
WCL15	144	.005	48.	3.000	0.152	0.141	.076	0.21	3.25	3.08
WCL13	132	.005	48.	3.000	0.049	0.049	.046	0.14	2.31	1.13
WCL13	132	.005	48.	3.000	0.099	0.097	.061	0.18	2.87	2.46
WCL13	132	.005	48.	3.000	0.122	0.116	.067	0.20	2.97	2.71
WCL13	132	.005	48.	3.000	0.148	0.137	.069	0.22	3.26	3.01

Table A-1 Model Test Data (cfs, ft) (Continued)

LENGTH	TEST	SO	SS	SB	QO	QI	D	BB	BS	LP*
22.9	85	.040	12.000	.125	.0020	.0020	.0152	.003	.207	.000
22.9	85	.040	12.000	.125	.0040	.0039	.0204	.003	.280	.000
22.9	85	.040	12.000	.125	.0050	.0048	.0238	.003	.290	.000
22.9	85	.040	12.000	.125	.0061	.0058	.0280	.003	.311	.000
26.7	97	.040	12.000	.125	.0027	.0027	.0226	.003	.223	.000
26.7	97	.040	12.000	.125	.0054	.0053	.0274	.003	.293	.000
26.7	97	.040	12.000	.125	.0068	.0065	.0320	.003	.305	.000
26.7	97	.040	12.000	.125	.0082	.0075	.0335	.003	.335	.000
30.5	109	.040	12.000	.125	.0035	.0035	.0213	.003	.253	.000
30.5	109	.040	12.000	.125	.0071	.0070	.0308	.003	.317	.000
30.5	109	.040	12.000	.125	.0088	.0083	.0338	.003	.360	.000
30.5	109	.040	12.000	.125	.0105	.0098	.0357	.003	.427	.000
34.3	121	.040	12.000	.125	.0043	.0043	.0238	.003	.274	.000
34.3	121	.040	12.000	.125	.0085	.0082	.0305	.003	.378	.000
34.3	121	.040	12.000	.125	.0108	.0100	.0366	.005	.451	.000
34.3	121	.040	12.000	.125	.0129	.0118	.0399	.006	.500	.000
38.1	133	.040	12.000	.125	.0061	.0061	.0290	.003	.317	.000
38.1	133	.040	12.000	.125	.0123	.0118	.0369	.006	.472	.000
38.1	133	.040	12.000	.125	.0152	.0139	.0433	.006	.564	.000

*Symbols are defined in nomenclature.

Table A-2 Model Test Data (cms, meters)

Length	Test	S_o	S_S	S_B	Q_T	Q_I	Depth	B_B	B_S	L'
22.9	87	.040	12.000	3.000	.0049	.0046	.0235	.079	.271	.000
22.9	87	.040	12.000	3.000	.0058	.0052	.0253	.082	.287	.000
26.7	99	.040	12.000	3.000	.0027	.0027	.0174	.070	.201	.000
26.7	99	.040	12.000	3.000	.0056	.0054	.0244	.079	.280	.000
26.7	99	.040	12.000	3.000	.0068	.0055	.0265	.082	.314	.000
26.7	99	.040	12.000	3.000	.0081	.0070	.0274	.088	.344	.000
30.5	111	.040	12.000	3.000	.0034	.0034	.0213	.073	.232	.000
30.5	111	.040	12.000	3.000	.0068	.0065	.0268	.082	.308	.000
30.5	111	.040	12.000	3.000	.0085	.0079	.0283	.091	.341	.000
30.5	111	.040	12.000	3.000	.0102	.0091	.0299	.091	.360	.000
34.3	123	.040	12.000	3.000	.0042	.0042	.0213	.076	.247	.000
34.3	123	.040	12.000	3.000	.0082	.0079	.0283	.085	.338	.000
34.3	123	.040	12.000	3.000	.0105	.0093	.0305	.104	.418	.000
34.3	123	.040	12.000	3.000	.0130	.0116	.0332	.104	.463	.000
38.1	133	.040	12.000	.125	.0183	.0161	.0512	.006	.616	.000
22.9	87	.040	12.000	3.000	.0020	.0020	.0152	.055	.185	.000
22.9	87	.040	12.000	3.000	.0039	.0037	.0213	.076	.244	.000

Table A-2 Model Test Data (cms, meters) (Continued)

Length	Test	S_o	S_S	S_B	Q_T	Q_I	Depth	B_B	B_S	L'
38.1	135	.040	12.000	3.000	.0045	.0045	.0226	.079	.268	.000
38.1	135	.040	12.000	3.000	.0091	.0088	.0277	.088	.402	.000
38.1	135	.040	12.000	3.000	.0113	.0105	.0308	.098	.445	.000
38.1	135	.040	12.000	3.000	.0139	.0127	.0332	.110	.475	.000
22.9	89	.020	12.000	.125	.0045	.0045	.0259	.021	.323	.000
22.9	89	.020	12.000	.125	.0091	.0090	.0372	.021	.418	.000
22.9	89	.020	12.000	.125	.0113	.0110	.0402	.021	.488	.152
22.9	89	.020	12.000	.125	.0136	.0125	.0411	.021	.530	.293
26.7	101	.020	12.000	.125	.0062	.0062	.0323	.021	.329	.000
26.7	101	.020	12.000	.125	.0125	.0122	.0393	.021	.512	.152
26.7	101	.020	12.000	.125	.0156	.0147	.0439	.024	.555	.445
26.7	101	.020	12.000	.125	.0187	.0170	.0497	.024	.594	.750
30.5	113	.020	12.000	.125	.0071	.0071	.0341	.021	.366	.152
30.5	113	.020	12.000	.125	.0142	.0136	.0421	.021	.536	.344
30.5	113	.020	12.000	.125	.0176	.0167	.0485	.024	.579	.649
30.5	113	.020	12.000	.125	.0212	.0198	.0536	.024	.610	.966
34.3	125	.020	12.000	.125	.0088	.0088	.0369	.021	.411	.152

Table A-2 Model Test Data (cms, meters) (Continued)

Length	Test	S_o	S_S	S_B	Q_T	Q_I	Depth	B_B	B_S	L'
34.3	125	.020	12.000	.125	.0176	.0170	.0482	.021	.579	.637
34.3	125	.020	12.000	.125	.0218	.0201	.0552	.024	.604	1.006
34.3	125	.020	12.000	.125	.0263	.0238	.0597	.024	.655	1.271
38.1	137	.020	12.000	.125	.0099	.0099	.0384	.021	.448	.381
38.1	137	.020	12.000	.125	.0198	.0190	.0512	.024	.591	.686
38.1	137	.020	12.000	.125	.0246	.0232	.0582	.024	.652	1.067
38.1	137	.020	12.000	.125	.0297	.0266	.0610	.024	.744	1.335
22.9	91	.020	12.000	3.000	.0037	.0037	.0238	.085	.287	.000
22.9	91	.020	12.000	3.000	.0074	.0073	.0299	.110	.360	.000
22.9	91	.020	12.000	3.000	.0094	.0090	.0357	.125	.427	.000
22.9	91	.020	12.000	3.000	.0112	.0102	.0387	.134	.463	.000
26.7	103	.020	12.000	3.000	.0044	.0044	.0241	.082	.287	.000
26.7	103	.020	12.000	3.000	.0089	.0086	.0317	.107	.411	.000
26.7	103	.020	12.000	3.000	.0111	.0104	.0360	.125	.427	.122
26.7	103	.020	12.000	3.000	.0135	.0125	.0399	.137	.463	.317
30.5	115	.020	12.000	3.000	.0060	.0060	.0296	.101	.308	.000
30.5	115	.020	12.000	3.000	.0119	.0114	.0363	.119	.442	.122

Table A-2 Model Test Data (cms, meters) (Continued)

Length	Test	S_o	S_S	S_B	Q_T	Q_I	Depth	B_B	B_S	L'
30.5	115	.020	12.000	3.000	.0150	.0138	.0405	.137	.475	.329
30.5	115	.020	12.000	3.000	.0180	.0156	.0454	.149	.539	.433
34.3	127	.020	12.000	3.000	.0064	.0064	.0296	.101	.332	.061
34.3	127	.020	12.000	3.000	.0128	.0123	.0378	.134	.472	.369
34.3	127	.020	12.000	3.000	.0159	.0148	.0408	.140	.512	.393
34.3	127	.020	12.000	3.000	.0191	.0169	.0454	.149	.539	.536
38.1	139	.020	12.000	3.000	.0079	.0079	.0326	.119	.369	.000
38.1	139	.020	12.000	3.000	.0158	.0154	.0418	.143	.512	.152
38.1	139	.020	12.000	3.000	.0200	.0180	.0457	.149	.579	.533
38.1	139	.020	12.000	3.000	.0238	.0212	.0482	.158	.649	.890
22.9	93	.005	12.000	.125	.0074	.0074	.0466	.021	.573	.229
22.9	93	.005	12.000	.125	.0147	.0139	.0591	.024	.747	.710
22.9	93	.005	12.000	.125	.0184	.0165	.0643	.024	.820	.914
22.9	93	.005	12.000	.125	.0220	.0189	.0695	.027	.881	1.091
26.7	105	.005	12.000	.125	.0087	.0087	.0494	.021	.616	.268
26.7	105	.005	12.000	.125	.0174	.0163	.0640	.024	.805	.878
26.7	105	.005	12.000	.125	.0218	.0190	.0592	.024	.881	1.082

Table A-2 Model Test Data (cms, meters) (Continued)

Length	Test	S_o	S_S	S_B	Q_T	Q_I	Depth	B_B	B_S	L'
26.7	105	.005	12.000	.125	.0259	.0214	.0762	.027	.957	1.256
30.5	117	.005	12.000	.125	.0089	.0089	.0491	.021	.619	.305
30.5	117	.005	12.000	.125	.0178	.0165	.0646	.024	.808	.890
30.5	117	.005	12.000	.125	.0221	.0193	.0701	.024	.884	1.167
30.5	117	.005	12.000	.125	.0266	.0224	.0771	.027	.963	1.295
34.3	129	.005	12.000	.125	.0092	.0092	.0500	.021	.622	.344
34.3	129	.005	12.000	.125	.0185	.0172	.0646	.024	.823	.930
34.3	129	.005	12.000	.125	.0231	.0199	.0732	.024	.899	1.146
34.3	129	.005	12.000	.125	.0276	.0230	.0777	.027	.978	1.347
38.1	141	.005	12.000	.125	.0105	.0105	.0518	.021	.655	.381
38.1	141	.005	12.000	.125	.0211	.0188	.0674	.024	.869	1.042
38.1	141	.005	12.000	.125	.0260	.0223	.0765	.027	.960	1.271
38.1	141	.005	12.000	.125	.0314	.0251	.0817	.030	1.030	1.500
22.9	95	.005	12.000	3.000	.0055	.0055	.0347	.113	.451	.229
22.9	95	.005	12.000	3.000	.0109	.0108	.0466	.149	.613	.329
22.9	95	.005	12.000	3.000	.0138	.0127	.0512	.168	.671	.469
22.9	95	.005	12.000	3.000	.0164	.0148	.0546	.186	.722	.597

Table A-2 Model Test Data (cms, meters) (Continued)

Length	Test	S_o	S_S	S_B	Q_T	Q_I	Depth	B_B	B_S	L'
26.7	107	.005	12.000	3.000	.0080	.0080	.0408	.137	.536	.268
26.7	107	.005	12.000	3.000	.0160	.0149	.0543	.180	.719	.585
26.7	107	.005	12.000	3.000	.0200	.0180	.0588	.198	.789	.730
26.7	107	.005	12.000	3.000	.0242	.0210	.0655	.219	.863	.902
30.5	119	.005	12.000	3.000	.0090	.0090	.0424	.143	.561	.305
30.5	119	.005	12.000	3.000	.0181	.0172	.0570	.192	.753	.661
30.5	119	.005	12.000	3.000	.0225	.0197	.0637	.207	.832	.814
30.5	119	.005	12.000	3.000	.0271	.0229	.0689	.226	.895	.978
34.3	131	.005	12.000	3.000	.0101	.0101	.0460	.152	.582	.344
34.3	131	.005	12.000	3.000	.0203	.0190	.0610	.204	.789	.738
34.3	131	.005	12.000	3.000	.0252	.0228	.0671	.219	.863	.917
34.3	131	.005	12.000	3.000	.0304	.0256	.0725	.238	.945	1.055
38.1	143	.005	12.000	3.000	.0126	.0126	.0500	.165	.649	.381
38.1	143	.005	12.000	3.000	.0252	.0231	.0671	.213	.875	.914
38.1	143	.005	12.000	3.000	.0311	.0270	.0738	.238	.965	1.091
38.1	143	.005	12.000	3.000	.0374	.0312	.0796	.259	1.036	1.295
22.9	86	.040	48.000	.125	.0013	.0013	.0104	.003	.491	.229

Table A-2 Model Test Data (cms, meters) (Continued)

Length	Test	S_o	S_S	S_B	Q_T	Q_I	Depth	B_B	B_S	L'
22.9	86	.040	48.000	.125	.0026	.0025	.0116	.003	.536	.634
22.9	86	.040	48.000	.125	.0032	.0031	.0122	.003	.549	.939
22.9	86	.040	48.000	.125	.0039	.0037	.0131	.003	.573	1.167
26.7	98	.040	48.000	.125	.0014	.0014	.0101	.003	.512	.268
26.7	98	.040	48.000	.125	.0028	.0026	.0119	.003	.549	.725
26.7	98	.040	48.000	.125	.0035	.0033	.0125	.003	.570	1.006
26.7	98	.040	48.000	.125	.0042	.0038	.0134	.003	.610	1.359
30.5	110	.040	48.000	.125	.0014	.0014	.0098	.003	.518	.305
30.5	110	.040	48.000	.125	.0028	.0027	.0116	.003	.570	.838
30.5	110	.040	48.000	.125	.0035	.0033	.0125	.003	.564	1.042
30.5	110	.040	48.000	.125	.0042	.0039	.0137	.003	.594	1.423
34.3	122	.040	48.000	.125	.0015	.0015	.0104	.003	.518	.344
34.3	122	.040	48.000	.125	.0029	.0028	.0110	.003	.613	1.311
34.3	122	.040	48.000	.125	.0037	.0034	.0128	.003	.613	1.387
34.3	122	.040	48.000	.125	.0044	.0040	.0140	.003	.668	1.475
38.1	134	.040	48.000	.125	.0019	.0019	.0101	.003	.479	.381
38.1	134	.040	48.000	.125	.0038	.0037	.0134	.003	.530	.966

Table A-2 Model Test Data (cms, meters) (Continued)

Length	Test	S_o	S_S	S_B	Q_T	Q_I	Depth	B_B	B_S	L'
38.1	134	.040	48.000	.125	.0047	.0043	.0146	.003	.567	1.347
38.1	134	.040	48.000	.125	.0056	.0051	.0152	.003	.655	1.829
22.9	88	.040	48.000	3.000	.0024	.0024	.0122	.027	.558	.229
22.9	88	.040	48.000	3.000	.0049	.0048	.0165	.046	.789	.991
22.9	88	.040	48.000	3.000	.0060	.0059	.0168	.049	.847	1.295
22.9	88	.040	48.000	3.000	.0073	.0067	.0186	.052	.939	1.753
26.7	100	.040	48.000	3.000	.0025	.0025	.0125	.030	.582	.268
26.7	100	.040	48.000	3.000	.0051	.0050	.0165	.046	.817	.917
26.7	100	.040	48.000	3.000	.0065	.0062	.0180	.049	.887	1.487
26.7	100	.040	48.000	3.000	.0076	.0069	.0186	.052	.975	1.832
30.5	112	.040	48.000	3.000	.0028	.0028	.0131	.034	.619	.305
30.5	112	.040	48.000	3.000	.0056	.0054	.0171	.046	.817	.991
30.5	112	.040	48.000	3.000	.0070	.0066	.0186	.052	.924	1.372
30.5	112	.040	48.000	3.000	.0084	.0076	.0186	.052	.960	1.600
34.3	124	.040	48.000	3.000	.0030	.0030	.0137	.040	.613	.344
34.3	124	.040	48.000	3.000	.0060	.0057	.0174	.049	.820	1.335
34.3	124	.040	48.000	3.000	.0074	.0067	.0183	.049	.908	1.679

Table A-2 Model Test Data (cms, meters) (Continued)

Length	Test	S_o	S_S	S_B	Q_T	Q_I	Depth	B_B	B_S	L'
34.3	124	.040	48.000	3.000	.0090	.0076	.0189	.052	.960	2.326
38.1	136	.040	48.000	3.000	.0032	.0032	.0140	.037	.664	.381
38.1	136	.040	48.000	3.000	.0065	.0063	.0180	.049	.939	1.067
38.1	136	.040	48.000	3.000	.0082	.0076	.0192	.052	.985	1.295
38.1	136	.040	48.000	3.000	.0097	.0085	.0192	.055	1.085	1.676
22.9	90	.020	48.000	.125	.0015	.0015	.0094	.012	.457	.229
22.9	90	.020	48.000	.125	.0029	.0027	.0110	.012	.552	1.067
22.9	90	.020	48.000	.125	.0037	.0034	.0119	.012	.579	1.524
22.9	90	.020	48.000	.125	.0044	.0038	.0152	.012	.732	2.134
26.7	102	.020	48.000	.125	.0019	.0019	.0098	.012	.497	.268
26.7	102	.020	48.000	.125	.0039	.0033	.0137	.012	.652	1.716
26.7	102	.020	48.000	.125	.0047	.0039	.0152	.012	.753	2.338
26.7	102	.020	48.000	.125	.0057	.0044	.0174	.012	.856	2.758
30.5	114	.020	48.000	.125	.0020	.0020	.0110	.012	.536	.305
30.5	114	.020	48.000	.125	.0040	.0038	.0149	.012	.640	1.347
30.5	114	.020	48.000	.125	.0050	.0044	.0162	.012	.677	1.829
30.5	114	.020	48.000	.125	.0060	.0052	.0177	.012	.808	2.262

Table A-2 Model Test Data (cms, meters) (Continued)

Length	Test	S_o	S_S	S_B	Q_T	Q_I	Depth	B_B	B_S	L'
34.3	126	.020	48.000	.125	.0021	.0021	.0125	.012	.552	.344
34.3	126	.020	48.000	.125	.0042	.0040	.0149	.012	.671	.978
34.3	126	.020	48.000	.125	.0053	.0048	.0158	.012	.732	1.500
34.3	126	.020	48.000	.125	.0064	.0057	.0174	.012	.792	1.984
38.1	138	.020	48.000	.125	.0022	.0022	.0125	.012	.543	.381
38.1	138	.020	48.000	.125	.0045	.0042	.0155	.012	.689	1.119
38.1	138	.020	48.000	.125	.0056	.0048	.0165	.012	.755	1.701
38.1	138	.020	48.000	.125	.0067	.0057	.0177	.012	.811	2.234
22.9	92	.020	48.000	3.000	.0010	.0010	.0104	.018	.497	.229
22.9	92	.020	48.000	3.000	.0021	.0021	.0116	.021	.561	.661
22.9	92	.020	48.000	3.000	.0025	.0024	.0122	.027	.597	.786
22.9	92	.020	48.000	3.000	.0030	.0028	.0128	.030	.625	.991
26.7	104	.020	48.000	3.000	.0011	.0011	.0088	.015	.469	.268
26.7	104	.020	48.000	3.000	.0022	.0022	.0110	.024	.625	.637
26.7	104	.020	48.000	3.000	.0029	.0027	.0128	.027	.658	.954
26.7	104	.020	48.000	3.000	.0033	.0030	.0134	.034	.685	1.271
30.5	116	.020	48.000	3.000	.0017	.0017	.0104	.024	.494	.305

Table A-2 Model Test Data (cms, meters) (Continued)

Length	Test	S_o	S_S	S_B	Q_T	Q_I	Depth	B_B	B_S	L'
30.5	116	.020	48.000	3.000	.0034	.0032	.0137	.037	.574	1.268
30.5	116	.020	48.000	3.000	.0042	.0038	.0155	.037	.716	1.573
30.5	116	.020	48.000	3.000	.0051	.0045	.0174	.049	.762	1.905
34.3	128	.020	48.000	3.000	.0015	.0016	.0098	.021	.546	.344
34.3	128	.020	48.000	3.000	.0031	.0029	.0128	.030	.677	1.070
34.3	128	.020	48.000	3.000	.0039	.0037	.0143	.037	.750	1.539
34.3	128	.020	48.000	3.000	.0047	.0042	.0155	.043	.768	1.740
38.1	140	.020	48.000	3.000	.0022	.0022	.0140	.034	.654	.381
38.1	140	.020	48.000	3.000	.0045	.0043	.0158	.043	.755	1.091
38.1	140	.020	48.000	3.000	.0057	.0054	.0180	.046	.850	1.625
38.1	140	.020	48.000	3.000	.0067	.0058	.0183	.049	.884	2.539
22.9	94	.005	48.000	.125	.0008	.0008	.0131	.012	.692	.229
22.9	94	.005	48.000	.125	.0016	.0015	.0158	.012	.704	.329
22.9	94	.005	48.000	.125	.0020	.0018	.0183	.012	.744	.686
22.9	94	.005	48.000	.125	.0024	.0022	.0189	.012	.792	.838
26.7	106	.005	48.000	.125	.0008	.0008	.0140	.012	.692	.268
26.7	106	.005	48.000	.125	.0016	.0015	.0174	.012	.704	.521

Table A-2 Model Test Data (cms, meters)(Continued)

Length	Test	S_o	S_S	S_B	Q_T	Q_I	Depth	B_B	B_S	L'
26.7	106	.005	48.000	.125	.0022	.0021	.0186	.012	.783	.789
26.7	106	.005	48.000	.125	.0025	.0023	.0195	.012	.878	.902
30.5	118	.005	48.000	.125	.0009	.0009	.0137	.012	.628	.305
30.5	118	.005	48.000	.125	.0018	.0017	.0165	.012	.725	.597
30.5	118	.005	48.000	.125	.0023	.0021	.0195	.012	.789	.786
30.5	118	.005	48.000	.125	.0027	.0024	.0198	.012	.838	.991
34.3	130	.005	48.000	.125	.0010	.0010	.0137	.012	.680	.344
34.3	130	.005	48.000	.125	.0020	.0019	.0171	.012	.744	.826
34.3	130	.005	48.000	.125	.0025	.0024	.0192	.012	.814	.917
34.3	130	.005	48.000	.125	.0030	.0027	.0204	.012	.881	1.131
38.1	142	.005	48.000	.125	.0011	.0011	.0146	.012	.701	.381
38.1	142	.005	48.000	.125	.0022	.0021	.0180	.012	.777	.838
38.1	142	.005	48.000	.125	.0029	.0027	.0213	.012	.890	1.015
38.1	142	.005	48.000	.125	.0033	.0030	.0213	.012	.908	1.167
22.9	96	.005	48.000	3.000	.0012	.0012	.0134	.043	.701	.229
22.9	96	.005	48.000	3.000	.0025	.0025	.0195	.052	.811	.509
22.9	96	.005	48.000	3.000	.0031	.0030	.0195	.053	.896	.586

Table A-2 Model Test Data (cms, meters) (Continued)

Length	Test	S_o	S_S	S_B	Q_T	Q_I	Depth	B_B	B_S	L'
22.9	96	.005	48.000	3.000	.0037	.0034	.0213	.061	.930	.814
26.7	108	.005	48.000	3.000	.0013	.0013	.0137	.034	.677	.268
26.7	108	.005	48.000	3.000	.0026	.0026	.0186	.052	.826	.585
26.7	108	.005	48.000	3.000	.0033	.0032	.0198	.058	.890	.738
26.7	108	.005	48.000	3.000	.0039	.0037	.0223	.064	.966	.826
30.5	120	.005	48.000	3.000	.0017	.0017	.0149	.046	.747	.305
30.5	120	.005	48.000	3.000	.0034	.0033	.0207	.061	.933	.710
30.5	120	.005	48.000	3.000	.0042	.0040	.0241	.067	1.067	.863
30.5	120	.005	48.000	3.000	.0051	.0047	.0259	.070	1.091	1.015
34.3	132	.005	48.000	3.000	.0014	.0014	.0140	.043	.704	.344
34.3	132	.005	48.000	3.000	.0028	.0027	.0186	.055	.875	.750
34.3	132	.005	48.000	3.000	.0035	.0033	.0204	.061	.905	.826
34.3	132	.005	48.000	3.000	.0042	.0039	.0210	.067	.994	.917
38.1	144	.005	48.000	3.000	.0014	.0014	.0140	.040	.580	.381
38.1	144	.005	48.000	3.000	.0029	.0029	.0189	.055	.860	.762
38.1	144	.005	48.000	3.000	.0036	.0035	.0216	.061	.945	.890
38.1	144	.005	48.000	3.000	.0043	.0040	.0232	.064	.991	.939

Table A-2 Model Test Data (cms, meters) (Continued)

BIBLIOGRAPHY

1. Appel, E., et al.
   HYDRAULIC PERFORMANACE OF PENNSYLVANIA HIGHWAY DRAINAGE INLETS INSTALLED IN GRASS CHANNELS, Lehigh University, Fritz Engineering Laboratory Report No. 364.4, Bethlehem, Pa. (January 1973).

2. Chow, V. T.
   OPEN-CHANNEL HYDRAULICS, McGraw-Hill Book Company, New York, New York (1959).

3. Einstein, H. A. and E. S. El-Samni
   HYDRODYNAMIC FORCES ON A ROUGH WALL, p. 521, Review of Modern Physics, Vol. 21 (1949).

4. Graf, W. H.
   HYDRAULICS OF SEDIMENT TRANSPORT, pp. 385-398, McGraw-Hill Book Company, New York, New York (1971).

5. Hansen, A. G.
   FLUID MECHANICS, pp. 395-413, Wiley, New York, New York, (1967).

6. Johns Hopkins University
   THE DESIGN OF STORM-WATER INLETS, Department of Sanitary Engineering and Water Resources, Report of the Storm Drainage Research Committee, Baltimore, Maryland (June 1956).

7. Larson, C. L. and L. G. Straub
   GRATE INLETS FOR SURFACE DRAINAGE OF STREETS AND HIGHWAYS, University of Minnesota, St. Anthony Falls Hydraulic Laboratory, Bulletin 2 (June 1949).

8. Li, Wen-Hsiung
   HYDRAULIC THEORY FOR DESIGN OF STORM-WATER INLETS, Highway Research Board, No. 33 (1954).

9. Morris, H. M.
   APPLIED HYDRAULICS IN ENGINEERING, The Ronald Press Company, New York, New York (1963).

10. Stevens, J. C. et al.
    HYDRAULICS MODELS, The Committee of the Hydraulic Division on Hydraulic Research, ASCE, Manual of Engineering Practice 25 (1942).

11. U. S. Army Corps of Engineers
    SURFACE DRAINAGE FACILITIES FOR AIRFIELDS, EM 1110-345-281 (1964).

12. Wasley, Richard J.
HYDRODYNAMICS OF FLOW INTO CURB-OPENING INLETS, Ph.D. Thesis, Stanford University, Berkeley, California, University Microfilms, Inc. Ann Arbor, Michigan (1961).

13. Yee, P. P. et al.
HYDRAULIC PERFORMANCE OF PENNSYLVANIA HIGHWAY DRAINAGE INLETS INSTALLED IN PAVED CHANNELS, Lehigh University, Fritz Engineering Laboratory Report 364.3, Bethlehem, Pa. (Nov. 1972).

14. Yee, P. P.
HYDRAULIC PERFORMANCE OF HIGHWAY DRAINAGE INLETS USED IN PENNSYLVANIA, MS Thesis, Lehigh University, Bethlehem, Pennsylvania (1972).

15. Yucel, O. et al.
DEVELOPMENT OF IMPROVED DRAINAGE INLETS, PHASE 1: LITERATURE SURVEY, Lehigh University, Fritz Engineering Laboratory Report No. 364.2 (1969).

VITA

Andrew Day Spear

I was born in Boston, Massachusetts on February 15, 1951. During my childhood, I lived in East Walpole, Massachusetts. I attended high school at Wilbraham Academy in Wilbraham, Massachusetts and graduate Cum Laude in June, 1969.

My college undergraduate work was performed at Lehigh University in Bethlehem, Pennsylvania. In June, 1973, I received a Bachelor of Arts degree in Applied Science. In June, 1974, I received a Bachelor of Science degree in Civil Engineering from the same University.

Since that time, also at Lehigh University, I have been associated with Fritz Engineering Laboratory Project 401: "The Optimal Dimensions of Pennsylvania Highway Drainage Inlets," while completing course work towards a Master of Science degree in Civil Engineering.